

**INFORMATION-BASED ASSET PRICING OF OPTIONS USING  
STOCHASTIC VOLATILITY MODELS**



**UNIVERSITY OF NAIROBI  
SCHOOL OF MATHEMATICS**

Cynthia Amai Ikamari  
I80/51961/2017

A research thesis submitted in partial fulfilment of the requirements for the award of the degree of Doctor of Philosophy in Actuarial Science of the University of Nairobi.

**January 2021**


**Declaration**

I, Cynthia Ikamari, whose student registration number is I80/51961/2017, hereby declare that this PhD Thesis entitled, “Information Based Asset Pricing using Stochastic Volatility Models” my own work and that, to the best of my knowledge and belief, it contains no material previously published or written by another person nor material which to a substantial extent has been accepted for the award of any other degree or diploma of the university or other institute of higher learning. Any uses made within it of the works of other authors in any form are properly acknowledged at the point of their use and a full list of the references employed has been included at the last page.

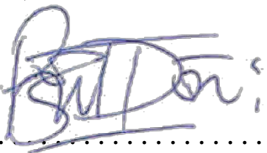
Signature: .....  ..... Date: ..... 23/08/2021 .....

Cynthia Ikamari,  
School of Mathematics,  
University of Nairobi

This thesis has been submitted for examination with our approval as the university supervisors.

Signature: .....  ..... Date: ..... 23/8/21 .....

Prof. Philip Ngare,  
School of Mathematics,  
University of Nairobi

Signature: .....  ..... Date: ..... 23.08.2021 .....

Prof. Patrick Weke,  
School of Mathematics,  
University of Nairobi

## **Dedication**

This work is lovingly dedicated to my daughter, Vivian. You made the process enjoyable and brought balance into this journey. The balance you created brought clarity to my thinking process that resulted in great ideas that enabled the completion of this work.

## **Acknowledgements**

The input of my two supervisors, Prof. Philip Ngare and Prof. Patrick Weke in this research work provided me with greatly needed assistance. Their guidance and support throughout the duration of the research greatly contributed to the completion of this work. I would like to express my appreciation to each of them for their commitment.

I also thank my family and friends for their unending support and consistently keeping me on track. Last but not the least; I thank the Lord, the Almighty, for his goodness and grace that have brought me this far.

## **Abstract**

In asset pricing, explicit models are being constructed for the flow of market information. Financial markets are making use of such models as a basis for asset pricing. With increased globalization of financial markets, investors and traders are becoming more interested in multi-asset products. Options that consist of a portfolio of assets are of interest to investors because they provide diversification across a number of market segments and assets. They are also cheaper in comparison to a portfolio that consists of similar single asset options. With these developments, financial markets are faced with the challenge of determining suitable prices for these multi-asset options.

This study looks at the valuation of such options incorporating information using a stochastic volatility model. An approximate price for multi-asset options is derived using the notion of comonotonicity and Wishart processes under the information-based asset pricing framework. The results show that the information flow rate parameter plays a significant role in the prices obtained in the model based on Brody, Hughson and Macrina's asset pricing framework. The prices obtained using the model give a relatively close fit to the prices observed in the market.

## **List of Abbreviations and Acronyms**

SDE - Stochastic Differential Equation

GBM - Geometric Brownian Motion

BHM - Brody Hughston Macrina

BS-BHM - Black Scholes-Brody Hughston Macrina

RMSE - Root Mean Square Error

CIR - Cox Ingersoll Ross

EKF - Extended Kalman Filter

PDE - Partial Differential Equation

SVM - Stochastic Volatility Model

ISVM - Information-Based Stochastic Volatility Model

BSM - Black Scholes Model

WAR - Wishart Autoregressive

MLE - Maximum Likelihood Estimation

## **List of Publications**

Ikamari, C., Ngare, P., & Weke, P. (2020). Multi-asset option pricing using an information-based model. *Scientific African*, 10, e00564.

Ikamari, C., Ngare, P., & Weke, P. (2021). Option pricing in an information-based model using the Crank-Nicolson finite difference method. *Far East Journal of Mathematical Sciences*, 130(2).

## Contents

<b>Declaration</b>	<b>i</b>
<b>Dedication</b>	<b>ii</b>
<b>Acknowledgements</b>	<b>iii</b>
<b>Abstract</b>	<b>iv</b>
<b>List of Abbreviations and Acronyms</b>	<b>v</b>
<b>1 Introduction</b>	<b>1</b>
1.1 Background of the study . . . . .	1
1.2 Statement of the problem . . . . .	6
1.3 Objectives of the study . . . . .	7
1.3.1 General Objective . . . . .	7
1.3.2 Specific Objectives . . . . .	7
1.4 Significance of the study . . . . .	8
<b>2 Literature Review</b>	<b>9</b>
<b>3 Multi-asset option pricing</b>	<b>14</b>
3.1 Modelling volatility in a multi-asset framework . . . . .	14
3.1.1 Asset pricing model with constant volatility . . . . .	14
3.1.2 Asset pricing model with stochastic volatility . . . . .	19
3.2 Dynamics of an option pricing model where the variance process depends on time and information in a multi-asset framework . . . . .	27
3.2.1 Information-based asset pricing framework model dynamics . . . . .	27
3.2.2 Multi-asset information-based asset pricing framework model dy- namics . . . . .	32
3.3 Asset pricing in an information-based framework . . . . .	38
3.3.1 Notion of comonotonicity in a multi-asset information-based frame- work . . . . .	38
3.3.2 Pricing multi-asset options under the BS-BHM model . . . . .	39
3.3.3 Pricing multi-asset options under the BS-BHM updated model . . . . .	45
3.3.4 Information-based framework model dynamics as a special case of the Black-Scholes model . . . . .	50



<b>4</b>	<b>Parameter estimation and non-linear filtering</b>	<b>52</b>
4.1	Estimation of model parameters . . . . .	52
4.1.1	Maximum likelihood estimation . . . . .	52
4.1.2	Pseudo-maximum likelihood estimation . . . . .	56
4.1.3	Method of moments . . . . .	60
4.1.4	Measurement of parameter sensitivity . . . . .	64
4.2	Comparison of volatility in a stochastic volatility model vs volatility in an information-based asset pricing model in a multivariate framework . . . . .	74
4.2.1	Preliminary concepts on non-linear filtering . . . . .	74
4.2.2	Non-linear filtering in the Heston model . . . . .	76
4.2.3	Non-linear filtering in an information-based framework . . . . .	80
<b>5</b>	<b>Data Analysis and Results</b>	<b>86</b>
5.1	Modelling volatility in a multi-asset framework . . . . .	92
5.1.1	Asset pricing model with constant volatility . . . . .	92
5.1.2	Asset pricing model with stochastic volatility . . . . .	99
5.2	Asset pricing in an information-based framework . . . . .	103
5.2.1	BS-BHM model . . . . .	103
5.2.2	BS-BHM updated model . . . . .	109
5.3	Estimation of model parameters . . . . .	117
5.3.1	Maximum likelihood estimation . . . . .	117
5.3.2	Method of moments . . . . .	117
5.3.3	Measurement of parameter sensitivity . . . . .	119
5.4	Comparison of volatility in a stochastic volatility model vs volatility in an information-based asset pricing model . . . . .	124
5.4.1	Volatility extraction in the Heston model . . . . .	124
5.4.2	Volatility extraction in the information-based asset pricing model . . . . .	129
<b>6</b>	<b>Conclusion and Recommendation</b>	<b>135</b>
	<b>List of References</b>	<b>138</b>

## List of Tables

1	SPX options data summary . . . . .	86
2	Dow Jones Euro Stoxx 50 options data summary . . . . .	90
3	The multi-asset Black-Scholes model option prices . . . . .	98
4	The multi-asset Heston model option prices . . . . .	101
5	Comparison of the multi-asset option prices between the BS-BHM model & the Black-Scholes model . . . . .	107
6	Comparison of the multi-asset option prices between the BS-BHM updated model & the Black-Scholes model . . . . .	114
7	RMSE values for the non-linear filters . . . . .	134

## List of Figures

1	Volatility surface . . . . .	2
2	Histogram of the SPX option strike prices . . . . .	87
3	Histogram of the SPX option underlying asset price . . . . .	88
4	Histogram of the SPX option implied volatility . . . . .	89
5	Histogram of the Dow Jones Euro Stoxx 50 option strike prices . . . . .	91
6	Simulated Black-Scholes model option prices . . . . .	93
7	Black-Scholes model surface wrt volatility . . . . .	94
8	Black-Scholes model surface wrt time to maturity . . . . .	95
9	Black-Scholes model price wrt strike price . . . . .	96
10	Comparison of the Black-Scholes model option prices and the empirical option prices . . . . .	97
11	The multi-asset Black-Scholes model option prices . . . . .	99
12	Simulated Heston model option price . . . . .	100
13	Heston model volatility surface . . . . .	101
14	Wishart processes . . . . .	102
15	BS-BHM model option prices vs. empirical option prices, $\gamma = 0.3$ . . . . .	104
16	BS-BHM model option prices vs. empirical option prices, $\gamma = 0.25$ . . . . .	105
17	Black-Scholes model vs. BS-BHM model option prices, $\gamma = 0.3$ . . . . .	106
18	Black-Scholes model vs. BS-BHM model option prices, $\gamma = 0.25$ . . . . .	107
19	Comparison of the multi-asset BS-BHM model and the multi-asset BSM . . . . .	108
20	BS-BHM model volatility surface . . . . .	109
21	BS-BHM updated model option prices vs. empirical option prices, $\gamma = 0.3$ . . . . .	110
22	BS-BHM updated model option prices vs. empirical option prices, $\gamma = 0.25$ . . . . .	111
23	Black-Scholes model vs. BS-BHM updated model option prices, $\gamma = 0.3$ . . . . .	112
24	Black-Scholes model vs. BS-BHM updated model option prices, $\gamma = 0.25$ . . . . .	113
25	Comparison of the multi-asset BS-BHM updated and the multi-asset BSM . . . . .	115
26	BS-BHM updated volatility surface . . . . .	116
27	Information flow rate wrt time . . . . .	118
28	Sensitivity of the option price wrt Delta . . . . .	119
29	Sensitivity of the option price wrt Gamma . . . . .	120
30	Sensitivity of the option price wrt Vega . . . . .	121
31	Sensitivity of the option price wrt Rho . . . . .	122
32	Sensitivity of the option price wrt Theta . . . . .	123
33	Heston model's simulated volatility . . . . .	126
34	Heston model's simulated volatility vs. estimated volatility using the EKF . . . . .	127

35	Heston model's simulated volatility vs. estimated volatility using the particle filter . . . . .	129
36	Information-based asset pricing model's simulated volatility . . . . .	130
37	Information-based framework simulated volatility vs. estimated volatility using the EKF . . . . .	132
38	Information-based framework simulated volatility vs. estimated volatility using the particle filter . . . . .	133

## 1. Introduction

### 1.1. Background of the study

With the globalization of financial markets, modern financial markets are facing an increasing level of complexity due to the rise in financial innovations that are designed to cater to the new market trends, (Khraisha and Arthur, 2018). Increased integration of financial markets has led to financial instruments which depend on more than one underlying asset becoming common. One such innovation relates to multi-asset options which, unlike standard options with one underlying asset, are based on several underlying asset. There has been an increase in the number of multi-asset options trading in financial markets. These options depend on the underlying assets' volatility and correlations. This means that, due to the underlying assets' correlation, there is increased multiple risk exposure to banks and other financial institutions.

The 2007-2009 financial crisis threatened the global financial markets with complete collapse as banks reduced the loans issued to businesses and other entities, (Thakor, 2015). It is regarded as the most severe period of financial difficulty since the Great Depression that occurred in the 1930s. The recession was partially a result of the financial institutions' co-movement illustrated on some of the financial markets' vulnerabilities. It was also due to increased innovations in financial products that led to increased multiple risks in the industry. This led to researchers in the field of mathematical finance to identify pricing models which are able to capture multiple sources of risk.

This study proposes to evaluate multi-asset European options which are a type of derivative instrument. In particular, the pricing of options that are dependent on several underlying assets incorporating information is examined. Options are a type of financial derivative, the value of which is based on the expectation of a change in the price of an underlying asset. It is a contract between a buyer and a seller in which the holder is entitled to trade in an underlying asset but is not obligated to do so at a pre-agreed price within a specified period of time. European call options offer the option holder the right to purchase the particular underlying asset, and the option can only be exercised at maturity.

In a multi-asset environment the balance between flexibility and tractability is very sensitive. The model should have enough flexibility to capture the features that are observable in actual option prices. In the case of several underlying assets, this may be a challenge since both the behavior of the individual assets and the joint behavior of the assets need to be taken into account. The need for mathematical structures to compute the option prices and the ability to calibrate the model to market prices is vital.

The multi-asset Black-Scholes model is one instance of a model used in pricing options whose underlying assets depend on one another (Bos and Ware, 2000). The model equations

are solved by making a substitution of the time-varying parameters with their constant averages. Another extension of the Black-Scholes model is the multi-dimensional Black-Scholes model where  $n$  assets are modelled using multi-dimensional geometric Brownian motion dynamics resulting in an approximate option price, (Carmona and Durrleman, 2006). The multi-dimensional Black-Scholes model assumes that options pay linear combinations of asset prices at maturity.

While the multi-asset Black-Scholes model pricing problem in a standard gaussian world may be already complex, the computation procedure is compounded by the significant evidence of variations from normality. Following the stock market crash in October 1987, variation in volatility has shown substantial deviations from normality, (Bernhardt and Eckblad, 2013). The downside of models used for pricing based on an inaccurate assumption of log-normality is the possibility of getting biased prices.

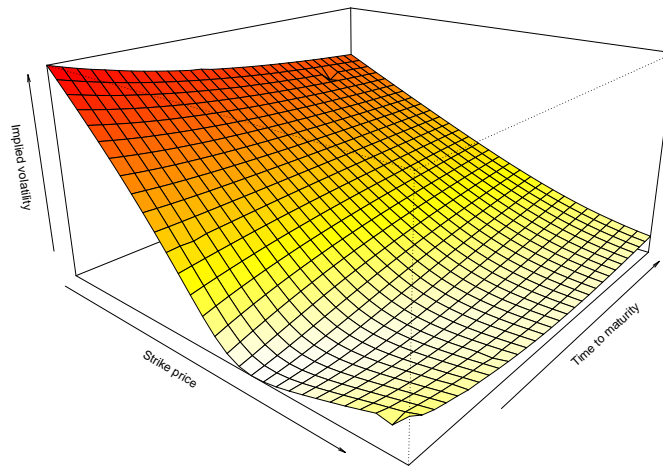


Figure 1: Volatility surface

Figure 1 illustrates the Black-Scholes model volatility surface. The main characteristic of the volatility surface is that options with a lower strike price tend to have a higher implied volatility. The volatility smile emerges from the fact that there are different implied volatilities for options with different strikes and maturities, (Wu and Elliott, 2017). The Black-Scholes assumption of constant volatility is invalidated by the volatility smile. However, it is inherently difficult to estimate stochastic volatility from historical data on asset returns because such states cannot be explicitly measured. Stochastic volatility models are often used to explain the dispersiveness of asset prices with respect to an underlying random

process, (Aït-Sahalia et al., 2020).

The multi-asset Heston model is an example of a stochastic volatility model that can capture multiple sources of risk, (Dimitroff et al., 2011; Gouriéroux and Sufana, 2010; Recchioni and Scoccia, 2014). It is an improvement on the multi-asset Black-Scholes model since it makes the stochastic volatility assumption. Furthermore, the model assumes that correlation exists between the underlying price of assets and volatility. The multi-asset Heston model is thus able to identify various characteristics of financial information which the multi-asset Black-Scholes model cannot. A multi-asset Heston model can be such that the single assets are affine Heston models, (Dimitroff et al., 2011).

However, since the assumptions about the variance process and the asset price process indicate an ad hoc nature, the reliability of the multi-asset Heston model is questionable. In addition, the model's variance process follows a Cox-Ingersoll-Ross process, (Cox et al., 1985). The multi-dimensional Black-Scholes model also shows an ad hoc nature by assuming that the asset prices follow an Ito process which is adapted to a filtration generated by multi-dimensional Brownian motions. This implies that the Brownian filtration in the models is seen to contain all relevant information and none that is irrelevant.

The Brownian filtration is pre-specified in the multi-asset extensions of the Black-Scholes model and the Heston model. In some aspects, this seems unsatisfactory because the Brownian filtration is generally considered to be cumulative information, learned over time evolution. In addition, the filtration does not take into account the nature of the information, and why this type of randomness provides useful information rather than noise is not clear. The arrival of any information relating to an expected cash flow from a particular asset is likely to have a substantial effect on the pricing decisions of the market traders. Due to this occurrence, this study looks at the information-based asset pricing framework which is based on Brody et al.'s asset pricing approach where the information available in the market is taken into account, (Brody et al., 2008; Macrina, 2006).

In financial markets, the most important factor in deciding the changes in the price of derivatives is the disclosure of financial information. Derivative prices change in reaction to the introduction of new information (whether real, partially true, false, or bogus) in the financial market, and they change again when the information is modified. The information-based asset pricing framework shows that asset price movements are in part due to the information on what the investor expects about the future cash flows associated with the asset and other information about the real value of the particular asset.

The information-based asset pricing framework will be studied based on the BS-BHM model proposed by Brody et al. and the BS-BHM updated model proposed by Mutijah et al., (Brody et al., 2008; Mutijah et al., 2012). The BS-BHM model is based on the

framework developed by Brody, Hughson and Macrina from a Black-Scholes perspective. A different result for the asset price process dynamics was later obtained by Mutijah et al. in their work which led to the authors coming up with the BS-BHM updated model.

The models adopt an incomplete information approach and the market information process is specified. An assumption is made that the market information process generates the market filtration from which the asset price dynamics are derived explicitly, (Brody et al., 2011). The information flow rate parameter is assumed to be constant. The models are inspired by the idea that, given the information circulating in the market, asset prices are determined by future cash flow expectations. The information-based asset pricing framework further assumes that market traders can only obtain partial noisy information about the associated cash flow.

The underlying asset price dynamics and volatility stochastic differential equations are not pre-specified in the information-based framework. In addition, the volatility process is seen to be stochastic, (Brody et al., 2008). Rather than imposing on the dynamics of volatility and the correlation model on the assets, the two are deduced from basic assumptions involving the related returns. The presence of an asset pricing kernel and the presence of an arbitrage-free market enable the use of a risk neutral probability measure,  $\mathbb{Q}$ , (Macrina and Parbhoo, 2010). This allows for risk-neutral pricing in the single asset case.

The aim of this study is to introduce and study a multi-asset extension of the information-based asset pricing framework from a Black-Scholes perspective. The notion of comonotonicity is used to obtain an approximate price for the multi-asset extension. Deelstra et al. and Dhaene et al., used the notion of comonotonicity on a basket option to obtain the price based on the Black-Scholes model, (Deelstra et al., 2004; Dhaene et al., 2020). With a suitable choice of parameter values, it is possible to derive the Black-Scholes model from the information-based framework. It is for this reason that the study finds an approach used for the Black-Scholes basket option to be suitable for pricing the multi-asset information-based framework. A lower bound and upper bound for the price is obtained using the notion of comonotonicity, this has been shown to be a useful tool in option pricing, (Chen et al., 2008).

In addition to using the theory of comonotonicity, this study examines a Wishart process-based multi-asset model that assumes stochastic volatility between the underlying assets, as well as between their volatilities. Gouriéroux and Sufana introduced the Wishart process into finance using a model where the process is used to describe the dynamics of the covariance matrix with the assumption that the asset price noises are independent, (Gouriéroux and Sufana, 2010). The study aims to develop multi-asset models which are tractable and in the one-dimensional case reduce to the corresponding single asset model.



A variance-in-mean effect is included in the asset price equation in the multi-asset model and the variance matrix is assumed to obey a Wishart process that is a multivariate extension of the CIR model. The CIR model is based on Wishart processes introduced by Bru which are able to capture the stochastic volatility and stochastic correlation between the underlying asset prices, (Bru, 1991). In the model, scalar variances are extended into covariance matrices as opposed to vectors of log-variances. The scale parameter underlying the conditional expectation of the asset covariance matrix in the Wishart distribution allows both correlations and variances to change with time stochastically.

Wishart processes have emerged as an efficient tool for modelling stochastic covariance structures. However, since they involve matrix processes, their numerical simulation may be difficult. Due to the flexibility of the models with a Wishart process in their system of dynamic equations, it makes it possible to have a better fit of the market data. The process allows the modelling of the dynamics of the volatilities and the evolution of co-volatilities. Risks in financial market are usually represented and measured by volatility and covalatility matrices. By modelling the dynamics of these matrices, Wishart processes can be used to analyse multivariate financial risk which makes them suitable to be used in risk management.

The asset price process and the volatility process which follows a Wishart process obtained in the multi-asset information-based framework are discretized to make the model suitable for numerical simulation. Various authors including Gauthier and Possamai have discretized multivariate stochastic volatility models, in particular the multifactor Heston model to obtain a simpler form that allows for numerical simulation, (Gauthier and Possamai, 2009). A multifactor Heston model consists of a single risky asset and several volatility processes which are assumed to be stochastic.

This study also looks at the estimation of parameters and measures parameter sensitivity using Greeks. Greeks are a series of risk measures that indicate the sensitivity of an option to time-value decay, variations in volatility, and price movements of its underlying security. They measure the sensitivity of derivative prices to variations in the parameters. This study looks at the following greeks: delta, gamma, vega, rho and theta.

The estimation of stochastic volatility from historical data on asset returns is inherently difficult because such states cannot be explicitly measured. In this study, a non linear filtering technique is used for the estimation of volatility in the multi-asset stochastic volatility models. In particular, the extended Kalman filter and particle filter also known as the sequential monte carlo approach are used. The state space model is first derived and for a specific discrete approximation of the model, a sequential method based on particle filters may be used estimate volatility.

## *1.2. Statement of the problem*

The information-based asset pricing framework observes the emergence of information, and its role as a driver of price dynamics is examined. The framework suggests a different approach aimed at improving the downside of the Black-Scholes and Heston models. In these two models, the Brownian filtration is considered to contain all the relevant information, and no irrelevant information. The unsatisfactory side of this approach is that it illustrates that the prices move as if they were spontaneous. However, in reality, a trend is expected in asset price processes.

The behaviors of investors is what forms the prices of assets when trading occurs. This study extends the information-based asset pricing model to the multi-asset case. This is because investors are becoming interested in investing in more than one asset due to the integration of financial markets. In addition, the options market is a constantly changing market which can allow investors to hedge and minimize the risk exposure of current positions. The traders and the hedgers would have to fully comprehend the option's Greeks to do so. Greeks indicate the sensitivity of the price of the option to a specific risk source. This study derives the Greeks under the information-based model.

### *1.3. Objectives of the study*

#### *1.3.1. General Objective*

The main objective of this work is to develop an appropriate model to be used in pricing derivatives incorporating the aspect of information in a multi-asset framework. The price of the derivative is constructed with a correlation between the underlying assets' price processes and the variance processes.

#### *1.3.2. Specific Objectives*

Specifically, the study aims;

**i) To derive a suitable model for option pricing in a multi-asset framework.**

In the derivatives market, it is observed that the implied volatility of options is not constant. This is because the volatility of an option at any moment is itself a stochastic quantity. An appropriate stochastic volatility model is obtained in the multi-asset framework.

**ii) To model the dynamics of an option pricing model where the variance process depends on time and information in a multi-asset framework.**

Asset prices change as time progresses. Asset price dynamics contain enough detail to specify the probability distributions of future prices. Previous studies have modelled the volatility without considering information. By adding information, this study improves on model accuracy in a multi-asset framework.

**iii) To price the derivative whose asset dynamics' volatility parameter depends on time and information in a multi-asset framework.**

Here, a Black-Scholes type formula for the price that is used to compute the value of a derivative in the multi-asset framework putting emphasis on analytic tractability is deduced.

**iv) To find the best estimates for the model parameters.**

A sensitivity analysis is performed to test the effect that a variation in the value of parameters has on the model. The sensitivity of the model in the multi-asset framework is investigated in regards to the information flow-rate parameter which is not known. This is necessary in determining the region in the space of the parameter for which an incorrect value of the flow-rate parameter yields significant errors in pricing of multi-asset European call options.

**v) To compare the volatility obtained in an asset where information is incorporated and that where information is fixed in a multi-asset framework.**

A comparison is done between the volatility in the pricing formula obtained under the multi-asset Heston model and multi-asset information-based asset pricing framework. By doing so, the study is able to determine the impact that information has on the asset price.

#### *1.4. Significance of the study*

Due to the globalization of financial markets, trading in several assets is becoming popular. This study obtains the price of a multi-asset option by incorporating the information available in the market. This improves on the existing asset pricing models as an investor is able to obtain the price of a multi-asset European option incorporating information.

Volatility has become a popular area of financial research, through the use of stochastic volatility models, the valuation actuary is able to obtain a closer match to the asset prices that are observed in the market. The risk control actuary is also able to identify the risk areas which may have been overlooked. By extending these models to the multi-asset case, better risk management practices will be adopted by financial institutions.

Options may also be used to hedge out risk in the financial markets. Speculators and hedgers often find it more attractive to trade in options rather than the underlying assets due to the reduced loss associated with options. As illustrated in the 2007-2008 recession, incorrect pricing of assets may result in a financial crisis which may eventually harm the overall economy. For a given initial deposit, options offer potentially higher returns since they can be traded on a higher leverage level compared to stocks.

## 2. Literature Review

The use of mathematics in financial modeling is attributed to Louis Bachelier dissertation that was based on speculation in markets in Paris, (Davis and Etheridge, 2006). However, studies on the behavior of assets over time found the equation proposed by Bachelier to be unsatisfactory as it allowed asset prices to be negative yet they were always observed to be positive.

Samuelson introduced the use of geometric Brownian motion in stock prices, (Samuelson, 1965). Samuelson used two parameters whose values were not known to denote the interest rate and the expected return. He discounted the expected value of the distribution taking into account all the possible values on maturity if the holder chooses to exercise it. This was later shown to be an inaccurate approach and an improvement was made by taking the option price to be a function of the asset price, (Samuelson et al., 1969). The resulting option pricing formula was shown to be dependent on the utility function curve that is assumed for a normal investor.

There was a major development in the field of financial economics in 1973 through Black and Scholes who derived a formula for option pricing, (Black and Scholes, 1973). Their work showed that if options are correctly priced, then arbitrage opportunities would not exist, that is, investors would not be guaranteed to make a profit by taking short or long positions in the underlying stocks and their options. The Black-Scholes model uses this as its basis in its option pricing framework.

Linders obtains an approximate price for a basket option using the theory of comonotonicity in a multivariate Black-Scholes model, (Linders, 2013). The basket option consists of underlying asset prices which have a lognormal distribution and are dependent on each other. An assumption is made of a structure of comonotonic dependence between the underlying asset prices. If they are all increasing or decreasing functions of the same random source, random variables are said to be comonotonic.

By making use of a synthetic share price, Linders obtains the basket option curve where the upper and lower bound obtained based on the notion of comonotonicity are combined to obtain an approximate price. It is shown that the first two moments of the option curve coincide with those of an actual basket option and a distribution can also be derived for this synthetic share price. He demonstrated that the dependence structure between the underlying assets plays a role in the price for a basket option.

The multivariate option pricing approach is regarded as a benchmark pricing approach for other extensions in the Black-Scholes model. The basket option is decomposed into a linear mix of one dimensional option prices for particular strike prices, (Chen et al., 2008). This results in a tractable model that is used to determine the upper and lower bounds for the

basket option price. The two bounds are then combined using an appropriately chosen weighting factor to give an approximate multivariate Black-Scholes model price.

The crucial assumption underlying the Black-Scholes model is that volatility is constant, (Black and Scholes, 1973). The second assumption is that the markets are efficient, which implies that people cannot consistently predict the market direction. In addition, it is assumed the underlying asset does not pay dividends on the option. In reality, a majority of companies pay their shareholders dividends. The original Black-Scholes model was later improved to include dividends, (Merton, 1973).

An assumption is also made regarding the interest rates; they are assumed to be constant and their value known; the risk-free rate is used to represent this rate. The model also assumed log-normally distributed asset prices which follow a geometric Brownian motion and European type of options which are only exercised on the expiry date. No transaction costs are incurred during the purchase of options and liquidity are also assumed.

In the real world, several of the assumptions that underlie the Black-Scholes model are violated to some extent, (Zuzana, 2018). Empirical studies illustrate that the constant volatility assumption made is not realistic (Blattberg and Gonedes, 1974; Scott, 1987). Hobson and Rogers introduced a class of models with non-constant volatility, (Hobson and Rogers, 1998). They propose the concept of stochastic volatility by expressing the volatility using exponentially-weighted moments of the historical log price. The paper does not introduce a new source of randomness as is done in other approaches, (Heston, 1993; Scott, 1987). This means that the market remains complete in the proposed model.

Ball and Torous illustrate that the correlation amongst financial quantities vary with time and are not stable, (Ball and Torous, 2000). In addition, Loretan and English show the presence of a connection between volatility and correlation, correlations amongst financial assets are seen to be high in periods of high volatility in the market, (Loretan and English, 2000). However, the price of options based on a number of assets are normally determined with the assumption of constant instantaneous correlations between assets.

The multi-asset Heston model assumes that volatility is stochastic which makes it an improvement to the multi-asset Black-Scholes model, (Gouriéroux and Sufana, 2010). It is an extension of the Heston model which is used in option pricing and is today among the most commonly utilized stochastic volatility models in the financial market, (Heston, 1993). The model depicts an alternative closed-form solution for determining option prices that aims at overcoming the weaknesses in the Black-Scholes model.

The Heston model allows for volatility to be stochastic which means that the volatility parameter has a stochastic process of its own. The Hull and White model is an example of a stochastic volatility model that was derived before the Heston model (Hull and White,

1987). In their original work, Hull and White analyzed their model and its predictions for option value using numerical methods to approximate the stochastic differential equation. The authors found that the prices obtained from the Black-Scholes model are often higher than the empirical price and the extent of this overpricing increases with an increase in time to maturity.

The assumptions underlying the Heston model include the following; the volatility of the underlying asset is itself a random variable, there are two Brownian motions: one for the underlying asset, and one for the variance; stochastic volatility models are thus two-factor models, the two processes are assumed to be correlated, the stochastic volatility is also assumed to be mean reverting, a frictionless market with no taxes or transaction costs is also assumed.

The extended Heston model demonstrates that highly reliable results for the price of European options can be obtained by the introduction of stochastic correlations, (Teng et al., 2018). This implies that stochastic correlations greatly improve the performance of the Heston model. The stochastic correlations are driven by stochastic differential equations. Monte Carlo simulation is used to simulate the price of the European call options.

Based on empirical evidence, Das et al., found that stochastic volatility models perform better than other models that can be used to model the volatility smile such as models that introduce jumps into the asset process, (Das et al., 1999). Despite stochastic volatility models outperforming the models that introduce jumps in the asset process, they noted that none of these models constituted an adequate explanation for volatility smiles.

In the models by Backus et al., it is shown that non-normality is allowed for by the introduction of kurtosis and skewness directly in the price of the option (David et al., 1997). It is shown that skewness can also be introduced in stochastic volatility models by allowing for correlation between the driving processes of the asset price stochastic differential equation and the volatility stochastic differential equation. A different approach of obtaining skewness by the introduction of jumps into the process that drives the underlying asset price is also illustrated by the authors.

The Heston model is extended to the multi-asset case by making use of Wishart processes. Wishart processes were first studied by Bru as an extension of square Bessel processes, Bru (1991). Bru realized that Wishart processes have a Wishart distribution which is a multivariate extension of the  $\chi^2$  distribution. A  $\chi^2$  distribution is derived from a sum of squares of independent standard normal random variables. The Wishart distribution plays a key role in the analysis of estimated covariance matrices. However, their numerical simulation can be difficult, because they make use of matrix processes.

Gourieroux assumes that the volatility matrix follows a Wishart autoregressive process in

the pricing of derivatives with multivariate stochastic volatility, (Gourieroux, 2006). The specification of the volatility matrix under this process is an extension of the CIR dynamic in the multivariate framework which ensures that the matrix is always positive, (Cox et al., 1985). Stochastic covariance structures can be efficiently modelled using Wishart processes. The Wishart process can be obtained from the CIR process by extending it to the multivariate case. Gourieroux shows that Wishart processes are ideal for modeling multivariate risk which arises in multi-asset options due to the dependence structure between the underlying assets. The author extends the CIR stochastic volatility model to the multi-asset case by considering a risk-free interest rate and two risky assets. A risk premium is introduced in the return equation and the stochastic volatility matrix process uses Wishart dynamics in the model.

The information-based asset pricing framework by Brody et al. is an improvement on the Black-Scholes model and Heston model which tend to be ad hoc, (Brody et al., 2008). The framework shows that fluctuations in asset prices are partially due to information on what the investor believes about the asset-related potential cash flows and other information on the actual value of the asset in question. This means that, as opposed to being an input into the transactions, the asset price should be an output of the decisions that affect the future transactions.

An incomplete information approach is adopted in the information-based asset pricing framework, this is contrary to the complete market assumption made by the Black-Scholes model, (Macrina, 2006). In a complete market, the information in the Brownian filtration is seen to be made up of only useful information and nothing that is not useful. The weakness of this approach is price movements happen as if they are random, which is contradictory to the fact that price changes have more structure. The market filtration in the information-based framework is assumed to be generated by the market information process. The dynamics for the asset price are then derived from the market filtration.

To make the multi-asset information-based model suitable for numerical simulation, it is discretized using an approach applied to the multifactor Heston model by Gauthier and Possamai and Kloeden and Platen, (Gauthier and Possamai, 2009; Kloeden and Platen, 1999). The Euler and Ornstein-Uhlenbeck are reviewed by the authors and a new discretization approach which is based in the Heston's Quadratic Exponential scheme is proposed, (Gauthier and Possamai, 2009). Empirical studies show that the proposed discretization approach is efficient in discretizing Wishart processes. A multifactor Heston model is made up of one risky asset and more than one variance process, (Da Fonseca et al., 2008).

Chen et al., price European call options and study Greek letters of options under a fuzzy environment by assuming that the asset return is a Gaussian fuzzy number, (Chen et al.,



2019). The sensitivity of call options to a parameter in the Heston model can be obtained by first-order and second-order derivatives of the in-the-money probabilities, (Rouah, 2013). A new Greek, omega is proposed to describe the influence of the skewness parameter on a new European call option price under a skew Brownian motion, (Zhu & He, 2017). Simulation can be effectively used as a valuable tool to estimate the options price derivatives, that is the Greeks under the Heston model where volatility is assumed to be stochastic, (Shafi et al., 2018).

Javaheri et al. define filtering as an iterative method that allows the estimation of the parameters of a model when the latter depends on a large amount of observable and unobservable data, (Javaheri et al., 2003). They present various filtering techniques which are used to obtain estimates for the stochastic volatility parameters from the underlying asset prices. In their study, an algorithm is constructed which includes a transition equation connecting two consecutive non-observable states and a measurement equation which relates this hidden state to the data observed. Empirical results based on the S&P500 time-series from 1996 to 2001 showed that the particle filter outperforms the other filters and that the extended Kalman filter becomes unreliable when the model becomes highly nonlinear.

Wang et al. use the consistent extended Kalman filter in the Heston model to estimate volatility by first discretizing the stochastic differential equations to make numerical simulation easier, (Wang et al., 2018). The extended Kalman filter linearizes the nonlinear equations in the model by making use of jacobian matrices, (Ewald et al., 2018). To compensate for the linearization error, the consistent extended Kalman filter is introduced so as to increase the accuracy of the estimation process.

Li et al. use particle filtering to estimate volatility in a stochastic volatility model in a discrete time framework (Li et al., 2015). Karamé uses several particle filters and a Hamilton filter to estimate unobserved state variables from stochastic volatility models, (Karamé, 2018). The particle filter is used to determine an estimate for the unobserved volatility and the hamilton filter reduces variation in the monte carlo estimates obtained. This study extends these approaches to the information-based asset pricing framework.

### 3. Multi-asset option pricing

#### 3.1. Modelling volatility in a multi-asset framework

In the derivatives market, it is observed that the volatility of option prices changes with time implying that the volatility of an option at any moment is itself stochastic. This invalidates the assumption of the Black-Scholes model that volatility is constant. An appropriate stochastic volatility model in this case the Heston model is examined. This work also shows that the Black-Scholes model can be obtained from the Heston model. The study first looks at the single asset model and then extends to the multi-asset case. The stochastic variance process in the multi-asset Heston model is assumed to follow a Wishart process.

##### 3.1.1. Asset pricing model with constant volatility

The Black-Scholes model is used to price options where volatility is assumed to be constant. The geometric Brownian motion shows the evolution of the price of assets over time. It has the following SDE:

$$dS_t = \mu S_t dt + \sigma S_t dW_t \quad (3.1.1)$$

where;

$t$  denotes the current time,

$W_t$  denotes a Weiner process or Brownian motion,

$S_t$  represents the current asset price,

$\mu$  is the drift term,

$\sigma$  denotes the asset price volatility.

Under  $\mathbb{Q}$ , the Black-Scholes model can be rewritten by substituting  $\mu$  with  $r$  in equation 3.1.1 as follows:

$$dS_t = r S_t dt + \sigma S_t dW_t \quad (3.1.2)$$

The European call price is as follows:

$$C_{BSMprice} = S_t \Phi(d_1) - K e^{-r(T-t)} \Phi(d_2) \quad (3.1.3)$$

where:

$$d_1 = \frac{\ln\left(\frac{S_t}{K}\right) + \left(r + \frac{1}{2}\sigma^2\right)(T-t)}{\sigma\sqrt{T-t}} \quad (3.1.4)$$

and

$$\begin{aligned} d_2 &= \frac{\ln\left(\frac{S_t}{K}\right) + \left(r - \frac{1}{2}\sigma^2\right)(T - t)}{\sigma\sqrt{T - t}} \\ &= d_1 - \sigma\sqrt{T - t} \end{aligned} \quad (3.1.5)$$

$K$  is the strike price,

$T$  is period to expiry,

$r$  is the risk-free rate of interest,

and

$$\Phi(x) = P[Z \leq x], \quad Z \sim N[0, 1]$$

Considering the multi-asset case with  $n$  assets, the asset price dynamics under  $\mathbb{Q}$  are given as:

$$dS_i(t) = rS_i(t)dt + \sigma_i S_i(t)dW_i(t)$$

for  $i = 1, 2, \dots, n$ .

There's correlation between  $dW_i$  and  $dW_j$  for  $i \neq j$  as follows:

$$E[dW_i(t)dW_j(t)] = \rho_{ij}dt$$

where the correlation coefficient is  $\rho_{ij}$ .

The price of the  $i^{th}$  asset is obtained as follows:

$$S_i(t) = S_i(0)e^{(r - \frac{1}{2}\sigma_i^2)t + \sigma_i dW_i(t)} \quad (3.1.6)$$

From equation 3.1.6, it follows that:

$$\log \frac{S_i(T)}{S_i(0)} \sim N\left(\left(r - \frac{1}{2}\sigma_i^2\right)T, \sigma_i^2 T\right) \quad (3.1.7)$$

Using the result in equation 3.1.7, the option price  $C_i[K, T]$  is given by:

$$C_i[K, T] = S_i(0)\Phi(d_{i,1}) - Ke^{-rT}\Phi(d_{i,2}) \quad (3.1.8)$$

where

$$d_{i,1} = \frac{\ln\left(\frac{S_i(0)}{K}\right) + \left(r + \frac{1}{2}\sigma_i^2\right)T}{\sigma_i\sqrt{T}} \quad (3.1.9)$$

and

$$\begin{aligned} d_{i,2} &= \frac{\ln\left(\frac{S_i(0)}{K}\right) + \left(r - \frac{1}{2}\sigma_i^2\right)T}{\sigma_i\sqrt{T}} \\ &= d_{i,1} - \sigma_i\sqrt{T} \end{aligned} \quad (3.1.10)$$

To obtain the price of the multi-asset Black-Scholes model with  $n$  underlying assets, the study proceeds as follows:

Let:

$$S(t) = \sum_{i=1}^n c_i S_i(t) \quad (3.1.11)$$

where  $c_i$  are constant nonnegative weights and  $S_i(t)$  denotes the  $i^{th}$  underlying asset.

An approximate value for the option price is obtained by combining the upper bound option price and the lower bound option price.

The upper bound option price is obtained as follows:

$$C^c[K] = e^{-rT} E_{\mathbb{Q}}[\max\{S^c - K, 0\}]$$

where:

$$S^c = c_1 F_{S_1}^{-1}(U) + \dots + c_n F_{S_n}^{-1}(U) \quad (3.1.12)$$

and  $U \sim U[0, 1]$ .

$$S^c = \sum_{i=1}^n c_i S_i(0) \exp\left[\left(r - \frac{\sigma_i^2}{2}\right)T + \sigma_i\sqrt{T}N^{-1}(U)\right]$$

Using the result from 3.1.7:

$$F_{S_i}^{-1}(p) = S_i(0) \exp\left[\left(r - \frac{\sigma_i^2}{2}\right)T + \sigma_i\sqrt{T}N^{-1}(p)\right] \quad (3.1.13)$$

The upper bound price is given as:

$$\begin{aligned} C^c[K] &= \sum_{i=1}^n c_i C_i[K_i^{*c}] \\ &= \sum_{i=1}^n c_i \left( S_i(0) \Phi(d_{i,1}^c) - K_i^{*c} e^{-rT} \Phi(d_{i,2}^c) \right) \end{aligned} \quad (3.1.14)$$

where

$$K_i^{*c} = S_i(0) \exp \left[ \left( r - \frac{\sigma_i^2}{2} \right) T + \sigma_i \sqrt{T} \phi^{-1} (F_{S^c}(K)) \right] \quad (3.1.15)$$

The value of  $F_{S^c}(K)$  is obtained from:

$$\sum_{i=1}^n c_i K_i^{*c} = K$$

and

$$d_{i,1}^c = \frac{\ln \left( \frac{S_i(0)}{K_i^{*c}} \right) + \left( r + \frac{1}{2} \sigma_i^2 \right) T}{\sigma_i \sqrt{T}}$$

$$d_{i,2}^c = d_{i,1}^c - \sigma_i \sqrt{T}$$

The lower bound price is as follows:

$$C^l[K] = e^{-rT} E_{\mathbb{Q}} [\max\{S^l - K, 0\}]$$

where:

$$S^l = \sum_{i=1}^n c_i \mathbb{E}[S_i | \Lambda]$$

and

$$\Lambda = \sum_{i=1}^n \lambda_i \ln \frac{S_i}{S_i(0)}$$

with  $\lambda_i > 0$  being given as:

$$\lambda_i = c_i S_i(0) e^{rT}$$

$$S^l = \sum_{i=1}^n c_i S_i(0) \exp \left[ \left( r - \frac{\sigma_i^2}{2} r_i^2 \right) T + r_i \sigma_i \sqrt{T} N^{-1}(U) \right]$$

The lower bound price is thus given as:

$$C^l[K] = \sum_{i=1}^n c_i e^{-rT} \mathbb{E} [\max(V_i - K_i^{*l}, 0)]$$

with:

$$V_i = S_i(0) \exp \left[ \left( r - \frac{\sigma_i^2}{2} r_i^2 \right) T + r_i \sigma_i \sqrt{T} N^{-1}(U) \right]$$

It follows that:

$$C^l[K] = \sum_{i=1}^n c_i(S_i(0)\Phi(d_{i,1}^l) - K_i^{*l}e^{-rT}\Phi(d_{i,2}^l)) \quad (3.1.16)$$

where

$$K_i^{*l} = S_i(0)\exp\left[\left(r - \frac{\sigma_i^2}{2}r_i^2\right)T + r_i\sigma_i\sqrt{T}N^{-1}(F_{S^l}(K))\right] \quad (3.1.17)$$

with

$$r_i = \frac{\sum_{j=1}^n \lambda_j \rho_{i,j} \sigma_j}{\sigma_\Lambda} \quad (3.1.18)$$

and

$$\sigma_\Lambda = \sqrt{\sum_{i=1}^n \lambda_i^2 \sigma_i^2 + 2 \sum_{i=1, j < i}^n \lambda_i \lambda_j \rho_{i,j} \sigma_i \sigma_j} \quad (3.1.19)$$

The value of  $F_{S^l}(K)$  is obtained from:

$$\sum_{i=1}^n c_i K_i^{*l} = K$$

and

$$d_{i,1}^l = \frac{\ln\left(\frac{S_i(0)}{K_i^{*l}}\right) + \left(r + \frac{1}{2}\sigma_i^2 r_i^2\right)T}{r_i \sigma_i \sqrt{T}}$$

$$d_{i,2}^l = d_{i,1}^l - r_i \sigma_i \sqrt{T}$$

A linear combination of the upper and lower bounds given by equation 3.1.14 and equation 3.1.16 respectively gives an approximate price as follows:

$$\begin{aligned} \bar{C}[K] &= e^{-rT} E_{\mathbb{Q}}[\max\{\bar{S} - K, 0\}] \\ &= zC^l[K] + (1-z)C^c[K] \quad \text{for all } K \geq 0. \end{aligned} \quad (3.1.20)$$

where  $0 \leq z \leq 1$ .

The cumulative distribution function  $F_{\bar{S}}$  of  $\bar{S}$  is given as:

$$F_{\bar{S}}(x) = zF_{S^l}(x) + (1-z)F_{S^c}(x), \quad \text{for all } x \in \mathbb{R}.$$

and

$$z = \frac{\mathbb{E}[u(S^c)] - \mathbb{E}[u(S)]}{\mathbb{E}[u(S^c)] - \mathbb{E}[u(S^l)]}$$

This implies that  $\mathbb{E}[u(\bar{S})] = \mathbb{E}[u(S)]$ .

where

$$u(x) = (x - \mathbb{E}[u(S)])^2$$

### 3.1.2. Asset pricing model with stochastic volatility

The Heston model is a popular stochastic volatility model where an assumption is made that the underlying asset price has a stochastic variance,  $V_t$ , that follows a CIR process. The model is represented by the following dynamic system of equations:

$$dS_t = rS_t dt + \sqrt{V_t} S_t dW_t^S \quad (3.1.21)$$

$$dV_t = \kappa(\theta - V_t) dt + \eta \sqrt{V_t} dW_t^\sigma \quad (3.1.22)$$

$$(dW_t^S dW_t^\sigma) = \rho dt$$

where  $\eta, \theta, \kappa$  are constants and  $\rho$  denotes the correlation coefficient.

The mean reversion of the variance process which is evident in the market is allowed for by the term  $\kappa(\theta - v)$ . The asset price is dependent on a drift and a variance, which is similar to the Black-Scholes model.

The Heston model's European call option price is as follows:

$$C_{Heston} = S_k e^{-q(\Delta k)} P_1 - K e^{-r(\Delta k)} P_2 \quad (3.1.23)$$

where  $P_j$  ( $j = 1, 2$ ) are the risk-adjusted probabilities of  $x_t = \ln(\frac{S_t}{S_{t-1}})$ .

$$P_j = \frac{1}{2} + \frac{1}{\pi} \int_0^\infty \text{Re} \frac{e^{-i\phi \ln K} f_j(\phi; x_k, V_k)}{i\phi} d\phi$$

for  $j = 1, 2$ .

The characteristic functions  $f_j(\phi; x_k, V_k)$  in the probabilities are given by:

$$f_j(\phi; x_k, V_k) = e^{i\phi \ln K + A_j(\phi, \Delta k) + B_j(\phi, \Delta k) V_k}$$

where

$$B_j(\phi, \Delta k) = \frac{b_j - \rho\sigma\phi i + d_j}{\sigma^2} \left[ \frac{1 - e^{d_j(\Delta k)}}{1 - g_j e^{d_j(\Delta k)}} \right]$$

$$A_j(\phi, \Delta k) = r\phi i(\Delta k) + \frac{a}{\sigma^2} \left[ (b_j - \rho\sigma\phi i + d_j) - 2\ln \left( \frac{1 - e^{d_j(\Delta k)}}{1 - g_j e^{d_j(\Delta k)}} \right) \right]$$

$$g_j = \frac{b_j - \rho\sigma\phi i + d_j}{b_j - \rho\sigma\phi i - d_j}$$

$$d_j = \sqrt{(\rho\sigma\phi i - b_j)^2 - \sigma^2(2u_j\phi i - \phi^2)}$$

and  $i = \sqrt{-1}$ ,  $\Delta k = T - k$ ,  $u_1 = \frac{1}{2}$ ,  $u_2 = -\frac{1}{2}$ ,  $a = \kappa\theta$ ,  $b_1 = \kappa - \rho\sigma$ ,  $b_2 = \kappa$  and  $\phi$  is called the integration variable or node.

The Black-Scholes model can be obtained from the Heston model by making use of the assumption of constant volatility. That is if  $V_t = \sigma^2$ , then equation 3.1.21 reduces to:

$$dS_t = rS_t dt + \sigma S_t dW_t^S \quad (3.1.24)$$

Equation 3.1.24 is the same equation for the Black-Scholes asset pricing model as given in equation 3.1.2 with  $dW_t^S = dW_t$ .

The Heston model can be extended to the multi-asset framework by making use of Wishart processes. Let  $\alpha \geq 0$ ,  $\lambda$  be a one-dimensional Brownian motion and  $x_0 \geq 0$ .

$$dZ_t = 2\sqrt{Z_t}d\lambda_t + \alpha dt, \quad X_0 = x_0 \quad (3.1.25)$$

A strong solution of equation 3.1.25 is called a square Bessel process with parameter  $\alpha$ . For the general Wishart process, let  $B_t^W$  be a matrix of standard Brownian motions in  $\mathbb{R}^{n \times n}$ ,  $\Omega, M, Q \in \mathbb{R}^{n \times n}$ , the Wishart stochastic differential equation is given by:

$$dX_t = [\Omega\Omega^\top + MX_t + X_tM^\top]dt + \sqrt{X_t}dB_t^WQ + Q^\top(dB_t^W)^\top\sqrt{X_t} \quad (3.1.26)$$

$Q$  denotes a matrix whose value determines the degree of variation in the state variable  $X$ ,  $M$  determines the speed at which the variable returns to its mean value, and

$$\Omega\Omega^\top = \beta Q^\top Q \quad (3.1.27)$$

where  $\beta, \beta > n-1$ , is an integer denoting the degrees of freedom determining the magnitude of the drift of  $Q^\top Q$  from zero.

Let  $\bar{S}_t$  be a vector of asset prices while  $\Sigma_t$  denotes the volatility matrix of  $n$  assets. Under



the multi-asset model, the SDEs are given by:

$$d \log \bar{S}_t = [\mu + (Tr(D_1 \Sigma_t), \dots, Tr(D_n \Sigma_t))^T] dt + \Sigma_t^{1/2} dW_t^s \quad (3.1.28)$$

$$d\Sigma_t = (\Omega \Omega^T + M \Sigma_t + \Sigma_t M^T) dt + \Sigma_t^{1/2} dW_t^\sigma Q + Q^T (dW_t^\sigma)^T \Sigma_t^{1/2} \quad (3.1.29)$$

where  $W_t^s$  is an  $n$ -dimensional vector and  $W_t^\sigma$  is an  $(n, n)$  matrix, the elements in both are independent standard Brownian motions. The volatility matrix,  $\Sigma_t$ , dynamics correspond to the continuous time Wishart autoregressive process. A volatility-in-mean effect is added to capture the tendency for the volatility and the asset prices moving together.

The Laplace transform of equation 3.1.29 is what is needed to solve the pricing equation for the European call option.

Considering the one-dimensional case, that is the case where  $n = 1$ , the equations 3.1.28 and 3.1.29 become:

$$d \log S_t = (\mu + \delta \sigma_t^2) dt + \sigma_t dW_t^s, \quad (3.1.30)$$

$$d(\sigma_t^2) = (w^2 + 2m\sigma_t^2) dt + 2q\sigma_t dW_t^\sigma \quad (3.1.31)$$

where  $\delta \sigma_t^2$  denotes the risk premium.

By setting  $V_t = \sigma_t^2$ ,  $w = \sqrt{\kappa \theta}$ ,  $m = -\frac{\kappa}{2}$  and  $q = \frac{\eta}{2}$ , the variance process in equation 3.1.31 is reduced to the Heston variance process represented by the dynamic equation 3.1.22.

To make the dynamic system represented in equation 3.1.28 and 3.1.29 suitable for numerical simulation, discretization is performed.

Ito's lemma is used to discretize the asset dynamic equation as follows:

$$d \ln(e^{-\mu t} \bar{S}_t) = \frac{\partial \ln(e^{-\mu t} \bar{S}_t)}{\partial t} dt + \frac{\partial \ln(e^{-\mu t} \bar{S}_t)}{\partial \bar{S}_t} d\bar{S}_t + \frac{1}{2} \frac{\partial^2 \ln(e^{-\mu t} \bar{S}_t)}{\partial \bar{S}_t^2} (d\bar{S}_t)^2$$

Rearranging equation 3.1.28:

$$d\bar{S}_t = \bar{S}_t [\mu + (Tr(D_1 \Sigma_t), \dots, Tr(D_n \Sigma_t))^T] dt + \bar{S}_t \Sigma_t^{1/2} dW_t^s \quad (3.1.32)$$

$$\begin{aligned} (d\bar{S}_t)^2 &= (\bar{S}_t)^2 \Sigma_t dt \\ \frac{\partial \ln(e^{-\mu t} \bar{S}_t)}{\partial t} &= -\mu, \quad \frac{\partial \ln(e^{-\mu t} \bar{S}_t)}{\partial \bar{S}_t} = \frac{1}{\bar{S}_t}, \quad \frac{\partial^2 \ln(e^{-\mu t} \bar{S}_t)}{\partial \bar{S}_t^2} = -\frac{1}{\bar{S}_t^2} \end{aligned}$$

$$\begin{aligned}
d\ln(e^{-\mu t}\bar{S}_t) &= -\mu dt + \frac{1}{S_t}d\bar{S}_t - \frac{1}{2\bar{S}_t^2}(d\bar{S}_t)^2 \\
d\ln(e^{-\mu t}\bar{S}_t) &= -\mu dt + \frac{1}{\bar{S}_t}\left(\bar{S}_t\left[r + (Tr(D_1\Sigma_t), \dots, Tr(D_n\Sigma_t))^\top\right]\right)dt + \Sigma_t^{1/2}dW_t^s - \frac{1}{2\bar{S}_t^2}(\bar{S}_t^2\Sigma_t dt) \\
d\ln(e^{-\mu t}\bar{S}_t) &= -\mu dt + \left(\mu + (Tr(D_1\Sigma_t), \dots, Tr(D_n\Sigma_t))^\top\right)dt + \Sigma_t^{1/2}dW_t^s - \frac{\Sigma_t dt}{2} \\
d\ln(e^{-\mu t}\bar{S}_t) &= (Tr(D_1\Sigma_t), \dots, Tr(D_n\Sigma_t))^\top dt + \Sigma_t^{1/2}dW_t^s - \frac{\Sigma_t}{2}dt \\
d[\ln(e^{-\mu t}\bar{S}_t)] &= (Tr(D_1\Sigma_t), \dots, Tr(D_n\Sigma_t))^\top dt + \Sigma_t^{1/2}dW_t^s - \frac{\Sigma_t}{2}dt \tag{3.1.33}
\end{aligned}$$

Integrating equation 3.1.33 over the interval  $[t, t + \Delta t]$  results in:

$$\begin{aligned}
\int_t^{t+\Delta t} d[\ln(e^{-\mu s}\bar{S}_s)] &= \int_t^{t+\Delta t} (Tr(D_1\Sigma_s), \dots, Tr(D_n\Sigma_s))^\top ds + \int_t^{t+\Delta t} \Sigma_s^{1/2}dW_s^s - \int_t^{t+\Delta t} \frac{\Sigma_s}{2}ds \\
\int_t^{t+\Delta t} d[\ln(e^{-\mu s}\bar{S}_s)] &= \ln(e^{-\mu(t+\Delta t)}\bar{S}_{(t+\Delta t)}) - \ln(e^{-\mu t}\bar{S}_t)
\end{aligned}$$

The predictor corrector scheme proposes to first handle the time integral in a centered manner, that is:

$$\begin{aligned}
\int_t^{t+\Delta t} (Tr(D_1\Sigma_s), \dots, Tr(D_n\Sigma_s))^\top ds &\approx \frac{\Delta t}{2}\left((Tr(D_1\Sigma_{t+\Delta t}), \dots, Tr(D_n\Sigma_{t+\Delta t}))^\top\right. \\
&\quad \left.+ (Tr(D_1\Sigma_t), \dots, Tr(D_n\Sigma_t))^\top\right) \\
\int_t^{t+\Delta t} \Sigma_s^{1/2}dW_s^s &\approx \sqrt{\Delta t}\sqrt{\Sigma_t}G
\end{aligned}$$

where  $G$  denotes a matrix of independent standard gaussian random variables.

$$\int_t^{t+\Delta t} \Sigma_s ds \approx \frac{\Delta t}{2}(\Sigma_{t+\Delta t} + \Sigma_t)$$

Thus, the following scheme is obtained:

$$\begin{aligned}
\log\left[\frac{e^{-\mu(t+\Delta t)}S_{t+\Delta t}}{e^{-\mu t}S_t}\right] &= \frac{\Delta t}{2}\left((Tr(D_1\Sigma_{t+\Delta t}), \dots, Tr(D_n\Sigma_{t+\Delta t}))^\top + (Tr(D_1\Sigma_t), \dots, Tr(D_n\Sigma_t))^\top\right) \\
&\quad + \sqrt{\Delta t}\sqrt{\Sigma_t}G - \frac{\Delta t}{4}(\Sigma_{t+\Delta t} + \Sigma_t) \tag{3.1.34}
\end{aligned}$$

Despite that the continuous-time process of the discounted price may be a martingale, the scheme given by equation 3.1.34 isn't. This implies that the discretized scheme for the asset price may not always be free of arbitrage.

The martingale correction modifies equation 3.1.34 to be such that:

$$\mathbb{E} \left[ e^{-\mu\Delta t} \bar{S}_{t+\Delta t} | \bar{S}_t \right] = \bar{S}_t$$

It follows that:

$$\begin{aligned} \exp \left[ \log \left[ \frac{e^{-\mu(t+\Delta t)} \bar{S}_{t+\Delta t}}{e^{-\mu t} \bar{S}_t} \right] \right] &= \exp \left[ \frac{\Delta t}{2} \left( (Tr(D_1 \Sigma_{t+\Delta t}), \dots, Tr(D_n \Sigma_{t+\Delta t}))^\top \right. \right. \\ &\quad \left. \left. + (Tr(D_1 \Sigma_t), \dots, Tr(D_n \Sigma_t))^\top \right) \right. \\ &\quad \left. + \sqrt{\Delta t} \sqrt{\Sigma_t} G - \frac{\Delta t}{4} (\Sigma_{t+\Delta t} + \Sigma_t) \right] \\ \left[ \frac{e^{-\mu(t+\Delta t)} \bar{S}_{t+\Delta t}}{e^{-\mu t} \bar{S}_t} \right] &= \left[ \frac{e^{-\mu\Delta t} \bar{S}_{t+\Delta t}}{\bar{S}_t} \right] \\ e^{-\mu\Delta t} \bar{S}_{t+\Delta t} &= \bar{S}_t \exp \left[ \frac{\Delta t}{2} \left( (Tr(D_1 \Sigma_{t+\Delta t}), \dots, Tr(D_n \Sigma_{t+\Delta t}))^\top \right. \right. \\ &\quad \left. \left. + (Tr(D_1 \Sigma_t), \dots, Tr(D_n \Sigma_t))^\top \right) + \sqrt{\Delta t} \sqrt{\Sigma_t} G - \frac{\Delta t}{4} (\Sigma_{t+\Delta t} + \Sigma_t) \right] \\ \mathbb{E} \left[ e^{-\mu\Delta t} \bar{S}_{t+\Delta t} | \bar{S}_t \right] &= \mathbb{E} \left[ \mathbb{E} \left[ e^{-r\Delta t} \bar{S}_{t+\Delta t} | \bar{S}_t, V_{t+\Delta t} \right] \right] \\ &= \bar{S}_t \exp \left( -\frac{\Delta t}{4} \Sigma_t \right) \mathbb{E} \left[ \exp \left( -\frac{\Delta t}{4} (\Sigma_{t+\Delta t}) \right) \times \mathbb{E}_t \left[ \exp \left[ \sqrt{\Delta t} \sqrt{\Sigma_t} G \right. \right. \right. \\ &\quad \left. \left. + \frac{\Delta t}{2} \left( (Tr(D_1 \Sigma_{t+\Delta t}), \dots, Tr(D_n \Sigma_{t+\Delta t}))^\top \right) \right. \right. \\ &\quad \left. \left. + (Tr(D_1 \Sigma_t), \dots, Tr(D_n \Sigma_t))^\top \right) | \Sigma_{t+\Delta t} \right] \\ &= \bar{S}_t \exp \left( -\frac{\Delta t}{4} \Sigma_t \right) \mathbb{E} \left[ \exp \left( -\frac{\Delta t}{4} (\Sigma_{t+\Delta t}) \right) \times \right. \\ &\quad \left. \mathbb{E}_t \left[ \exp \left( \sqrt{\Delta t} \sqrt{\Sigma_t} G \right) | \Sigma_{t+\Delta t} \right] \right. \\ &\quad \left. \mathbb{E}_t \left[ \exp \left( \frac{\Delta t}{2} \left( (Tr(D_1 \Sigma_{t+\Delta t}), \dots, Tr(D_n \Sigma_{t+\Delta t}))^\top \right) \right. \right. \right. \\ &\quad \left. \left. + (Tr(D_1 \Sigma_t), \dots, Tr(D_n \Sigma_t))^\top \right) | \Sigma_{t+\Delta t} \right] \right] \end{aligned}$$

$$\mathbb{E}_t \left[ \exp(\sqrt{\Delta t} \sqrt{\Sigma_t} G) | \Sigma_{t+\Delta t} \right] = \exp\left(\frac{\Delta t \Sigma_t}{2}\right)$$

$$\begin{aligned} \mathbb{E}_t \left[ \exp\left(\frac{\Delta t}{2} \left( (Tr(D_1 \Sigma_{t+\Delta t}), \dots, Tr(D_n \Sigma_{t+\Delta t}))^\top + (Tr(D_1 \Sigma_t), \dots, Tr(D_n \Sigma_t))^\top \right) \middle| \Sigma_{t+\Delta t} \right) \right] \\ = \exp\left(\frac{\Delta t}{2} \left( (Tr(D_1 \Sigma_{t+\Delta t}), \dots, Tr(D_n \Sigma_{t+\Delta t}))^\top + (Tr(D_1 \Sigma_t), \dots, Tr(D_n \Sigma_t))^\top \right) \right) \end{aligned}$$

$$\begin{aligned} \mathbb{E} \left[ e^{-\mu \Delta t} \bar{S}_{t+\Delta t} | \bar{S}_t \right] &= \bar{S}_t \exp\left(-\frac{\Delta t}{4} \Sigma_t + \frac{\Delta t}{2} (Tr(D_1 \Sigma_t), \dots, Tr(D_n \Sigma_t))^\top\right) \\ &\quad \mathbb{E} \left[ \exp\left(-\frac{\Delta t}{4} (\Sigma_{t+\Delta t}) + \left(\frac{\Delta t \Sigma_t}{2}\right) \right. \right. \\ &\quad \left. \left. + \left(\frac{\Delta t}{2} \left( (Tr(D_1 \Sigma_{t+\Delta t}), \dots, Tr(D_n \Sigma_{t+\Delta t}))^\top \right. \right. \right. \right. \\ &\quad \left. \left. \left. + (Tr(D_1 \Sigma_t), \dots, Tr(D_n \Sigma_t))^\top \right) \right) \middle| \Sigma_t \right] \\ &= \bar{S}_t \exp\left(\frac{\Delta t}{4} \Sigma_t + \frac{\Delta t}{2} (Tr(D_1 \Sigma_t), \dots, Tr(D_n \Sigma_t))^\top\right) \\ &\quad \mathbb{E} \left[ \exp\left(-\frac{\Delta t}{4} (\Sigma_{t+\Delta t}) + \left(\frac{\Delta t}{2} \left( (Tr(D_1 \Sigma_{t+\Delta t}), \dots, Tr(D_n \Sigma_{t+\Delta t}))^\top \right) \right) \right) \middle| \Sigma_t \right] \end{aligned}$$

Let

$$M = \mathbb{E} \left[ \exp\left(-\frac{\Delta t}{4} (\Sigma_{t+\Delta t}) + \left(\frac{\Delta t}{2} \left( (Tr(D_1 \Sigma_{t+\Delta t}), \dots, Tr(D_n \Sigma_{t+\Delta t}))^\top \right) \right) \right) \middle| \Sigma_t \right]$$

If the scheme in equation 3.1.34 is modified as follows:

$$\begin{aligned} \log \left[ \frac{e^{-\mu(t+\Delta t)} \bar{S}_{t+\Delta t}}{e^{-\mu t} \bar{S}_t} \right] &= -\log M - \frac{\Delta t}{2} \left( Tr(D_1 \Sigma_t), \dots, Tr(D_n \Sigma_t) \right)^\top - \frac{\Delta t}{4} \Sigma_t \\ &\quad + \frac{\Delta t}{2} \left( (Tr(D_1 \Sigma_{t+\Delta t}), \dots, Tr(D_n \Sigma_{t+\Delta t}))^\top + (Tr(D_1 \Sigma_t), \dots, Tr(D_n \Sigma_t))^\top \right) \\ &\quad + \sqrt{\Delta t} \sqrt{\Sigma_t} G - \frac{\Delta t}{4} (\Sigma_{t+\Delta t} + \Sigma_t) \end{aligned} \quad (3.1.35)$$

then the martingale condition would be satisfied.

To discretize the variance process, integrating equation 3.1.29, over the interval  $[t, t + \Delta t]$

yields:

$$\begin{aligned} \int_t^{t+\Delta t} d\Sigma_s &= \int_t^{t+\Delta t} (\Omega\Omega^\top + M\Sigma_s + \Sigma_s M^\top) ds + \int_t^{t+\Delta t} \Sigma_s^{1/2} dW_s^\sigma Q \\ &\quad + \int_t^{t+\Delta t} Q^\top (dW_s^\sigma)^\top \Sigma_s^{1/2} \end{aligned} \quad (3.1.36)$$

An approximation to equation 3.1.36 is done using a slightly modified Euler scheme as follows:

$$\begin{aligned} \int_t^{t+\Delta t} d\Sigma_s &= \int_t^{t+\Delta t} \Omega\Omega^\top ds + \int_t^{t+\Delta t} M\Sigma_s ds + \int_t^{t+\Delta t} \Sigma_s M^\top ds + \int_t^{t+\Delta t} \Sigma_s^{1/2} dW_s^\sigma Q \\ &\quad + \int_t^{t+\Delta t} Q^\top (dW_s^\sigma)^\top \Sigma_s^{1/2} \end{aligned}$$

$$\int_t^{t+\Delta t} d\Sigma_s \approx \Sigma_{t+\Delta t} - \Sigma_t$$

$$\int_t^{t+\Delta t} \Omega\Omega^\top ds \approx \Delta t \Omega\Omega^\top$$

$$\int_t^{t+\Delta t} M\Sigma_s ds \approx \Delta t M\Sigma_t$$

$$\int_t^{t+\Delta t} \Sigma_s M^\top ds \approx \Delta t M^\top \Sigma_t$$

$$\int_t^{t+\Delta t} \sqrt{\Sigma_s} dW_s^\sigma Q \approx \sqrt{\Delta t} \sqrt{\Sigma_t} G Q$$

$$\int_t^{t+\Delta t} Q^\top (dW_s^\sigma)^\top \sqrt{\Sigma_s} \approx Q^\top G^\top \sqrt{\Delta t} \sqrt{\Sigma_t}$$

$$\Sigma_{t+\Delta t} = \Sigma_t + \Delta t \Omega\Omega^\top + \Delta t M\Sigma_t + \Delta t M^\top \Sigma_t + \sqrt{\Delta t} \sqrt{\Sigma_t} G Q + Q^\top G^\top \sqrt{\Delta t} \sqrt{\Sigma_t}$$

Thus:

$$\Sigma_{t+\Delta t} = \Sigma_t + \left( \Omega\Omega^\top + M\Sigma_t + M^\top \Sigma_t \right) \Delta t + \sqrt{\Delta t} \sqrt{\Sigma_t} G Q + Q^\top G^\top \sqrt{\Delta t} \sqrt{\Sigma_t} \quad (3.1.37)$$

Equation 3.1.37 is referred to as a discretized Wishart process and can be used to simulate  $\Sigma$  for any fixed step size  $\Delta t > 0$ . This process can become negative definite since the square root is no longer well defined. A solution to this problem is to make use of the full truncation scheme which involves taking the positive value of the variance denoted by  $\Sigma_t^+$ ,

that is  $\Sigma_t^+ = \max(0, \Sigma_t)$ . Thus:

$$\begin{aligned} \Sigma_{t+\Delta t} = \Sigma_t + & \left( \Omega\Omega^\top + (\Sigma_t)^+ M + M^\top (\Sigma_t)^+ \right) \Delta t + \sqrt{(\Sigma_t)^+} G Q \sqrt{\Delta t} \\ & + Q^\top G^\top \sqrt{\Delta t} \sqrt{(\Sigma_t)^+} \end{aligned} \quad (3.1.38)$$

Equation 3.1.38 can be written as:

$$\begin{aligned} \Sigma_{t+\Delta t} = \Sigma_t + & \left( \beta Q Q^\top + (\Sigma_t)^+ M + M^\top (\Sigma_t)^+ \right) \Delta t + \sqrt{(\Sigma_t)^+} G Q \sqrt{\Delta t} \\ & + Q^\top G^\top \sqrt{\Delta t} \sqrt{(\Sigma_t)^+} \end{aligned} \quad (3.1.39)$$

The price of an option written on  $\log \bar{S}_t$  and  $\Sigma_t$  can be obtained as follows:

$$C_{\log \bar{S}_t, \Sigma_t}(t, \zeta, h) = e^{-rh} \exp \left[ \zeta^\top \log S_t + \text{Tr}(A(h) \Sigma_t) + c(h) \right]$$

where:

$$A(h) = (\varphi A_2^1(h) + A_2^2(h))^{-1} (\varphi A_1^1(h) + A_1^2(h))$$

with

$$\begin{pmatrix} A_1^1(h) & A_1^2(h) \\ A_2^1(h) & A_2^2(h) \end{pmatrix} = e^h \begin{pmatrix} M + Q^\top \rho \zeta^\top & -2Q^\top Q \\ \frac{1}{2}(\zeta \zeta^\top - \sum_{i=1}^n \zeta_i D_i) & -(M^\top + \zeta \rho^\top Q) \end{pmatrix}$$

and

$$c(h) = -\frac{\beta}{2} \text{Tr} \left[ \log(\varphi A_2^1(h) + A_2^2(h)) + h M^\top + h \zeta (\rho^\top Q) \right] + hr(\zeta^\top I - 1)$$

$A(0) = \varphi$ ,  $b(0) = \zeta$  and  $c(0)=0$ .

### 3.2. Dynamics of an option pricing model where the variance process depends on time and information in a multi-asset framework

Here, the asset price process dynamics and the variance process dynamics for the information-based framework are looked at and the derivation is extended to the multi-asset case.

#### 3.2.1. Information-based asset pricing framework model dynamics

The information-based model is modelled under the probability space  $(\Omega, \mathcal{F}, \mathbb{Q})$ .  $\mathcal{F}_t$  denotes the market filtration.

An assumption is made on the presence of an existing kernel for pricing which is assumed to be adapted to  $\mathcal{F}_t$  and that the market is free of arbitrage opportunities. Arbitrage opportunities exploit the price difference between two markets to make a profit. These assumptions allow for the use of a risk neutral measure.

A return,  $X_T$ , that is expected to happen at time  $T$  is considered. The value of  $X_T$  will only be known at maturity and at current time,  $t$ , it's value is given as follows:

$$S_t = P_{tT} \mathbb{E}[X_T | \mathcal{F}_t] \quad (3.2.1)$$

where  $P_{tT}$  denotes the discount factor.

Equation 3.2.1 is the discounted conditional expectation of  $X_T$  under  $\mathbb{Q}$ . An assumption is made that a given quantity of partial information that relates to the value of the return is available at an earlier period of time.

The asset price is determined by the expectation of discounted returns involved, subject to the information available. By making use of a Brownian bridge, it is possible to create explicit formulas, and semi-analytical terms for derivative prices.

To ensure that the market information process reveals the value of the return at maturity, it is taken to be a function of the return, that is:

$$\xi_t = f(X_T)$$

Prior to maturity,  $\xi_t$  contains only partial information relating to the return.

The market information process denoted by  $\{\xi_t\}_{0 \leq t \leq T}$  is given by:

$$\xi_t = \gamma t X_T + \beta_{tT} \quad (3.2.2)$$

where  $X_T \sim N[0, 1]$ .

The information process given in equation 3.2.2 has two terms; the first term,  $\gamma t X_T$  is the market signal which contains the true market information, and the second term,  $\beta_{tT}$  denotes

the market noise.

$\{\beta_{tT}\}_{0 \leq t \leq T}$  is a  $\mathbb{Q}$  Brownian bridge over the interval  $[0, T]$  with  $\beta_{0T} = 0$  and  $\beta_{TT} = 0$ . It follows that:

$$E[\beta_{tT}] = 0$$

and

$$Var[\beta_{tT}] = \frac{t(T-t)}{T}$$

A Brownian bridge is used to represent market noise because at the beginning, all the market information is used in asset pricing but as time goes by, new information is revealed and this is accounted for by increasing the variance of the bridge for the first half of its trajectory.

When the return value is revealed at maturity, the variance value is equal to 0. The information flow rate parameter,  $\gamma$  denotes the speed with which the true value of  $X_T$  is revealed. If it is low, then it implies that the value of  $X_T$  is hidden until almost at maturity while if the value of  $\gamma$  is high, then, the value of the return is revealed quickly.

An assumption is made that  $X_T$  and the Brownian bridge are independent. It follows that:

$$\beta_{tT} = W_t - \frac{t}{T}W_T$$

Thus:

$$\beta_{tT} \sim N\left(0, \frac{t(T-t)}{T}\right)$$

The information about the real value of  $X_T$  will increase steadily, as this happens, the masking factors will also initially increase in value but will in the long run vanish as the maturity date nears.

$\beta_{tT}$  is not adapted to the market filtration process. Thus,  $\beta_{tT}$  can be seen as representing speculation, rumour, overreaction or any other misrepresentation that may occur relating to financial transactions.

The dynamics of the asset price process satisfies the following SDE;

$$dS_t = r_t S_t dt + \Gamma_{tT} dW_t$$

In this study, an assumption will be made that  $r_t$  which denotes the interest rate at time  $t$  is a constant implying that  $r_t = r$ . Thus;

$$dS_t = r S_t dt + \Gamma_{tT} dW_t \tag{3.2.3}$$



where:

$$\Gamma_{tT} = P_{tT} \frac{\gamma T}{T-t} V_t \quad (3.2.4)$$

and  $V_t$  denotes the conditional variance of  $X_T$ .

Let:

$$\begin{aligned} X_{tT} &= \mathbb{E}[X_T/\xi_t] \\ &= \int_0^\infty x \pi_t(x) dx \end{aligned}$$

where  $\pi_t(x)$  denotes the conditional probability density for the random variable  $X_T$  such that:

$$\begin{aligned} \pi_t(x) &= \frac{d}{dx} \mathbb{Q}[X_T \leq x/\xi_t] \\ d\pi_t(x) &= \frac{\gamma T}{T-t} (x - X_{tT}) \pi_t(x) dZ_t^\pi \end{aligned}$$

where  $Z_t^\pi$  denotes a Brownian motion.

Since  $V_t$  is the conditional variance, its value depends on the market information process at time  $t$ , that is:

$$\begin{aligned} V_t &= \mathbb{E}[(X_T/\xi_t - \mathbb{E}[X_T/\xi_t])^2] \\ &= \mathbb{E}[(X_T/\xi_t)^2] - (\mathbb{E}[X_T/\xi_t])^2 \\ &= \int_0^\infty x^2 \pi_t(x) dx - X_{tT}^2 \end{aligned} \quad (3.2.5)$$

The process  $\{W_t\}_{0 \leq t \leq T}$  is given as:

$$W_t = \xi_t - \int_0^t \frac{1}{T-s} (\gamma T X_{sT} - \xi_s) ds \quad (3.2.6)$$

Differentiating both sides of equation 3.2.6 with respect to  $t$  gives:

$$dW_t = d\xi_t - \frac{1}{T-t} (\gamma T X_{tT} - \xi_t) dt \quad (3.2.7)$$

By rearranging equation 3.2.7, the SDE for the market information process is as follows:

$$d\xi_t = \frac{1}{T-t} (\gamma T X_{tT} - \xi_t) dt + dW_t \quad (3.2.8)$$

The SDE for  $X_{tT}$  is given as:

$$dX_{tT} = \frac{\gamma T}{T-t} V_t \left[ \frac{1}{T-t} (\xi_t - \gamma T X_{tT}) dt + d\xi_t \right] \quad (3.2.9)$$

Rearranging equation 3.2.9 leads to:

$$dX_{tT} = \frac{\gamma T}{T-t} V_t \left[ d\xi_t - \frac{1}{T-t} (\gamma T X_{tT} - \xi_t) dt \right]$$

Thus:

$$dX_{tT} = \frac{\gamma T}{T-t} V_t dW_t$$

$V_t$  is a function of  $\pi_t(x)$  and  $X_{tT}$ . Applying Ito's lemma to equation 3.2.5 gives:

$$dV_t = \frac{\partial V_t}{\partial \pi_t(x)} d\pi_t(x) + \frac{\partial V_t}{\partial X_{tT}} dX_{tT} + \frac{1}{2} \frac{\partial^2 V_t}{\partial X_{tT}^2} (dX_{tT})^2$$

$$\begin{aligned} \frac{\partial V_t}{\partial \pi_t(x)} &= \int_0^\infty x^2 dx, & \frac{\partial V_t}{\partial X_{tT}} &= -2X_{tT}, & \frac{\partial^2 V_t}{\partial X_{tT}^2} &= -2 \\ (dX_{tT})^2 &= \left( \frac{\gamma T}{T-t} V_t dW_t \right)^2 \\ &= \left( \frac{\gamma T}{T-t} \right)^2 V_t^2 dt \end{aligned}$$

$$dV_t = \left( \int_0^\infty x^2 dx \right) d\pi_t(x) + (-2X_{tT}) dX_{tT} + \frac{1}{2} (-2) (dX_{tT})^2$$

$$\begin{aligned}
dV_t &= \left( \int_0^\infty x^2 dx \right) \left( \frac{\gamma T}{T-t} (x - X_{tT}) \pi_t(x) dW_t \right) + (-2X_{tT}) \left( \frac{\gamma T}{T-t} V_t dW_t \right) + \frac{1}{2} (-2) \left( \frac{\gamma T}{T-t} \right)^2 V_t^2 dt \\
&= \left( \frac{\gamma T}{T-t} \int_0^\infty x^2 dx \right) \left( (x - X_{tT}) \pi_t(x) dW_t \right) - 2X_{tT} \left( \frac{\gamma T}{T-t} V_t dW_t \right) - \left( \frac{\gamma T}{T-t} \right)^2 V_t^2 dt \\
&= \left( \frac{\gamma T}{T-t} \int_0^\infty x^2 dx \right) \left( (x \pi_t(x) dW_t - X_{tT} \pi_t(x) dW_t) \right) - 2X_{tT} \left( \frac{\gamma T}{T-t} V_t dW_t \right) - \left( \frac{\gamma T}{T-t} \right)^2 V_t^2 dt \\
&= \left( \frac{\gamma T}{T-t} \left( \int_0^\infty x^3 \pi_t(x) dx - X_{tT} \int_0^\infty x^2 \pi_t(x) dx \right) dW_t \right) - 2X_{tT} \left( \frac{\gamma T}{T-t} V_t dW_t \right) - \left( \frac{\gamma T}{T-t} \right)^2 V_t^2 dt \\
&= \left( \frac{\gamma T}{T-t} \left( \int_0^\infty x^3 \pi_t(x) dx - X_{tT} \int_0^\infty x^2 \pi_t(x) dx \right) dW_t \right) \\
&\quad - 2X_{tT} \left( \frac{\gamma T}{T-t} \left( \int_0^\infty x^2 \pi_t(x) dx - X_{tT}^2 \right) dW_t \right) - \left( \frac{\gamma T}{T-t} \right)^2 V_t^2 dt \\
&= \left( \frac{\gamma T}{T-t} \left( \int_0^\infty x^3 \pi_t(x) dx - X_{tT} \int_0^\infty x^2 \pi_t(x) dx \right) dW_t \right) \\
&\quad - 2 \left( \frac{\gamma T}{T-t} X_{tT} \int_0^\infty x^2 \pi_t(x) dx + 2X_{tT}^3 \right) dW_t - \left( \frac{\gamma T}{T-t} \right)^2 V_t^2 dt \\
&= \left( \frac{\gamma T}{T-t} \left( \int_0^\infty x^3 \pi_t(x) dx - X_{tT} \int_0^\infty x^2 \pi_t(x) dx \right. \right. \\
&\quad \left. \left. - 2X_{tT} \int_0^\infty x^2 \pi_t(x) dx + 2X_{tT}^3 \right) dW_t \right) - \left( \frac{\gamma T}{T-t} \right)^2 V_t^2 dt \\
&= \left( \frac{\gamma T}{T-t} \left( \int_0^\infty x^3 \pi_t(x) dx - 3X_{tT} \int_0^\infty x^2 \pi_t(x) dx + 2X_{tT}^3 \right) dW_t \right) - \left( \frac{\gamma T}{T-t} \right)^2 V_t^2 dt
\end{aligned}$$

Let

$$\begin{aligned}
\kappa_t &= \mathbb{E}[(X_T - \mathbb{E}[X_T])^3] \\
&= \int_0^\infty x^3 \pi_t(x) dx - 3X_{tT} \int_0^\infty x^2 \pi_t(x) dx + 2X_{tT}^3
\end{aligned}$$

Thus

$$dV_t = \left( \frac{\gamma T}{T-t} \kappa_t dW_t \right) - \left( \frac{\gamma T}{T-t} \right)^2 V_t^2 dt$$

The deterministic nonnegative process  $\{g_t\}_{0 \leq t \leq T}$  is defined by:

$$g_t = \gamma_t + \frac{1}{T-t} \int_0^t \gamma_s ds$$

If  $\gamma$  is a constant, then:

$$g_t = \frac{\gamma T}{T-t} \quad (3.2.10)$$

The dynamics for  $V_t$  are therefore given as:

$$dV_t = -g_t^2 V_t^2 dt + g_t \kappa_t dW_t \quad (3.2.11)$$

### 3.2.2. Multi-asset information-based asset pricing framework model dynamics

**Proposition 3.1.** *The joint dynamics of  $\bar{S}_t$  and  $\Sigma_t$  under the multi-asset model are given by:*

$$d\bar{S}_t = [r\bar{S}_t + (Tr(D_1\Sigma_t), \dots, Tr(D_n\Sigma_t))^T] dt + P_{tT} g_t \Sigma_t dW_t^S \quad (3.2.12)$$

$$d\Sigma_t = (\Omega\Omega^T + M\Sigma_t + \Sigma_t M^T) dt + \sqrt{\Sigma_t} dW_t^\sigma Q + Q^T (dW_t^\sigma)^T \sqrt{\Sigma_t} \quad (3.2.13)$$

where  $W_t^S$  is an  $n$ -dimensional vector and  $W_t^\sigma$  is an  $(n, n)$  matrix. The elements in both are independent unidimensional standard Brownian motions.  $r$  is a constant  $n$ -dimensional vector denoting the risk-free rate of interest,  $D_i$ ,  $i = 1, \dots, n$ ,  $\Omega$ ,  $M$ ,  $Q$  are  $(n, n)$  matrices with  $\Omega$  invertible.  $P_{tT}$  and  $g_t$  are both  $n$ -dimensional vectors.

*Proof.* Using Ito's lemma, it is shown that the variance process for the information-based asset pricing framework takes a similar form to the square Bessel process which is the one dimensional Wishart process.

Substituting for the value of  $\Gamma_{tT}$  given by equation 3.2.4 and  $g_t$  given by equation 3.2.10, the asset price dynamics given by equation 3.2.3 can be rewritten as:

$$dS_t = rS_t dt + P_{tT} g_t V_t dW_t \quad (3.2.14)$$

The dynamics for the variance process are as given in equation 3.2.11.

Let  $\beta_t$  denote the coefficient of skewness at time  $t$  such that:

$$\beta_t = \frac{\kappa_t}{V_t^{3/2}}$$

Substituting for  $\kappa_t$  in equation 3.2.11 gives:

$$dV_t = -g_t^2 V_t^2 dt + g_t \beta_t V_t^{3/2} dW_t \quad (3.2.15)$$

Using Ito's lemma, let  $X_t = V_t^{-1}$ , the following result is obtained:

$$dX_t = \frac{\partial X_t}{\partial t} dt + \frac{\partial X_t}{\partial V_t} dV_t + \frac{1}{2} \frac{\partial^2}{\partial V_t^2} (dV_t)^2$$

$$\frac{\partial X_t}{\partial t} = 0, \quad \frac{\partial X_t}{\partial V_t} = -V_t^{-2}, \quad \frac{\partial^2 X_t}{\partial V_t^2} = 2V_t^{-3}$$

$$(dV_t)^2 = \beta_t^2 v_t^2 V_t^3 dt$$

$$\begin{aligned} dX_t &= -V_t^{-2}(-v_t^2 V_t^2 dt + g_t \beta_t V_t^{3/2} dW_t) + V_t^{-3} (dV_t)^2 \\ &= -V_t^{-2}(-g_t^2 V_t^2 dt) + (-V_t^{-2})(g_t \beta_t V_t^{3/2} dW_t) + V_t^{-3}(\beta_t^2 g_t^2 V_t^3 dt) \\ &= g_t^2 dt - \beta_t g_t V_t^{-1/2} dW_t + \beta_t^2 g_t^2 dt \\ &= g_t^2(1 + \beta_t^2)dt - \beta_t g_t V_t^{-1/2} dW_t \\ &= g_t^2(1 + \beta_t^2)dt - \beta_t g_t \sqrt{X_t} dW_t \end{aligned}$$

Thus, the variance process for the single asset case can be given as:

$$dX_t = g_t^2(1 + \beta_t^2)dt - \beta_t g_t \sqrt{X_t} dW_t \quad (3.2.16)$$

where  $X_t^{-1}$  denotes the inverse of the variance process.

The dynamics of the volatility matrix  $\Sigma_t$  in equation 3.2.13 represents a continuous-time process of stochastic matrices which correspond to the continuous time WAR.

A volatility-in-mean effect is introduced in the drift to account for the risk premium and to capture the tendency for the volatility and the stock prices moving together by introducing interactions between covolatilities and expected returns. The drift in equation 3.2.12 is an affine function of factor volatilities and co-volatilities:

$$E_t(d\bar{S}_{i,t}) = [r\bar{S}_{i,t} + Tr(D_i \Sigma_t)] dt, \quad i = 1, \dots, n, \quad (3.2.17)$$

$E_t$  is the expectation conditional on the information available at time  $t$ .

Considering the one-dimensional case, that is the case where  $n = 1$ , the equations 3.2.12 and 3.2.13 become:

$$dS_t = (rS_t + \delta V_t)dt + P_{tT} g_t V_t dW_t \quad (3.2.18)$$

and

$$d(V_t) = (w^2 + 2mV_t)dt + 2q\sqrt{V_t}dW_t \quad (3.2.19)$$

respectively.

The variance process can be seen to be a CIR process and the model is reduced to the one-dimensional information-based model.

Considering the two-dimensional case, the Wishart process in equation 3.2.13 is given as:

$$\begin{aligned}
d\Sigma_t &= d \begin{pmatrix} \Sigma_t^{11} & \Sigma_t^{12} \\ \Sigma_t^{12} & \Sigma_t^{22} \end{pmatrix} \\
&= \left[ \begin{pmatrix} \Omega_{11} & \Omega_{12} \\ \Omega_{21} & \Omega_{22} \end{pmatrix} \begin{pmatrix} \Omega_{11} & \Omega_{21} \\ \Omega_{12} & \Omega_{22} \end{pmatrix} + \begin{pmatrix} M_{11} & M_{12} \\ M_{21} & M_{22} \end{pmatrix} \begin{pmatrix} \Sigma_t^{11} & \Sigma_t^{12} \\ \Sigma_t^{12} & \Sigma_t^{22} \end{pmatrix} + \right. \\
&\quad \left. \begin{pmatrix} \Sigma_t^{11} & \Sigma_t^{12} \\ \Sigma_t^{12} & \Sigma_t^{22} \end{pmatrix} \begin{pmatrix} M_{11} & M_{21} \\ M_{12} & M_{22} \end{pmatrix} \right] dt + \begin{pmatrix} \Sigma_t^{11} & \Sigma_t^{12} \\ \Sigma_t^{12} & \Sigma_t^{22} \end{pmatrix}^{\frac{1}{2}} \begin{pmatrix} dW_t^{11} & dW_t^{12} \\ dW_t^{21} & dW_t^{22} \end{pmatrix} \begin{pmatrix} Q_{11} & Q_{12} \\ Q_{21} & Q_{22} \end{pmatrix} + \begin{pmatrix} Q_{11} & Q_{21} \\ Q_{12} & Q_{22} \end{pmatrix} \\
&\quad \begin{pmatrix} dW_t^{11} & dW_t^{21} \\ dW_t^{12} & dW_t^{22} \end{pmatrix} \begin{pmatrix} \Sigma_t^{11} & \Sigma_t^{12} \\ \Sigma_t^{12} & \Sigma_t^{22} \end{pmatrix}^{\frac{1}{2}}
\end{aligned}$$

$$\text{Let } \sigma_t = \Sigma_t^{\frac{1}{2}} = \begin{pmatrix} \Sigma_t^{11} & \Sigma_t^{12} \\ \Sigma_t^{12} & \Sigma_t^{22} \end{pmatrix}^{\frac{1}{2}} = \begin{pmatrix} \sigma_t^{11} & \sigma_t^{12} \\ \sigma_t^{12} & \sigma_t^{22} \end{pmatrix}$$

$$\text{this implies that } \sigma_t^2 = \Sigma_t = \begin{pmatrix} (\sigma_t^{11})^2 + (\sigma_t^{12})^2 & \sigma_t^{11}\sigma_t^{12} + \sigma_t^{12}\sigma_t^{22} \\ \sigma_t^{11}\sigma_t^{12} + \sigma_t^{12}\sigma_t^{22} & (\sigma_t^{12})^2 + (\sigma_t^{22})^2 \end{pmatrix}$$

$$\begin{aligned}
&\begin{pmatrix} \Sigma_t^{11} & \Sigma_t^{12} \\ \Sigma_t^{12} & \Sigma_t^{22} \end{pmatrix}^{\frac{1}{2}} \begin{pmatrix} dW_t^{11} & dW_t^{12} \\ dW_t^{21} & dW_t^{22} \end{pmatrix} \begin{pmatrix} Q_{11} & Q_{12} \\ Q_{21} & Q_{22} \end{pmatrix} \\
&= \begin{pmatrix} \sigma_t^{11} & \sigma_t^{12} \\ \sigma_t^{12} & \sigma_t^{22} \end{pmatrix} \begin{pmatrix} dW_t^{11} & dW_t^{12} \\ dW_t^{21} & dW_t^{22} \end{pmatrix} \begin{pmatrix} Q_{11} & Q_{12} \\ Q_{21} & Q_{22} \end{pmatrix} \\
&= \left[ \begin{aligned} &\sigma_t^{11} dW_t^{11} Q_{11} + \sigma_t^{12} dW_t^{21} Q_{11} + \sigma_t^{11} dW_t^{12} Q_{21} + \sigma_t^{12} dW_t^{22} Q_{21} \\ &\sigma_t^{12} dW_t^{11} Q_{11} + \sigma_t^{22} dW_t^{21} Q_{11} + \sigma_t^{12} dW_t^{12} Q_{12} + \sigma_t^{22} dW_t^{22} Q_{21} \\ &\sigma_t^{11} dW_t^{11} Q_{12} + \sigma_t^{12} dW_t^{21} Q_{12} + \sigma_t^{11} dW_t^{12} Q_{22} + \sigma_t^{12} dW_t^{22} Q_{22} \\ &\sigma_t^{12} dW_t^{11} Q_{12} + \sigma_t^{22} dW_t^{21} Q_{12} + \sigma_t^{12} dW_t^{12} Q_{22} + \sigma_t^{22} dW_t^{22} Q_{22} \end{aligned} \right] \\
&\begin{pmatrix} Q_{11} & Q_{21} \\ Q_{12} & Q_{22} \end{pmatrix} \begin{pmatrix} dW_t^{11} & dW_t^{21} \\ dW_t^{12} & dW_t^{22} \end{pmatrix} \begin{pmatrix} \Sigma_t^{11} & \Sigma_t^{12} \\ \Sigma_t^{12} & \Sigma_t^{22} \end{pmatrix}^{\frac{1}{2}} \\
&= \begin{pmatrix} Q_{11} & Q_{21} \\ Q_{12} & Q_{22} \end{pmatrix} \begin{pmatrix} dW_t^{11} & dW_t^{21} \\ dW_t^{12} & dW_t^{22} \end{pmatrix} \begin{pmatrix} \sigma_t^{11} & \sigma_t^{12} \\ \sigma_t^{12} & \sigma_t^{22} \end{pmatrix} \\
&= \left[ \begin{aligned} &\sigma_t^{11} dW_t^{11} Q_{11} + \sigma_t^{11} dW_t^{12} Q_{21} + \sigma_t^{12} dW_t^{21} Q_{11} + \sigma_t^{12} dW_t^{22} Q_{21} \\ &\sigma_t^{11} dW_t^{11} Q_{12} + \sigma_t^{11} dW_t^{12} Q_{22} + \sigma_t^{12} dW_t^{21} Q_{12} + \sigma_t^{12} dW_t^{22} Q_{22} \\ &\sigma_t^{12} dW_t^{11} Q_{11} + \sigma_t^{12} dW_t^{12} Q_{21} + \sigma_t^{22} dW_t^{21} Q_{11} + \sigma_t^{22} dW_t^{22} Q_{21} \\ &\sigma_t^{12} dW_t^{11} Q_{12} + \sigma_t^{12} dW_t^{12} Q_{22} + \sigma_t^{22} dW_t^{21} Q_{12} + \sigma_t^{22} dW_t^{22} Q_{22} \end{aligned} \right]
\end{aligned}$$

$$\begin{aligned}
d\Sigma_t^{11} &= (\Omega_{11}^2 + \Omega_{12}^2 + 2M_{11}\Sigma_{11})dt + 2\sigma_t^{11}(dW_t^{11}Q_{11} + dW_t^{12}Q_{21}) + 2\sigma_t^{12}(dW_t^{21}Q_{11} + dW_t^{22}Q_{21}) \\
d\Sigma_t^{12} &= (\Omega_{11}\Omega_{21} + \Omega_{12}\Omega_{22} + 2M_{12}\Sigma_{12})dt + \sigma_t^{11}(dW_t^{11}Q_{12} + dW_t^{12}Q_{22}) + \sigma_t^{12}(dW_t^{21}Q_{12} + dW_t^{22}Q_{22}) \\
&\quad + dW_t^{11}Q_{11} + dW_t^{12}Q_{21}) + \sigma_t^{22}(dW_t^{21}Q_{11} + dW_t^{22}Q_{21}) \\
d\Sigma_t^{22} &= (\Omega_{22}^2 + \Omega_{21}^2 + 2M_{22}\Sigma_{22})dt + 2\sigma_t^{12}(dW_t^{11}Q_{12} + dW_t^{12}Q_{22}) + 2\sigma_t^{22}(dW_t^{21}Q_{12} + dW_t^{22}Q_{22})
\end{aligned}$$

**Proposition 3.2.** *The infinitesimal generator associated with the Wishart process in equation 3.2.13 is given by:*

$$\mathcal{L}_\Sigma = \text{Tr}[(\beta Q^\top Q + M\Sigma + \Sigma M^\top)D + 2\Sigma D Q^\top Q D] \quad (3.2.20)$$

where

$$D = \left( \frac{\partial}{\partial \Sigma^{ij}} \right)_{1 \leq i, j \leq n}$$

*Proof.* The following equations are used to generate the infinitesimal generator of the process:

$$\begin{aligned}
d \langle \Sigma^{11}, \Sigma^{11} \rangle_t &= (d\Sigma^{11})(d\Sigma^{11}) \\
&= 4(\sigma_t^{11})^2 Q_{11}^2 dt + 4(\sigma_t^{12})^2 Q_{21}^2 dt + 4(\sigma_t^{12})^2 Q_{11}^2 dt + 4(\sigma_t^{11})^2 Q_{21}^2 dt \\
&= 4\Sigma_t^{11} [Q_{11}^2 + Q_{21}^2]
\end{aligned}$$

$$d \langle \Sigma^{12}, \Sigma^{12} \rangle_t = \Sigma_t^{11} [Q_{11}^2 + Q_{22}^2] + \Sigma_t^{12} [Q_{11}Q_{12} + Q_{21}Q_{22}] + \Sigma_t^{22} [Q_{11}^2 + Q_{21}^2]$$

$$\begin{aligned}
d \langle \Sigma^{22}, \Sigma^{22} \rangle_t &= 4Q_{12}^2 [\sigma_{12}^2 + \sigma_{22}^2] + 4Q_{22}^2 [\sigma_{12}^2 + \sigma_{22}^2] dt \\
&= 4\Sigma_t^{22} [Q_{12}^2 + Q_{22}^2] dt
\end{aligned}$$

$$d \langle \Sigma^{11}, \Sigma^{12} \rangle_t = (2\Sigma_t^{11}(Q_{11}Q_{12} + Q_{21}Q_{22}) + 2\Sigma_t^{12}(Q_{11}^2 + Q_{21}^2))dt$$

$$d \langle \Sigma^{11}, \Sigma^{22} \rangle_t = 4\Sigma_t^{12}(Q_{11}Q_{12} + Q_{21}Q_{22})dt$$

$$d \langle \Sigma^{12}, \Sigma^{22} \rangle_t = 2(\Sigma_t^{12}(Q_{12}^2 + Q_{22}^2) + \Sigma_t^{22}(Q_{11}Q_{12} + Q_{21}Q_{22}))dt$$

The trace of the matrix  $2\Sigma_t DQ^T QD$  is as follows:

$$\begin{aligned}
Tr[2\Sigma_t DQ^T QD] &= 2Tr[\Sigma_t DQ^T QD] \\
&= 2\Sigma_t^{11}(Q_{11}^2 + Q_{21}^2) \frac{\partial^2}{(\partial\Sigma^{11})^2} \\
&\quad + 2\left(\Sigma_t^{11}(Q_{12}^2 + Q_{22}^2) + 2\Sigma_t^{12}(Q_{11}Q_{12} + Q_{21}Q_{22}) + \Sigma_t^{22}(Q_{11}^2 + Q_{21}^2)\right) \frac{\partial^2}{(\partial\Sigma^{12})^2} \\
&\quad + 2\Sigma_t^{22}(Q_{12}^2 + Q_{22}^2) \frac{\partial^2}{(\partial\Sigma^{22})^2} \\
&\quad + 4\left(\Sigma_t^{11}(Q_{11}Q_{12} + Q_{21}Q_{22}) + \Sigma_t^{12}(Q_{11}^2 + Q_{21}^2)\right) \frac{\partial^2}{\partial\Sigma^{11}\Sigma^{12}} \\
&\quad + 4\Sigma_t^{12}(Q_{11}Q_{12} + Q_{21}Q_{22}) \frac{\partial^2}{\partial\Sigma^{11}\Sigma^{22}} \\
&\quad + 4\left(\Sigma_t^{12}(Q_{12}^2 + Q_{22}^2) + 2\Sigma_t^{22}(Q_{11}Q_{12} + Q_{21}Q_{22})\right) \frac{\partial^2}{\partial\Sigma^{12}\Sigma^{22}}
\end{aligned}$$

and

$$\begin{aligned}
\mathcal{L}_\Sigma &= Tr[(\Omega\Omega^\top + M\Sigma + \Sigma M^\top)D] + \frac{1}{2}\left(\langle \Sigma^{11}, \Sigma^{11} \rangle_t \frac{\partial^2}{(\partial\Sigma^{11})^2} \right. \\
&\quad + 2\langle \Sigma^{12}, \Sigma^{12} \rangle_t \frac{\partial^2}{(\partial\Sigma^{12})^2} + \langle \Sigma^{22}, \Sigma^{22} \rangle_t \frac{\partial^2}{(\partial\Sigma^{22})^2} + 4\langle \Sigma^{11}, \Sigma^{12} \rangle_t \frac{\partial^2}{\partial\Sigma^{11}\Sigma^{12}} \\
&\quad \left. + 2\langle \Sigma^{11}, \Sigma^{22} \rangle_t \frac{\partial^2}{\partial\Sigma^{11}\Sigma^{22}} + 4\langle \Sigma^{12}, \Sigma^{22} \rangle_t \frac{\partial^2}{\partial\Sigma^{12}\Sigma^{22}} \right)
\end{aligned}$$

In order to discretize the asset price process, for every  $t \in \mathbb{R}_+$ ,  $\Delta t > 0$ , equation 3.2.12 is integrated over the interval  $[t, t + \Delta t]$ :

$$\begin{aligned}
\int_t^{t+\Delta t} d\bar{S}_u &= \int_t^{t+\Delta t} [r\bar{S}_u + (Tr(D_1\Sigma_u), \dots, Tr(D_n\Sigma_u))^\top] du + \int_t^{t+\Delta t} P_{uT} g_u \Sigma_u dW_u \\
&= \int_t^{t+\Delta t} r\bar{S}_u du + \int_t^{t+\Delta t} [(Tr(D_1\Sigma_u), \dots, Tr(D_n\Sigma_u))^\top] du + \int_t^{t+\Delta t} P_{uT} g_u \Sigma_u dW_u
\end{aligned} \tag{3.2.21}$$

To make equation 3.2.21 suitable for numerical simulation, a slightly modified Euler scheme is used as follows:

$$\int_t^{t+\Delta t} d\bar{S}_u \approx \bar{S}_{t+\Delta t} - \bar{S}_t$$



$$\int_t^{t+\Delta t} r\bar{S}_u du \approx r\Delta t\bar{S}_t$$

$$\int_t^{t+\Delta t} [(Tr(D_1\Sigma_u), \dots, Tr(D_n\Sigma_u))^T] du \approx \Delta t [(Tr(D_1\Sigma_t), \dots, Tr(D_n\Sigma_t))^T]$$

$$\int_t^{t+\Delta t} P_{uT}g_u\Sigma_u dW_u \approx P_{tT}g_t\Sigma_t\sqrt{\Delta t}G$$

Thus:

$$\bar{S}_{t+\Delta t} = \bar{S}_t + r\Delta t\bar{S}_t + \Delta t [(Tr(D_1\Sigma_t), \dots, Tr(D_n\Sigma_t))^T] + P_{tT}g_t\Sigma_t\sqrt{\Delta t}G \quad (3.2.22)$$

Equation 3.2.22 can be used to simulate  $S$  for any fixed step size  $\Delta t > 0$ . This process can become negative definite since the square root is no longer well defined. A solution to this problem is to make use of the full truncation scheme which involves taking the positive value of the variance such that:

$$\bar{S}_{t+\Delta t} = \bar{S}_t + r\Delta t\bar{S}_t + \Delta t\bar{S}_t [(Tr(D_1\Sigma_t^+), \dots, Tr(D_n\Sigma_t^+))^T] + P_{tT}g_t\Sigma_t^+\sqrt{\Delta t}G \quad (3.2.23)$$

For the variance process, the discretization process is done by using the same approach used in the Heston model resulting in the discretized Wishart process given in equation 3.1.38.

### 3.3. Asset pricing in an information-based framework

The study starts with a valuation formula for an option written on one underlying asset and extends to the case of an option written on  $n$  underlying assets. The two approaches for the information-based asset pricing framework; that is the BS-BHM model and the BS-BHM updated model are looked at.

Risk-neutral pricing is used where the model has one underlying asset. The notion of comonotonicity is used for the case of  $n$  underlying assets by obtaining a lower bound and an upper bound for the price by assuming a comonotonic dependence structure between the underlying assets. The approach is based on the assumption that an increase in the value of one of the variables results in an increase in the value of all the variables.

#### 3.3.1. Notion of comonotonicity in a multi-asset information-based framework

Let:

$$D_t = \sum_{i=1}^n c_i S_{i,t} \quad (3.3.1)$$

where  $c_i$  denotes the weight and  $(S_{1,t}, \dots, S_{n,t})$  are assumed to be comonotonic, which implies that an increase in the price of one asset results in all the other asset prices increasing at the same time.

Let  $\Sigma$  denote the variance-covariance matrix such that:

$$\Sigma = \begin{pmatrix} \Sigma_{1,1} & \Sigma_{1,2} & \cdots & \Sigma_{1,n} \\ \Sigma_{2,1} & \Sigma_{2,2} & \cdots & \Sigma_{2,n} \\ \vdots & \vdots & \ddots & \vdots \\ \Sigma_{n,1} & \Sigma_{n,2} & \cdots & \Sigma_{n,n} \end{pmatrix}$$

The upper bound price is obtained as follows:

$$C^u[K] = E_{\mathbb{Q}}[\max\{D^u - K, 0\}]$$

where:

$$D^u = \sum_{i=1}^n c_i F_{S_{i,t}}^{-1}(U) \quad (3.3.2)$$

$U \sim U[0, 1]$ .

The lower bound price is given by:

$$C^l[K] = E_{\mathbb{Q}}[\max\{D^l - K, 0\}] \quad (3.3.3)$$

where:

$$D^l = \sum_{i=1}^n c_i \mathbb{E}[S_{i,t} | \Psi] \quad (3.3.4)$$

and

$$\Psi = \sum_{i=1}^n \psi_i \ln \frac{S_{i,t}}{S_{i,0}} \quad (3.3.5)$$

with  $\psi_i > 0$  being given as:

$$\psi_i = c_i S_{i,0} e^{rt} \quad (3.3.6)$$

The upper and lower bound are combined using a linear association to obtain the price of the multi-asset derivative as follows:

$$C[K] = zC^l[K] + (1-z)C^u[K] \quad \text{for all } K \geq 0. \quad (3.3.7)$$

$z$  represents an interpolation weight given as:

$$z = \frac{V(D^u) - V(D)}{V(D^u) - V(D^l)} \quad (3.3.8)$$

### 3.3.2. Pricing multi-asset options under the BS-BHM model

**Proposition 3.3.** *The price of a European call option under the BS-BHM model is given as follows:*

$$C_{bhm} = S_0 e^{\varphi + \frac{1}{2}\delta^2} \Phi(d_1) - K \Phi(-d_2)$$

where:

$$d_1 = \frac{\log\left(\frac{S_0}{K}\right) + \varphi}{\delta} + \delta$$

and

$$d_2 = d_1 - \delta$$

*Proof.* Under the BS-BHM model, the value for  $S_t$  is given as:

$$S_t = S_0 \exp\left(rt - \frac{1}{2}v^2T + \frac{1}{2}\frac{v\sqrt{T}}{\gamma^2\tau + 1} + \frac{\gamma\tau v\sqrt{T}}{t(\gamma^2\tau + 1)}\xi_t\right) \quad (3.3.9)$$

where  $\tau = \frac{tT}{T-t}$  and  $v$  is a constant.

Introducing logs in equation 3.3.9 leads to:

$$\log\left(\frac{S_t}{S_0}\right) = \left(rt - \frac{1}{2}v^2T + \frac{1}{2}\frac{v\sqrt{T}}{\gamma^2\tau + 1} + \frac{\gamma\tau v\sqrt{T}}{t(\gamma^2\tau + 1)}\xi_t\right) \quad (3.3.10)$$

Equation 3.3.10 follows the lognormal distribution given as:

$$\log\left(\frac{S_t}{S_0}\right) \sim N\left[rt - \frac{1}{2}v^2T + \frac{1}{2}\frac{v\sqrt{T}}{\gamma^2\tau + 1}, \left(\frac{\gamma\tau v\sqrt{T}}{t(\gamma^2\tau + 1)}\right)^2\left(\gamma^2t^2 + \frac{t(T-t)}{T}\right)\right] \quad (3.3.11)$$

Let:

$$\varphi = rt - \frac{1}{2}v^2T + \frac{1}{2}\frac{v\sqrt{T}}{\gamma^2\tau + 1}$$

and

$$\delta^2 = \left(\frac{\gamma\tau v\sqrt{T}}{t(\gamma^2\tau + 1)}\right)^2\left(\gamma^2t^2 + \frac{t(T-t)}{T}\right)$$

This implies that:

$$\log\left(\frac{S_t}{S_0}\right) \sim N\left[\varphi, \delta^2\right] \quad (3.3.12)$$

$$S_t \sim N\left[S_0e^\varphi, S_0^2e^{2\varphi+\delta^2}\left(e^{\delta^2} - 1\right)\right]$$

Let  $C_{bhm}$  denote the value of the derivative at the current time  $t$ .

$$C_{bhm} = E_{\mathbb{Q}}[\max\{S_t - K, 0\}] \quad (3.3.13)$$

Equation 3.3.9 can be re-written as follows:

$$S_t = \exp\left(\log S_0 + rt - \frac{1}{2}v^2T + \frac{1}{2}\frac{v\sqrt{T}}{\gamma^2\tau + 1} + \frac{\gamma\tau v\sqrt{T}}{t(\gamma^2\tau + 1)}\xi_t\right) \quad (3.3.14)$$

Define  $\alpha = \log S_0 + \varphi$ .

Substituting for the value of  $\alpha$  in equation 3.3.14 gives:

$$S_t = e^{\alpha+\delta Z} \quad (3.3.15)$$

Let  $K = e^{\alpha+\delta z}$ , making  $z$  to be the subject leads to:

$$\begin{aligned} z &= \frac{\log K - \alpha}{\delta} \\ &= \frac{\log K - \log S_0 - \varphi}{\delta} \\ &= \frac{\log\left(\frac{K}{S_0}\right) - \varphi}{\delta} \end{aligned} \quad (3.3.16)$$

Substituting for the values of  $S_t$  and  $K$  in equation 3.3.13 gives:

$$\begin{aligned}
C_{bhm} &= E_{\mathbb{Q}}[\max\{e^{\alpha+\delta Z} - e^{\alpha+\delta z}, 0\}] \\
&= e^{\alpha+\delta z} E_{\mathbb{Q}}[\max\{e^{\delta(Z-z)} - 1, 0\}] \\
&= e^{\alpha+\delta z} \int_{-\infty}^{\infty} \max\{e^{\delta(y-z)} - 1, 0\} f(y) dy \\
&= e^{\alpha+\delta z} \left[ \int_z^{\infty} e^{\delta(y-z)} f(y) dy - \int_z^{\infty} f(y) dy \right] \\
&= e^{\alpha+\delta z} \left[ e^{-\delta z} \int_z^{\infty} e^{\delta y} f(y) dy - \int_z^{\infty} f(y) dy \right] \tag{3.3.17}
\end{aligned}$$

where  $f(y) = \frac{1}{\sqrt{2\pi}} e^{-\frac{1}{2}y^2}$

$$\begin{aligned}
C_{bhm} &= e^{\alpha+\delta z} \left[ e^{-\delta z} \int_z^{\infty} \frac{1}{\sqrt{2\pi}} e^{\delta y - \frac{1}{2}y^2} dy - \int_z^{\infty} \frac{1}{\sqrt{2\pi}} e^{-\frac{1}{2}y^2} dy \right] \\
&= e^{\alpha+\delta z} \left[ e^{-\delta z + \frac{1}{2}\delta^2} \int_z^{\infty} \frac{1}{\sqrt{2\pi}} e^{-\frac{1}{2}(y-\delta)^2} dy - \int_z^{\infty} \frac{1}{\sqrt{2\pi}} e^{-\frac{1}{2}y^2} dy \right] \\
&= e^{\alpha+\delta z} \left[ e^{-\delta z + \frac{1}{2}\delta^2} \Phi(\delta - z) - \Phi(-z) \right] \\
&= e^{\alpha + \frac{1}{2}\delta^2} \Phi(\delta - z) - e^{\alpha+\delta z} \Phi(-z) \tag{3.3.18}
\end{aligned}$$

$$\alpha + \frac{1}{2}\delta^2 = \log S_0 + \varphi + \frac{1}{2}\delta^2 \quad (3.3.19)$$

$$\begin{aligned} \delta - z &= \delta - \frac{\log\left(\frac{K}{S_0}\right) - \varphi}{\delta} \\ &= \frac{\delta^2 + \log\left(\frac{S_0}{K}\right) + \varphi}{\delta} \\ &= \frac{\log\left(\frac{S_0}{K}\right) + \varphi}{\delta} + \delta \\ &= d_1 \end{aligned} \quad (3.3.20)$$

$$\begin{aligned} \alpha + \delta z &= \log S_0 + \varphi + \delta \frac{\log\left(\frac{K}{S_0}\right) - \varphi}{\delta} \\ &= \log K \end{aligned} \quad (3.3.21)$$

$$\begin{aligned} -z &= -\frac{\log\left(\frac{K}{S_0}\right) - \varphi}{\delta} \\ &= \frac{\log\left(\frac{S_0}{K}\right) + \varphi}{\delta} \\ &= d_1 - \delta \\ &= d_2 \end{aligned} \quad (3.3.22)$$

Substituting for equations 3.3.19, 3.3.20, 3.3.21 and 3.3.22 in equation 3.3.18 gives:

$$\begin{aligned} C_{bhm} &= e^{\log S_0 + \varphi + \frac{1}{2}\delta^2} \Phi(d_1) - e^{\log K} \Phi(-d_2) \\ &= S_0 e^{\varphi + \frac{1}{2}\delta^2} \Phi(d_1) - K \Phi(-d_2) \end{aligned} \quad (3.3.23)$$

Equation 3.3.23 represents the valuation formula for the derivative price under the BS-BHM model. This formula is similar to that obtained in the Black-Scholes model.

**Proposition 3.4.** *The price of a multi-asset European call option under the BS-BHM model is given as follows:*

$$C[K] = zC^l[K] + (1 - z)C^u[K]$$

where:

$$C^u[K] = \sum_{i=1}^n c_i [S_{i,0} e^{\varphi_i + \frac{1}{2}\delta_i^2} \Phi(d_{i,1}^u) - K_i^u \Phi(d_{i,2}^u)]$$

and

$$C^l[K] = \sum_{i=1}^n c_i [S_{i,0} e^{\varphi_i + \frac{1}{2}\delta_i^2} \Phi(d_{i,1}^l) - K_i^l \Phi(d_{i,2}^l)]$$

*Proof.* Considering the multi-asset information-based asset pricing framework under the

BS-BHM model, let

$$S_{i,t} = S_{i,0} \exp\left(rt - \frac{1}{2}v_i^2T + \frac{1}{2}\frac{v_i\sqrt{T}}{\gamma_i^2\tau + 1} + \frac{\gamma_i\tau v_i\sqrt{T}}{t(\gamma_i^2\tau + 1)}\xi_{i,t}\right) \quad (3.3.24)$$

$\rho_{i,j}$  denote the correlation coefficient such that:

$$\rho_{i,j} = \text{Corr}\left[\frac{\gamma_i\tau v_i\sqrt{T}}{t(\gamma_i^2\tau + 1)}\xi_{i,t}, \frac{\gamma_j\tau v_j\sqrt{T}}{t(\gamma_j^2\tau + 1)}\xi_{j,t+s}\right]$$

where  $s \geq 0$ .

$$\Sigma_{i,j} = \text{Cov}\left[\frac{\gamma_i\tau v_i\sqrt{T}}{t(\gamma_i^2\tau + 1)}\xi_{i,t}, \frac{\gamma_j\tau v_j\sqrt{T}}{t(\gamma_j^2\tau + 1)}\xi_{j,t+s}\right]$$

and

$$F_{S_{i,t}}^{-1}(U) = S_{i,0} \exp\left(rt - \frac{1}{2}v_i^2T + \frac{1}{2}\frac{v_i\sqrt{T}}{\gamma_i^2\tau + 1} + \frac{\gamma_i\tau v_i\sqrt{T}}{t(\gamma_i^2\tau + 1)}\sqrt{\gamma_i^2t^2 + \frac{t(T-t)}{T}}N^{-1}(U)\right) \quad (3.3.25)$$

The upper bound price is given as follows:

$$C^u[K] = \sum_{i=1}^n c_i [S_{i,0}e^{\varphi_i + \frac{1}{2}\delta_i^2}\Phi(d_{i,1}^u) - K_i^u\Phi(d_{i,2}^u)] \quad (3.3.26)$$

Using the result from equation 3.3.11 gives:

$$K_i^u = S_{i,0} \exp\left[rt - \frac{1}{2}v_i^2T + \frac{1}{2}\frac{v_i\sqrt{T}}{\gamma_i^2\tau + 1} + \frac{\gamma_i\tau v_i\sqrt{T}}{t(\gamma_i^2\tau + 1)}\sqrt{\gamma_i^2t^2 + \frac{t(T-t)}{T}}N^{-1}(F_{D^u}(K))\right] \quad (3.3.27)$$

Let

$$\varphi_i = rt - \frac{1}{2}v_i^2T + \frac{1}{2}\frac{v_i\sqrt{T}}{\gamma_i^2\tau + 1} \quad (3.3.28)$$

and

$$\delta_i = \left(\frac{\gamma_i\tau v_i\sqrt{T}}{t(\gamma_i^2\tau + 1)}\right)\sqrt{\left(\gamma_i^2t^2 + \frac{t(T-t)}{T}\right)} \quad (3.3.29)$$

Substituting equation 3.3.28 and 3.3.29 into 3.3.27 gives:

$$K_i^u = S_{i,0} \exp\left[\varphi_i + \delta_i N^{-1}(F_{D^u}(K))\right] \quad (3.3.30)$$

$F_{D^u}(K)$  is determined using the relation:

$$\sum_{i=1}^n c_i K_i^u = K \quad (3.331)$$

and

$$d_{i,1}^u = \frac{\log\left(\frac{S_{i,0}}{K_i^u}\right) + \varphi_i}{\delta_i} + \delta_i,$$

$$d_{i,2}^u = d_{i,1}^u - \delta_i$$

The variance of  $D^u$  is as follows:

$$V[D^u] = \sum_{i=1}^n \sum_{j=1}^n c_i c_j S_{i,0} S_{j,0} e^{(2\varphi_i \varphi_j + \delta_i \delta_j)} [e^{\delta_i \delta_j} - 1]$$

The price  $C^l[K]$  can be expressed as:

$$C^l[K] = \sum_{i=1}^n c_i [S_{i,0} e^{\varphi_i + \frac{1}{2}\delta_i^2} \Phi(d_{i,1}^l) - K_i^l \Phi(d_{i,2}^l)] \quad (3.332)$$

where

$$K_i^l = S_{i,0} \exp\left[rt - \frac{1}{2}v_i^2 T + \frac{1}{2} \frac{v_i \sqrt{T}}{y_i^2 \gamma_i^2 \tau + 1} + \frac{y_i \gamma_i \tau v_i \sqrt{T}}{t(y_i^2 \gamma_i^2 \tau + 1)} \sqrt{y_i^2 \gamma_i^2 t^2 + \frac{t(T-t)}{T}} N^{-1}(F_{D^l}(K))\right] \quad (3.333)$$

Let

$$\varphi_{i^*} = rt - \frac{1}{2}y_i^2 v_i^2 T + \frac{1}{2} \frac{y_i v_i \sqrt{T}}{\gamma_i^2 \tau + 1} \quad (3.334)$$

and

$$\delta_{i^*} = \left(\frac{y_i \gamma_i \tau v_i \sqrt{T}}{t(\gamma_i^2 \tau + 1)}\right) \sqrt{\left(\gamma_i^2 t^2 + \frac{t(T-t)}{T}\right)} \quad (3.335)$$

Substituting equation 3.334 and 3.335 into equation 3.333 gives:

$$K_i^l = S_{i,0} \exp\left[\varphi_{i^*} + \delta_{i^*} N^{-1}(F_{D^l}(K))\right] \quad (3.336)$$

with

$$y_i = \frac{\sum_{j=1}^n \psi_j \rho_{i,j} \delta_j}{\sigma_\Psi} \quad (3.337)$$



and

$$\sigma_{\Psi}^2 = \sum_{i=1}^n \psi_i^2 \delta_i^2 + 2 \sum_{i=1, j < i}^n \psi_i \psi_j \rho_{i,j} \delta_i \delta_j \quad (3.3.38)$$

$F_{D^l}(K)$  is determined using the relation:

$$\sum_{i=1}^n c_i K_i^l = K \quad (3.3.39)$$

and

$$d_{i,1}^l = \frac{\log\left(\frac{S_{i,0}}{K_i^l}\right) + \varphi_{i^*}}{\delta_{i^*}} + \delta_{i^*},$$

$$d_{i,2}^l = d_{i,1}^l - \delta_{i^*}$$

The variance for  $D^l$  is as follows:

$$V[D^l] = \sum_{i=1}^n \sum_{j=1}^n c_i c_j S_{i,0} S_{j,0} e^{(2\varphi + \delta_{i^*} \delta_{j^*})} [e^{\delta_{i^*} \delta_{j^*}} - 1]$$

### 3.3.3. Pricing multi-asset options under the BS-BHM updated model

**Proposition 3.5.** *The price of a European call option under the BS-BHM updated model is given as follows:*

$$C_{updated} = S\Phi(d_1) - Ke^{-(A + \frac{B^2}{2})}\Phi(d_2)$$

where:

$$d_1 = \frac{\log\left(\frac{S_0}{K}\right) + A}{B} + B$$

and

$$d_2 = d_1 - B$$

*Proof.* Under the BS-BHM updated model, the value for  $S_t$  is as follows:

$$S_t = S_0 \exp\left(rt - \frac{1}{2} \frac{\gamma^2 \tau}{\gamma^2 \tau + 1} v^2 T + \frac{\gamma \tau v \sqrt{T}}{t(\gamma^2 \tau + 1)} \xi_t\right) \quad (3.3.40)$$

The lognormal distribution for  $\frac{S_t}{S_0}$  is given by:

$$\log\left(\frac{S_t}{S_0}\right) \sim N\left[rt - \frac{1}{2} \frac{\gamma^2 \tau}{\gamma^2 \tau + 1} v^2 T, \left(\frac{\gamma \tau v \sqrt{T}}{t(\gamma^2 \tau + 1)}\right)^2 \left(\gamma^2 t^2 + \frac{t(T-t)}{T}\right)\right] \quad (3.3.41)$$

Let:

$$A = rt - \frac{1}{2} \frac{\gamma^2 \tau}{\gamma^2 \tau + 1} v^2 T$$

and

$$B = \frac{\gamma \tau v \sqrt{T}}{t(\gamma^2 \tau + 1)} \sqrt{\left( \gamma^2 t^2 + \frac{t(T-t)}{T} \right)}$$

$$\log\left(\frac{S_t}{S_0}\right) \sim N\left[A, B^2\right] \quad (3.3.42)$$

$$S_t \sim N\left[S_0 e^A, S_0^2 e^{2A} \left(e^{B^2} - 1\right)\right]$$

Thus:

$$S_t = S_0 e^{A+BZ} \quad (3.3.43)$$

where  $Z \sim N[0, 1]$ .

Equation 3.3.41 a density function given as follows:

$$f\left(\frac{S_t}{S_0}\right) = \frac{1}{B\sqrt{2\pi}\left(\frac{S_t}{S_0}\right)} \exp\left(-\frac{1}{2}\left[\frac{\log\left(\frac{S_t}{S_0}\right) - A}{B}\right]^2\right) \quad (3.3.44)$$

Let  $C_{updated}$  denote the derivative price under the BS-BHM updated model with one underlying asset. It follows that:

$$C_{updated} = E_{\mathbb{Q}}[\max\{S_t - K, 0\}] \quad (3.3.45)$$

An assumption is made that there's a default-free deterministic interest rate.

$$\begin{aligned} C_{updated} &= \int_0^{\infty} \max\{S_t - K, 0\} f(s_t) ds_t \\ &= \int_K^{\infty} \{S_t - K, 0\} f(s_t) ds_t \end{aligned}$$

Using the result from equation 3.3.43, it follows that;

$$Z = \frac{\log\left(\frac{S_t}{S_0}\right) - A}{B}$$

For the lower bound, when  $S_t = K$ ;

$$Z = \frac{\log\left(\frac{K}{S_0}\right) - A}{B}$$

$$\begin{aligned}
C_{updated} &= \int_{\frac{\log(\frac{K}{S_0})-A}{B}}^{\infty} (S_0 e^{A+BZ} - K) f(z) dz \\
&= \int_{\frac{\log(\frac{K}{S_0})-A}{B}}^{\infty} S_0 e^{A+BZ} f(z) dz - \int_{\frac{\log(\frac{K}{S_0})-A}{B}}^{\infty} K f(z) dz \\
&= \int_{\frac{\log(\frac{K}{S_0})-A}{B}}^{\infty} S_0 e^{A+BZ} f(z) dz - K \int_{\frac{\log(\frac{K}{S_0})-A}{B}}^{\infty} f(z) dz
\end{aligned}$$

$$f(z) = \frac{1}{\sqrt{2\pi}} e^{-\frac{z^2}{2}}$$

$$\begin{aligned}
C_{updated} &= S_0 e^A \int_{\frac{\log(\frac{K}{S_0})-A}{B}}^{\infty} e^{BZ} \frac{1}{\sqrt{2\pi}} e^{-\frac{z^2}{2}} dz - K \int_{\frac{\log(\frac{K}{S_0})-A}{B}}^{\infty} \frac{1}{\sqrt{2\pi}} e^{-\frac{z^2}{2}} dz \\
&= S_0 e^A \int_{\frac{\log(\frac{K}{S_0})-A}{B}}^{\infty} e^{BZ - \frac{z^2}{2}} \frac{1}{\sqrt{2\pi}} dz - K \int_{\frac{\log(\frac{K}{S_0})-A}{B}}^{\infty} \frac{1}{\sqrt{2\pi}} e^{-\frac{z^2}{2}} dz
\end{aligned}$$

$$BZ - \frac{z^2}{2} = \frac{B^2}{2} - \frac{(z-B)^2}{2}$$

$$\begin{aligned}
C_{updated} &= S_0 e^A \int_{\log\left(\frac{K}{S_0}\right) - A}^{\infty} \frac{e^{\frac{B^2}{2} - \frac{(z-B)^2}{2}}}{\sqrt{2\pi}} dz - K \int_{\log\left(\frac{K}{S_0}\right) - A}^{\infty} \frac{1}{\sqrt{2\pi}} e^{-\frac{z^2}{2}} dz \\
&= S_0 e^{A + \frac{B^2}{2}} \int_{\log\left(\frac{K}{S_0}\right) - A}^{\infty} \frac{1}{\sqrt{2\pi}} e^{-\frac{(z-B)^2}{2}} dz - K \int_{\log\left(\frac{K}{S_0}\right) - A}^{\infty} \frac{1}{\sqrt{2\pi}} e^{-\frac{z^2}{2}} dz \\
&= S_0 e^{A + \frac{B^2}{2}} P\left[N(B, 1) > \frac{\log\left(\frac{K}{S_0}\right) - A}{B}\right] - KP\left[N(0, 1) > \frac{\log\left(\frac{K}{S_0}\right) - A}{B}\right] \\
&= S_0 e^{A + \frac{B^2}{2}} \left(1 - \Phi\left(\frac{\log\left(\frac{K}{S_0}\right) - A}{B} - B\right)\right) - K\left(1 - \Phi\left(\frac{\log\left(\frac{K}{S_0}\right) - A}{B}\right)\right) \\
&= S_0 e^{A + \frac{B^2}{2}} \Phi\left(B - \frac{\log\left(\frac{K}{S_0}\right) - A}{B}\right) - K\Phi\left(\frac{A - \log\left(\frac{K}{S_0}\right)}{B}\right) \\
&= S_0 e^{A + \frac{B^2}{2}} \Phi\left(\frac{\log\left(\frac{S_0}{K}\right) + A}{B} + B\right) - K\Phi\left(\frac{\log\left(\frac{S_0}{K}\right) + A}{B}\right) \\
&= S_0 \Phi\left(\frac{\log\left(\frac{S_0}{K}\right) + A}{B} + B\right) - K e^{-(A + \frac{B^2}{2})} \Phi\left(\frac{\log\left(\frac{S_0}{K}\right) + A}{B}\right)
\end{aligned}$$

Thus:

$$C_{updated} = S\Phi(d_1) - K e^{-(A + \frac{B^2}{2})} \Phi(d_2) \quad (3.3.46)$$

where

$$d_1 = \frac{\log\left(\frac{S_0}{K}\right) + A}{B} + B$$

and

$$d_2 = d_1 - B$$

**Proposition 3.6.** *The price of a multi-asset European call option under the BS-BHM updated model is given as follows:*

$$C[K] = zC^l[K] + (1 - z)C^u[K]$$

where:

$$C^u[K] = \sum_{i=1}^n c_i (S_i \Phi(d_{i,1}) - K_i^u e^{-(A_i + \frac{B_i^2}{2})} \Phi(d_{i,2}))$$

and

$$C^l[K] = \sum_{i=1}^n c_i (S_i \Phi(d_{i,1}) - K_i^l e^{-(A_i + \frac{B_i^2}{2})} \Phi(d_{i,2}))$$

*Proof.* Let

$$S_{i,t} = S_{i,0} \exp\left(rt - \frac{1}{2} \frac{\gamma_i^2 \tau}{\gamma_i^2 \tau + 1} v_i^2 T + \frac{\gamma_i \tau v_i \sqrt{T}}{t(\gamma_i^2 \tau + 1)} \xi_{i,t}\right) \quad (3.3.47)$$

The correlation between the  $i^{th}$  asset and  $j^{th}$  asset is given by:

$$\rho_{i,j} = \text{Corr}\left[\frac{\gamma_i \tau v_i \sqrt{T}}{t(\gamma_i^2 \tau + 1)} \xi_{i,t}, \frac{\gamma_j \tau v_j \sqrt{T}}{t(\gamma_j^2 \tau + 1)} \xi_{j,t+s}\right]$$

$s \geq 0$  and  $\rho_{i,j}$  is assumed to be constant for all time periods.

$$\Sigma_{i,j} = \text{Cov}\left[\frac{\gamma_i \tau v_i \sqrt{T}}{t(\gamma_i^2 \tau + 1)} \xi_{i,t}, \frac{\gamma_j \tau v_j \sqrt{T}}{t(\gamma_j^2 \tau + 1)} \xi_{j,t+s}\right]$$

and

$$F_{S_{i,t}}^{-1}(U) = S_{i,0} \exp\left(rt - \frac{1}{2} \frac{\gamma_i^2 \tau}{\gamma_i^2 \tau + 1} v_i^2 T + \frac{\gamma_i \tau v_i \sqrt{T}}{t(\gamma_i^2 \tau + 1)} \sqrt{\gamma_i^2 t^2 + \frac{t(T-t)}{T}} N^{-1}(U)\right) \quad (3.3.48)$$

The upper bound price  $C^u[K]$  can be expressed as:

$$C^u[K] = \sum_{i=1}^n c_i (S_i \Phi(d_{i,1}) - K_i^u e^{-(A_i + \frac{B_i^2}{2})} \Phi(d_{i,2})) \quad (3.3.49)$$

with

$$d_{i,1} = \frac{\log\left(\frac{S_0}{K_i^u}\right) + A_i}{B_i} + B_i,$$

$$d_{i,2} = d_{i,1} - B_i$$

Using the result from equation 3.3.11:

$$K_i^u = S_i \exp\left[rt - \frac{1}{2} \frac{\gamma_i^2 \tau}{\gamma_i^2 \tau + 1} v_i^2 T + \left(\frac{\gamma_i \tau v_i \sqrt{T}}{t(\gamma_i^2 \tau + 1)}\right) \sqrt{\left(\gamma_i^2 t^2 + \frac{t(T-t)}{T}\right)} \phi^{-1}(F_{D^u}(K))\right] \quad (3.3.50)$$

Let

$$A_i = rt - \frac{1}{2} \frac{\gamma_i^2 \tau}{\gamma_i^2 \tau + 1} v_i^2 T \quad (3.3.51)$$

and

$$B_i = \left( \frac{\gamma_i \tau v_i \sqrt{T}}{t(\gamma_i^2 \tau + 1)} \right) \sqrt{\left( \gamma_i^2 t^2 + \frac{t(T-t)}{T} \right)} \quad (3.3.52)$$

$F_{D^u}(K)$  is determined using the relation in equation 3.3.31.

The variance of  $D^u$  is as follows:

$$V[D^u] = \sum_{i=1}^n \sum_{j=1}^n c_i c_j S_{i,0} S_{j,0} e^{(2A_i A_j + B_i B_j)} [e^{B_i B_j} - 1]$$

The price  $C^l[K]$  can be expressed as:

$$C^l[K] = \sum_{i=1}^n c_i (S_i \Phi(d_{i,1}) - K_i^l e^{-(A_i + \frac{B_i^2}{2})} \Phi(d_{i,2})) \quad (3.3.53)$$

with

$$d_{i,1} = \frac{\log\left(\frac{S_0}{K_i^l}\right) + rt - \frac{1}{2} \frac{\gamma_i^2 \tau}{\gamma_i^2 \tau + 1} v_i^2 y_i T}{y_i B_i} + y_i B_i, \quad (3.3.54)$$

$$d_{i,2} = d_{i,1} - y_i B_i \quad (3.3.55)$$

where

$$K_i^l = S_i \exp \left[ rt - \frac{1}{2} \frac{\gamma_i^2 \tau}{\gamma_i^2 \tau + 1} v_i^2 y_i T + \left( \frac{y_i \gamma_i \tau v_i \sqrt{T}}{t(\gamma_i^2 \tau + 1)} \right) \sqrt{\left( \gamma_i^2 t^2 + \frac{t(T-t)}{T} \right)} \phi^{-1}(F_{D^l}(K)) \right] \quad (3.3.56)$$

with  $y_i$  as given in equation 3.3.37 and  $\sigma_\gamma^2$  given in equation 3.3.38.

$F_{D^l}(K)$  is determined using the relation in equation 3.3.39.

### 3.3.4. Information-based framework model dynamics as a special case of the Black-Scholes model

The Black-Scholes asset pricing model can be recovered from the information-based framework model dynamics.

The asset price process  $\{S_t\}_{(0 \leq t \leq T)}$  can be obtained by rearranging equation 3.1.2 as follows:

$$\frac{dS_t}{S_t} = r dt + \sigma dW_t$$

$$d \log S_t = r dt + \sigma dW_t$$

Using Ito's lemma, let  $b = \log S_t$ :

$$\begin{aligned}
db &= \frac{\partial b}{\partial t} dt + \frac{\partial b}{\partial S_t} dS_t + \frac{1}{2} \frac{\partial^2 b}{\partial S_t^2} (S_t)^2 \\
\frac{\partial b}{\partial t} &= 0, \quad \frac{\partial b}{\partial S_t} = \frac{1}{S_t}, \quad \frac{\partial^2 b}{\partial S_t^2} = -\frac{1}{S_t^2} \\
(dS_t)^2 &= \sigma^2 dS_t^2 dt \\
d \log S_t &= \frac{1}{S_t} dS_t - \frac{1}{S_t^2} (dS_t)^2 \\
d \log S_t &= \frac{1}{S_t} S_t (rdt + \sigma dW_t) - \frac{1}{2S_t^2} \sigma^2 S_t^2 dt \\
&= (rdt + \sigma dW_t) - \frac{1}{2} \sigma^2 dt \\
&= \left( r - \frac{1}{2} \sigma^2 \right) dt + \sigma dW_t \tag{3.3.57}
\end{aligned}$$

Integrating both sides of equation 3.3.57 from 0 to  $t$  gives:

$$\begin{aligned}
\int_0^t d \log S_r &= \int_0^t \left( r - \frac{1}{2} \sigma^2 \right) dr + \int_0^t \sigma dW_r \\
\log S_t - \log S_0 &= \left( r - \frac{1}{2} \sigma^2 \right) t + \sigma W_t \\
\log \left( \frac{S_t}{S_0} \right) &= \left( r - \frac{1}{2} \sigma^2 \right) t + \sigma W_t \\
S_t &= S_0 \exp \left[ \left( r - \frac{1}{2} \sigma^2 \right) t + \sigma W_t \right] \tag{3.3.58}
\end{aligned}$$

Considering the case where  $\gamma^2 T = 1$ , the asset pricing model in equation 3.3.40 reduces to:

$$S_t = S_0 \exp \left[ \left( r - \frac{1}{2} v^2 \right) t + v \xi_t \right] \tag{3.3.59}$$

Equation 3.3.59 takes a similar form to the Black-Scholes asset pricing model given in equation 3.3.58 with  $\sigma = v$  and  $W_t = \xi_t$ .

## 4. Parameter estimation and non-linear filtering

### 4.1. Estimation of model parameters

Parameters in the models discussed in the previous sections will be estimated using MLE, pseudo-MLE and the method of moments.

#### 4.1.1. Maximum likelihood estimation

The method of MLE can be used to estimate parameters in the Black-Scholes model and the information-based asset pricing framework.

Let:

$$x_{t_k} = \left( \frac{S_{t_k}}{S_{t_{k-1}}} \right) \quad (4.1.1)$$

For discrete time points  $t_k$ ,  $k = 1, 2, \dots$ , equation 3.3.58 can be written as:

$$S_{t_k} = S_{t_{k-1}} \exp \left[ \left( r - \frac{1}{2} \sigma^2 \right) \Delta t + \sigma \Delta W \right] \quad (4.1.2)$$

where  $\Delta t = t_k - t_{k-1}$  and  $\Delta W = W_{t_k} - W_{t_{k-1}}$ .

Taking the logs of equation 4.1.2:

$$\log S_{t_k} - \log S_{t_{k-1}} = \left( r - \frac{1}{2} \sigma^2 \right) \Delta t + \sigma \Delta W \quad (4.1.3)$$

The mean and variance of equation 4.1.3 are as follows:

$$\log S_{t_k} - \log S_{t_{k-1}} \sim N \left[ \left( r - \frac{1}{2} \sigma^2 \right) \Delta t, \sigma^2 \Delta t \right] \quad (4.1.4)$$

The parameter to be estimated in the BSM is  $\sigma$ .

Given that there are  $N$  observations, the log likelihood function is given by:

$$L(\sigma) = \sum_{k=1}^N \log f_{\sigma}(x_{t_k}) \quad (4.1.5)$$

where

$$f_{\sigma}(x_{t_k}) = \frac{1}{\sigma x_{t_k} \sqrt{2\pi \Delta t}} \exp \left( - \frac{[\log x_{t_k} - (r - \frac{1}{2} \sigma^2) \Delta t]^2}{2\sigma^2 \Delta t} \right) \quad (4.1.6)$$

Using the method of MLE, the derivative of equation 4.1.5 is taken with respect to the unknown parameters and equating the result to zero.



The mean can be estimated using:

$$m\hat{e}an = \left( r - \frac{1}{2}\hat{\sigma}^2 \right) \Delta t \quad (4.1.7)$$

The estimate for the parameter  $\sigma$  is obtained from the  $m\hat{e}an$  as follows:

$$\begin{aligned} m\hat{e}an &= \sum_{k=1}^n \frac{\log x_{t_k}}{N} \\ &= \bar{x} \end{aligned} \quad (4.1.8)$$

Equation 4.1.7 is equated to equation 4.1.8 and a solution is found for  $\sigma$ .

In the information-based asset pricing framework, the parameters to be estimated are  $\gamma$  and  $v$ . Two models will be considered: the BS-BHM model and the BS-BHM updated model.

In the BS-BHM model, the MLE is done as follows:

For discrete time points, equation 3.3.9 can be written as:

$$S_{t_k} = S_{t_{k-1}} \exp \left( r\Delta t - \frac{1}{2}v^2T + \frac{1}{2} \frac{v\sqrt{T}}{\gamma^2\tau + 1} + \frac{\gamma\tau v\sqrt{T}}{\Delta t(\gamma^2\tau + 1)} \xi_{t_k} \right)$$

Taking the logs of equation 4.1.1:

$$\log S_{t_k} = \log S_{t_{k-1}} + r\Delta t - \frac{1}{2}v^2T + \frac{1}{2} \frac{v\sqrt{T}}{\gamma^2\tau + 1} + \frac{\gamma\tau v\sqrt{T}}{\Delta t(\gamma^2\tau + 1)} \xi_{t_k} \quad (4.1.9)$$

where

$$\tau = \frac{\Delta t T}{T - \Delta t}$$

Equation 4.1.9 has the following distribution:

$$\begin{aligned} \log(x_{t_k}) \sim N \left[ r\Delta t - \frac{1}{2}v^2T + \frac{1}{2} \frac{v\sqrt{T}}{\gamma^2\tau + 1}, \left( \frac{\gamma\tau v\sqrt{T}}{\Delta t(\gamma^2\tau + 1)} \right)^2 \right. \\ \left. \left( \gamma^2\Delta t^2 + \frac{\Delta t(T - \Delta t)}{T} \right) \right] \end{aligned} \quad (4.1.10)$$

Let

$$A' = r\Delta t - \frac{1}{2}v^2T + \frac{1}{2} \frac{v\sqrt{T}}{\gamma^2\tau + 1} \quad (4.1.11)$$

and

$$B'^2 = \left( \frac{\gamma\tau v\sqrt{T}}{\Delta t(\gamma^2\tau + 1)} \right)^2 \gamma^2\Delta t^2 + \frac{\Delta t(T - \Delta t)}{T} \quad (4.1.12)$$

This implies that:

$$\log(x_{t_k}) \sim N\left[A', B'^2\right] \quad (4.1.13)$$

From equation 4.1.13,  $x_{t_k}$  has the following distribution:

$$f_{\gamma, v}(x_{t_k}) = \frac{1}{B' x_k \sqrt{2\pi}} \exp\left(-\frac{1}{2} \left[\frac{\log x_{t_k} - A'}{B'}\right]^2\right) \quad (4.1.14)$$

The log likelihood function is given by:

$$L(\gamma, v) = \sum_{k=1}^N \log f_{\gamma, v}(x_{t_k}) \quad (4.1.15)$$

The derivative of equation 4.1.15 is taken with respect to the unknown parameters and equating the result to zero.

The mean can be estimated using:

$$\widehat{mean}' = \widehat{A}' \quad (4.1.16)$$

and the variance can be estimated as:

$$\widehat{variance}' = \widehat{B}'^2 \quad (4.1.17)$$

The estimates for the parameters are obtained from the  $\widehat{mean}'$  and  $\widehat{variance}'$ .

$$\widehat{mean}' = \bar{x} \quad (4.1.18)$$

and

$$\widehat{variance}' = \sum_{k=1}^N \frac{(\log x_{t_k} - \widehat{mean}')^2}{N} \quad (4.1.19)$$

Equation 4.1.16 is equated to equation 4.1.18 and similarly, equation 4.1.17 is equated to equation 4.1.19 to obtain estimates for  $\gamma$  and  $v$ .

In the BS-BHM updated model, the parameters to be estimated are  $\gamma$  and  $v$ . Using the method of MLE, the estimation of the parameters is done as follows:

For discrete time points in equation 3.3.40 gives:

$$S_{t_k} = S_{t_{k-1}} \exp\left(r\Delta t - \frac{1}{2} \frac{\gamma^2 \tau}{\gamma^2 \tau + 1} v^2 T + \frac{\gamma \tau v \sqrt{T}}{\Delta t (\gamma^2 \tau + 1)} \xi_{t_k}\right) \quad (4.1.20)$$

Equation 4.1.20 leads to:

$$\log(x_{t_k}) \sim N \left[ r\Delta t - \frac{1}{2} \frac{\gamma^2 \tau}{\gamma^2 \tau + 1} v^2 T, \left( \frac{\gamma \tau v \sqrt{T}}{\Delta t (\gamma^2 \tau + 1)} \right)^2 \left( \gamma^2 \Delta t^2 + \frac{\Delta t (T - \Delta t)}{T} \right) \right] \quad (4.1.21)$$

Let

$$A^* = r\Delta t - \frac{1}{2} \frac{\gamma^2 \tau}{\gamma^2 \tau + 1} v^2 T \quad (4.1.22)$$

and

$$B^{*2} = \left( \frac{\gamma \tau v \sqrt{T}}{\Delta t (\gamma^2 \tau + 1)} \right)^2 \left( \gamma^2 \Delta t^2 + \frac{\Delta t (T - \Delta t)}{T} \right) \quad (4.1.23)$$

This implies that:

$$\log(x_{t_k}) \sim N \left[ A^*, B^{*2} \right] \quad (4.1.24)$$

The log likelihood function is given by:

$$L(\gamma, v) = \sum_{k=1}^n \log f_{\gamma, v}(x_{t_k}) \quad (4.1.25)$$

The derivative of equation 4.1.25 is taken with respect to the unknown parameters and equating the result to zero.

The mean can be estimated using:

$$mean^* = \hat{A}^* \quad (4.1.26)$$

and the variance can be estimated as:

$$variance^* = \hat{B}^{*2} \quad (4.1.27)$$

The estimates for the parameters  $\gamma$  and  $v$  are obtained from the  $mean^*$  and  $variance^*$ .

$$mean^* = \bar{x} \quad (4.1.28)$$

and

$$\widehat{variance}^* = \sum_{k=1}^N \frac{(\log x_{t_k} - m\hat{e}an^*)^2}{N} \quad (4.1.29)$$

Equation 4.1.26 is equated to equation 4.1.28 and similarly, equation 4.1.27 is equated to equation 4.1.29 to obtain estimates for  $\gamma$  and  $v$ .

#### 4.1.2. Pseudo-maximum likelihood estimation

This technique is used to estimate parameters in the Heston model, an assumption is made that the volatility parameter,  $V_t$  has been extracted. The unknown parameters to be estimated are  $\kappa$ ,  $\theta$ ,  $\eta$  and  $\rho$ .

The Heston model is specified by the SDEs given by equation 3.1.21 and equation 3.1.22. An approximation is made to equation 3.1.22 over the interval  $[0, T]$  such that:

$$dV_t = \kappa(\theta - V_t)dt + \eta\sqrt{V_{t-\Delta t}}dW_t^\sigma \quad (4.1.30)$$

An assumption is made that  $V_t$  remains constant in a small time interval  $[t - \Delta t, t)$ , where  $\Delta t$  represents the sampling step.

From equation 4.1.30, it follows that:

$$V_t - V_{t-\Delta t} = \kappa \int_{t-\Delta t}^t (\theta - V_s)ds + \eta\sqrt{V_{t-\Delta t}} \int_{t-\Delta t}^t dW_s^\sigma \quad (4.1.31)$$

The discretized model corresponding to 4.1.31 is given as:

$$V_t = e^{-\kappa\Delta t}V_{t-\Delta t} + \theta[1 - e^{-\kappa\Delta t}] + \varepsilon_t \quad for \ t = 1, 2, \dots, T$$

where  $E[\varepsilon_t] = 0$ ,  $E[\varepsilon_t\varepsilon_s] = 0$  for  $s \neq t$  and

$$\begin{aligned} E[\varepsilon_t^2] &= \int_{t-\Delta t}^t e^{-2\kappa\Delta t(t-\tau)}\eta^2V(t-\Delta t)d\tau \\ &= \frac{1}{2}\eta^2\kappa^{-1}(1 - e^{-2\kappa\Delta t})V_{t-\Delta t} \end{aligned}$$

and

$$Var[\varepsilon_t] = \frac{1}{2}\eta^2\kappa^{-1}(1 - e^{-2\kappa\Delta t})V_{t-\Delta t}$$

The pseudo log-likelihood function of  $\varepsilon_t$  is given as follows:

$$\log L(\kappa, \theta, \eta) = - \sum_{k=1}^n \left[ \frac{1}{2} \log \{ \text{Var}(\varepsilon_t) \} + \frac{1}{2} \text{Var}^{-1}(\varepsilon_t) \{ V_k - e^{-\kappa \Delta t} V_{k-1} - \theta(1 - e^{-\kappa \Delta t}) \}^2 \right]$$

By differentiating the log-likelihood with respect to the parameters  $\kappa$ ,  $\theta$  and  $\eta$ , the following result is obtained:

$$\hat{\kappa} = -\frac{1}{\Delta t} \log(\hat{\beta}_1), \quad \hat{\theta} = \hat{\beta}_2 \quad \text{and} \quad \hat{\eta}^2 = \frac{2\hat{\kappa}\hat{\beta}_3}{1 - \hat{\beta}_1^2}$$

where

$$\begin{aligned} \hat{\beta}_1 &= \frac{n^{-2} \sum_{k=1}^n V_k \sum_{k=1}^n V_{k-1}^{-1} - n^{-1} \sum_{k=1}^n V_k V_{k-1}^{-1}}{n^{-2} \sum_{k=1}^n V_{k-1} \sum_{k=1}^n V_{k-1}^{-1} - 1}, \\ \hat{\beta}_2 &= \frac{n^{-1} \sum_{k=1}^n V_k V_{k-1}^{-1} - \hat{\beta}_1}{(1 - \hat{\beta}_1) n^{-1} \sum_{k=1}^n V_{k-1}^{-1}}, \\ \hat{\beta}_3 &= n^{-1} \sum_{k=1}^n \{ V_k - V_{k-1} \hat{\beta}_1 - \hat{\beta}_2 (1 - \hat{\beta}_1)^2 \} V_{k-1}^{-1} \end{aligned}$$

Once the parameters  $\kappa$ ,  $\eta$  and  $\theta$  have been estimated, the estimation of  $\rho$  can be done. By applying Ito's lemma, equation 3.1.21 can be written as:

$$d \ln S_t = (r - \frac{1}{2} V_t) dt + \sqrt{V_t} dW_t^S$$

To remove correlation between equation 3.1.21 and equation 3.1.22, let:

$$dW_t^S = \rho dW_t^\sigma + \sqrt{1 - \rho^2} dW_t^B \quad (4.1.32)$$

where  $W_t^\sigma$  and  $W_t^B$  are uncorrelated Brownian motions.

This leads to:

$$\begin{aligned} d \ln S_t &= (r - \frac{1}{2} V_t) dt + \sqrt{V_t} (\rho dW_t^\sigma + \sqrt{1 - \rho^2} dW_t^B) \\ &= (r - \frac{1}{2} V_t) dt + \sqrt{V_t} \rho dW_t^\sigma + \sqrt{V_t} \sqrt{1 - \rho^2} dW_t^B \end{aligned} \quad (4.1.33)$$

From equation 3.1.22, it follows that:

$$\sqrt{V_t} dW_t^\sigma = \frac{1}{\eta} \left( dV_t - \kappa(\theta - V_t) dt \right) \quad (4.1.34)$$

Substituting equation 4.1.34 into equation 4.1.33 gives:

$$d \ln S_t = \left( r - \frac{1}{2} V_t \right) dt + \frac{\rho}{\eta} \left( dV_t - \kappa(\theta - V_t) dt \right) + \sqrt{V_t} \sqrt{1 - \rho^2} dW_t^B \quad (4.1.35)$$

An approximation for  $\ln S_t$  can be obtained as follows:

$$\ln S_t = \ln S_{t-1} + \left[ r - \frac{1}{2} V_{t-\Delta t} - \frac{\rho}{\eta} \kappa(\theta - V_{t-\Delta t}) \right] \Delta t + \frac{\rho}{\eta} (V_t - V_{t-\Delta t}) + \xi_t \quad (4.1.36)$$

where  $E[\xi_t] = 0$ ,  $E[\xi_t \xi_s] = 0$ , if  $t \neq s$ , and  $E[\xi_t^2] = V_{t-\Delta t} (1 - \rho^2) \Delta t$ .

An assumption is made that  $\xi_t$  follows a normal distribution, thus:

$$\xi_t \sim N(0, V_{t-\Delta t} (1 - \rho^2) \Delta t) \quad (4.1.37)$$

In this case, the pseudo log-likelihood function will be given as:

$$\log L(\rho) = - \sum_{k=1}^n \left[ \frac{1}{2} \log \{ \text{Var}(\xi_k) \} + \frac{1}{2} \text{Var}^{-1}(\xi_k) \{ b \}^2 \right] \quad (4.1.38)$$

where

$$b = \ln S_{t_k} - \ln S_{t_{k-1}} + \left[ r - \frac{1}{2} V_{k-1} - \frac{\rho}{\eta} \kappa(\theta - V_{k-1}) \right] \Delta k + \frac{\rho}{\eta} (V_k - V_{k-1}) \quad (4.1.39)$$

The estimate for  $\rho$  can then be obtained by obtaining the derivative of equation 4.1.38 with respect to  $\rho$  and equating it to zero. The second derivative can be obtain to check that the estimator is indeed a maximum point.

$$\begin{aligned} b^2 &= \left( \ln S_{t_k} - \ln S_{t_{k-1}} + \left[ r - \frac{1}{2} V_{k-1} - \frac{\rho}{\eta} \kappa(\theta - V_{k-1}) \right] \Delta k + \frac{\rho}{\eta} (V_k - V_{k-1}) \right)^2 \\ &= \left( \ln S_{t_k} - \ln S_{t_{k-1}} + \left( r - \frac{1}{2} V_{k-1} \right) \Delta k - \frac{\rho}{\eta} \kappa(\theta - V_{k-1}) \Delta k + \frac{\rho}{\eta} (V_k - V_{k-1}) \right)^2 \\ &= \left( \ln S_{t_k} - \ln S_{t_{k-1}} + \left( r - \frac{1}{2} V_{k-1} \right) \Delta k - \frac{\rho}{\eta} \left[ \kappa(\theta - V_{k-1}) \Delta k - (V_k - V_{k-1}) \right] \right)^2 \\ &= \left( \ln S_{t_k} - \ln S_{t_{k-1}} + \left( r - \frac{1}{2} V_{k-1} \right) \Delta k \right)^2 - 2 \left( \ln S_{t_k} - \ln S_{t_{k-1}} + \left( r - \frac{1}{2} V_{k-1} \right) \Delta k \right) \times \\ &\quad \frac{\rho}{\eta} \left[ \kappa(\theta - V_{k-1}) \Delta k - (V_k - V_{k-1}) \right] + \left( \frac{\rho}{\eta} \right)^2 \left[ \kappa(\theta - V_{k-1}) \Delta k - (V_k - V_{k-1}) \right]^2 \end{aligned}$$

$$\begin{aligned}
\frac{\partial}{\partial \rho} \log L(\rho) &= - \frac{\partial}{\partial \rho} \sum_{k=1}^n \left[ \frac{1}{2} \log \{ \text{Var}(\xi_k) \} + \frac{1}{2} \text{Var}^{-1}(\xi_k) \{b\}^2 \right] \\
&= - \frac{\partial}{\partial \rho} \sum_{k=1}^n \frac{1}{2} \log \{ \text{Var}(\xi_k) \} - \frac{\partial}{\partial \rho} \sum_{k=1}^n \frac{1}{2} \text{Var}^{-1}(\xi_k) \{b\}^2 \\
&= - \frac{\partial}{\partial \rho} \sum_{k=1}^n \frac{1}{2} \text{Var}^{-1}(\xi_k) \{b\}^2 \\
&= - \sum_{k=1}^n \frac{1}{2} \text{Var}^{-1}(\xi_k) \frac{\partial}{\partial \rho} \{b\}^2
\end{aligned}$$

$$\begin{aligned}
\frac{\partial}{\partial \rho} \log L(\rho) &= - \sum_{k=1}^n \frac{1}{2} \text{Var}^{-1}(\xi_k) \frac{\partial}{\partial \rho} \left[ \left( \ln S_{t_k} - \ln S_{t_{k-1}} + \left( r - \frac{1}{2} V_{k-1} \right) \Delta k \right)^2 \right. \\
&\quad \left. - 2 \left( \ln S_{t_k} - \ln S_{t_{k-1}} + \left( r - \frac{1}{2} V_{k-1} \right) \Delta k \right) \frac{\rho}{\eta} \left[ \kappa(\theta - V_{k-1}) \Delta k - (V_k - V_{k-1}) \right] \right. \\
&\quad \left. + \left( \frac{\rho}{\eta} \right)^2 \left[ \kappa(\theta - V_{k-1}) \Delta k - (V_k - V_{k-1}) \right]^2 \right] \\
&= - \sum_{k=1}^n \frac{1}{2} \text{Var}^{-1}(\xi_k) \left[ \frac{\partial}{\partial \rho} \left( \ln S_{t_k} - \ln S_{t_{k-1}} + \left( r - \frac{1}{2} V_{k-1} \right) \Delta k \right)^2 \right. \\
&\quad \left. - 2 \frac{\partial}{\partial \rho} \left( \ln S_{t_k} - \ln S_{t_{k-1}} + \left( r - \frac{1}{2} V_{k-1} \right) \Delta k \right) \frac{\rho}{\eta} \left[ \kappa(\theta - V_{k-1}) \Delta k - (V_k - V_{k-1}) \right] \right. \\
&\quad \left. + \frac{\partial}{\partial \rho} \left( \frac{\rho}{\eta} \right)^2 \left[ \kappa(\theta - V_{k-1}) \Delta k - (V_k - V_{k-1}) \right]^2 \right] \\
&= - \sum_{k=1}^n \frac{1}{2} \text{Var}^{-1}(\xi_k) \left[ - 2 \left( \ln S_{t_k} - \ln S_{t_{k-1}} + \left( r - \frac{1}{2} V_{k-1} \right) \Delta k \right) \times \right. \\
&\quad \left. \frac{1}{\eta} \left[ \kappa(\theta - V_{k-1}) \Delta k - (V_k - V_{k-1}) \right] + \left( \frac{2\rho}{\eta^2} \right) \left[ \kappa(\theta - V_{k-1}) \Delta k - (V_k - V_{k-1}) \right]^2 \right]
\end{aligned}$$

Equating the derivative of the log-likelihood with respect to  $\rho$  to zero and solving for  $\rho$ :

$$\frac{\partial}{\partial \rho} \log L(\rho) = 0$$

$$-\sum_{k=1}^n \frac{1}{2} \text{Var}^{-1}(\xi_k) \left[ -2 \left( \ln S_{t_k} - \ln S_{t_{k-1}} + \left(r - \frac{1}{2} V_{k-1}\right) \Delta k \right) \frac{1}{\eta} \left[ \kappa(\theta - V_{k-1}) \Delta k - (V_k - V_{k-1}) \right] \right. \\ \left. + \left( \frac{2\rho}{\eta^2} \right) \left[ \kappa(\theta - V_{k-1}) \Delta k - (V_k - V_{k-1}) \right]^2 \right] = 0$$

$$\left[ -2 \sum_{k=1}^n \frac{1}{2} \text{Var}^{-1}(\xi_k) \left( \ln S_{t_k} - \ln S_{t_{k-1}} + \left(r - \frac{1}{2} V_{k-1}\right) \Delta k \right) \frac{1}{\eta} \left[ \kappa(\theta - V_{k-1}) \Delta k - (V_k - V_{k-1}) \right] \right. \\ \left. + \left( \frac{2\rho}{\eta^2} \right) \sum_{k=1}^n \frac{1}{2} \text{Var}^{-1}(\xi_k) \left[ \kappa(\theta - V_{k-1}) \Delta k - (V_k - V_{k-1}) \right]^2 \right] = 0$$

$$\rho \sum_{k=1}^n \text{Var}^{-1}(\xi_k) \left[ \kappa(\theta - V_{k-1}) \Delta k - (V_k - V_{k-1}) \right]^2 \\ = -\eta \sum_{k=1}^n \text{Var}^{-1}(\xi_k) \left( \ln S_{t_k} - \ln S_{t_{k-1}} + \left(r - \frac{1}{2} V_{k-1}\right) \Delta k \right) \left( \kappa(\theta - V_{k-1}) \Delta k - (V_k - V_{k-1}) \right)$$

$$\hat{\rho} = \frac{-\eta \sum_{k=1}^n \text{Var}^{-1}(\xi_k) \left( \ln S_{t_k} - \ln S_{t_{k-1}} + \left(r - \frac{1}{2} V_{k-1}\right) \Delta k \right) \left( \kappa(\theta - V_{k-1}) \Delta k - (V_k - V_{k-1}) \right)}{\sum_{k=1}^n \text{Var}^{-1}(\xi_k) \left[ \kappa(\theta - V_{k-1}) \Delta k - (V_k - V_{k-1}) \right]^2} \quad (4.1.40)$$

thus, an estimate of  $\rho$  can be obtained from equation 4.1.40.

#### 4.1.3. Method of moments

The method of moments can also be used to estimate parameters in the information-based asset pricing model.

The  $\log x_{t_k}$  where  $x_{t_k}$  is as defined in 4.1.1 are assumed to be independent of each other and denote the log of the ratio of the underlying asset prices.

Given that there are  $N$  observations, the first sample moment which denotes the sample mean is given as:

$$m_1 = \frac{1}{N} \sum_{k=1}^N \log x_{t_k} \quad (4.1.41)$$



Similarly, the second sample moment is given as:

$$m_2 = \frac{1}{N} \sum_{k=1}^N (\log x_{t_k})^2 \quad (4.1.42)$$

Suppose that  $\mu_1^*$  and  $\mu_2^*$  denote the first and second moments respectively for the BS-BHM model. Using equation 4.1.10, it follows that:

$$\begin{aligned} \mu_1^* &= E[\log x_{t_k}] \\ &= r\Delta t - \frac{1}{2}v^2T + \frac{1}{2} \frac{v\sqrt{T}}{\gamma^2\tau + 1} \end{aligned} \quad (4.1.43)$$

and

$$\begin{aligned} \mu_2^* &= E[\log x_{t_k}]^2 \\ &= \text{Var}[\log x_{t_k}] + (E[\log x_{t_k}])^2 \\ &= \left( \frac{\gamma\tau v\sqrt{T}}{\Delta t(\gamma^2\tau + 1)} \right)^2 \left( \gamma^2\Delta t^2 + \frac{\Delta t(T - \Delta t)}{T} \right) + \left( r\Delta t - \frac{1}{2}v^2T + \frac{1}{2} \frac{v\sqrt{T}}{\gamma^2\tau + 1} \right)^2 \end{aligned} \quad (4.1.44)$$

The next step is to equate the sample moments to the moments from the BS-BHM model as follows:

$$\begin{aligned} m_1 &= \mu_1^* \\ m_1 &= r\Delta t - \frac{1}{2}v^2T + \frac{1}{2} \frac{v\sqrt{T}}{\gamma^2\tau + 1} \end{aligned} \quad (4.1.45)$$

Making  $v^2$  to be the subject:

$$v^2 = \frac{2(m_1 - r\Delta t)}{T} - \frac{v\sqrt{T}}{(\gamma^2\tau + 1)T} \quad (4.1.46)$$

Similarly:

$$m_2 = \mu_2^* = \left( \frac{\gamma\tau v\sqrt{T}}{\Delta t(\gamma^2\tau + 1)} \right)^2 \left( \gamma^2\Delta t^2 + \frac{\Delta t(T - \Delta t)}{T} \right) + \left( r\Delta t - \frac{1}{2}v^2T + \frac{1}{2}\frac{v\sqrt{T}}{\gamma^2\tau + 1} \right)^2 \quad (4.1.47)$$

$$= \left( \frac{\gamma\tau v\sqrt{T}}{\Delta t(\gamma^2\tau + 1)} \right)^2 \left( \gamma^2\Delta t^2 + \frac{\Delta t(T - \Delta t)}{T} \right) + m_1^2$$

$$v^2 = \frac{(m_2 - m_1^2)\Delta t(\gamma^2\tau + 1)^2}{\gamma^2\tau^2(\gamma^2\Delta tT + (T - \Delta t))} \quad (4.1.48)$$

Equating equation 4.1.55 and equation 4.1.56 yields:

$$\frac{2(m_1 - r\Delta t)}{T} - \frac{v\sqrt{T}}{(\gamma^2\tau + 1)T} = \frac{(m_2 - m_1^2)\Delta t(\gamma^2\tau + 1)^2}{\gamma^2\tau^2(\gamma^2\Delta tT + (T - \Delta t))} \quad (4.1.49)$$

Making  $v$  to be the subject:

$$v = \frac{(\gamma^2\tau + 1)T}{\sqrt{T}} \left[ \frac{2(m_1 - r\Delta t)}{T} - \frac{(m_2 - m_1^2)\Delta t(\gamma^2\tau + 1)^2}{\gamma^2\tau^2(\gamma^2\Delta tT + (T - \Delta t))} \right] \quad (4.1.50)$$

Suppose that  $\mu_1$  and  $\mu_2$  denote the first and second moments respectively for the BS-BHM updated model. Using equation 4.1.21, it follows that:

$$\begin{aligned} \mu_1 &= E[\log x_{t_k}] \\ &= r\Delta t - \frac{1}{2}\frac{\gamma^2\tau}{\gamma^2\tau + 1}v^2T \end{aligned} \quad (4.1.51)$$

and

$$\begin{aligned} \mu_2 &= E[\log x_{t_k}]^2 \\ &= Var[\log x_{t_k}] + (E[\log x_{t_k}])^2 \\ &= \left( \frac{\gamma\tau v\sqrt{T}}{\Delta t(\gamma^2\tau + 1)} \right)^2 \left( \gamma^2\Delta t^2 + \frac{\Delta t(T - \Delta t)}{T} \right) + \left( r\Delta t - \frac{1}{2}\frac{\gamma^2\tau}{\gamma^2\tau + 1}v^2T \right)^2 \end{aligned} \quad (4.1.52)$$

The next step is to equate the sample moments to the moments from the BS-BHM updated

model as follows:

$$\begin{aligned}
 m_1 &= \mu_1 \\
 m_1 &= r\Delta t - \frac{1}{2} \frac{\gamma^2 \tau}{\gamma^2 \tau + 1} v^2 T
 \end{aligned} \tag{4.1.53}$$

Making  $v^2$  to be the subject:

$$v^2 = \frac{2(r\Delta t - m_1)(\gamma^2 \tau + 1)}{\gamma^2 \tau T} \tag{4.1.54}$$

$$v^2 = \frac{2(r\Delta t - m_1)}{T} + \frac{2(r\Delta t - m_1)}{\gamma^2 \tau T} \tag{4.1.55}$$

Similarly:

$$\begin{aligned}
 m_2 &= \mu_2 \\
 &= \left( \frac{\gamma \tau v \sqrt{T}}{\Delta t (\gamma^2 \tau + 1)} \right)^2 \left( \gamma^2 \Delta t^2 + \frac{\Delta t (T - \Delta t)}{T} \right) + \left( r\Delta t - \frac{1}{2} \frac{\gamma^2 \tau}{\gamma^2 \tau + 1} v^2 T \right)^2 \\
 &= \left( \frac{\gamma \tau v \sqrt{T}}{\Delta t (\gamma^2 \tau + 1)} \right)^2 \left( \gamma^2 \Delta t^2 + \frac{\Delta t (T - \Delta t)}{T} \right) + m_1^2 \\
 v^2 &= \frac{(m_2 - m_1^2) \Delta t (\gamma^2 \tau + 1)^2}{\gamma^2 \tau^2 (\gamma^2 \Delta t T + (T - \Delta t))}
 \end{aligned} \tag{4.1.56}$$

Equating equation 4.1.55 and equation 4.1.56 yields:

$$\begin{aligned}
 \frac{2(r\Delta t - m_1)(\gamma^2 \tau + 1)}{\gamma^2 \tau T} &= \frac{(m_2 - m_1^2) \Delta t (\gamma^2 \tau + 1)^2}{\gamma^2 \tau^2 (\gamma^2 \Delta t T + (T - \Delta t))} \\
 \frac{2(r\Delta t - m_1)}{T} &= \frac{(m_2 - m_1^2) \Delta t (\gamma^2 \tau + 1)}{\tau (\gamma^2 \Delta t T + (T - \Delta t))}
 \end{aligned}$$

Making  $\gamma^2$  to be the subject:

$$\begin{aligned}
 2\tau(r\Delta t - m_1)(\gamma^2 \Delta t T + (T - \Delta t)) &= \Delta t T (m_2 - m_1^2) (\gamma^2 \tau + 1) \\
 2\tau \gamma^2 \Delta t T (r\Delta t - m_1) + 2\tau (r\Delta t - m_1)(T - \Delta t) &= \Delta t T \gamma^2 \tau (m_2 - m_1^2) + \Delta t T (m_2 - m_1^2) \\
 \gamma^2 &= \frac{\Delta t T (m_2 - m_1^2) - 2\tau (r\Delta t - m_1)(T - \Delta t)}{2\tau \Delta t T (r\Delta t - m_1) - \Delta t T \tau (m_2 - m_1^2)}
 \end{aligned} \tag{4.1.57}$$

Thus:

$$\hat{\gamma} = \sqrt{\frac{\Delta t T (m_2 - m_1^2) + 2\tau(r\Delta t - m_1)(T - \Delta t)}{2\tau\Delta t T(r\Delta t - m_1) - \Delta t T \tau(m_2 - m_1^2)}} \quad (4.1.58)$$

Substituting equation 4.1.57 into equation 4.1.55, an estimate for  $v$  can be obtained as follows:

$$v^2 = \frac{2(r\Delta t - m_1)}{T} + \frac{2(r\Delta t - m_1)[2\Delta t(r\Delta t - m_1) - \Delta t(m_2 - m_1^2)]}{\Delta t T (m_2 - m_1^2) + 2\tau(r\Delta t - m_1)(T - \Delta t)} \quad (4.1.59)$$

Thus:

$$\hat{v} = \sqrt{\frac{2(r\Delta t - m_1)}{T} + \frac{2(r\Delta t - m_1)[2\Delta t(r\Delta t - m_1) - \Delta t(m_2 - m_1^2)]}{\Delta t T (m_2 - m_1^2) + 2\tau(r\Delta t - m_1)(T - \Delta t)}} \quad (4.1.60)$$

#### 4.1.4. Measurement of parameter sensitivity

An option's delta measures the variation in the price of an option with respect to changes in the underlying asset assuming that the other parameters are unchanged at that time. It is defined as follows:

$$delta = \frac{\partial f}{\partial S}$$

where  $f$  is a function denoting the option price and  $S$  denotes the underlying asset price. For the Black-Scholes model, it is given as:

$$delta = \Phi(d_1)$$

**Proposition 4.1.** *A European call option's delta under the BS-BHM model is given as follows:*

$$delta = e^{\varphi + \frac{1}{2}\delta^2} \left[ \Phi(d_1) + \frac{1}{\delta} \Phi'(d_1) \right] + \frac{K}{\delta S} \Phi'(-d_2) \quad (4.1.61)$$

*Proof.* For the BS-BHM model, delta is computed as follows:

$$\begin{aligned}
\text{delta} &= \frac{\partial(S e^{\varphi + \frac{1}{2}\delta^2} \Phi(d_1) - K \Phi(-d_2))}{\partial S} \\
&= \frac{\partial(S e^{\varphi + \frac{1}{2}\delta^2} \Phi(d_1))}{\partial S} - \frac{\partial(K \Phi(-d_2))}{\partial S} \\
&= e^{\varphi + \frac{1}{2}\delta^2} \frac{\partial(S \Phi(d_1))}{\partial S} - K \frac{\partial(\Phi(-d_2))}{\partial S} \\
&= e^{\varphi + \frac{1}{2}\delta^2} \left[ \Phi(d_1) \frac{\partial S}{\partial S} + S \frac{\partial(\Phi(d_1))}{\partial S} \right] - K \frac{\partial(\Phi(-d_2))}{\partial S} \\
&= e^{\varphi + \frac{1}{2}\delta^2} \left[ \Phi(d_1) + S \Phi'(d_1) \frac{\partial d_1}{\partial S} \right] + K \Phi'(-d_2) \frac{\partial(d_2)}{\partial S} \tag{4.1.62}
\end{aligned}$$

The partial derivative of  $d_1$  with respect to  $S$  is given by:

$$\begin{aligned}
\frac{\partial d_1}{\partial S} &= \frac{\partial\left(\frac{\log\left(\frac{S}{K}\right) + \varphi}{\delta} + \delta\right)}{\partial S} \\
&= \frac{\partial\left(\frac{\log\left(\frac{S}{K}\right) + \varphi}{\delta}\right)}{\partial S} \\
&= \frac{1}{\delta} \frac{\partial(\log\left(\frac{S}{K}\right))}{\partial S} \\
&= \frac{1}{\delta S} \tag{4.1.63}
\end{aligned}$$

Substituting for  $\frac{\partial d_1}{\partial S}$  as given in equation 4.1.63 into equation 4.1.62 leads to:

$$\text{delta} = e^{\varphi + \frac{1}{2}\delta^2} \left[ \Phi(d_1) + \frac{1}{\delta} \Phi'(d_1) \right] + \frac{K}{\delta S} \Phi'(-d_2) \tag{4.1.64}$$

An option's gamma measures the rate of variation in delta with respect to changes in the underlying asset assuming that the other parameters are unchanged at that time.

It is useful in assessing delta stability, which can be used to determine the probability of an option attaining the strike price value at expiry and is given as follows:

$$\text{gamma} = \frac{\partial^2 f}{\partial S^2}$$

For the Black-Scholes model, it is given as:

$$\text{gamma} = \frac{\Phi(d_1)}{\sigma S \sqrt{T-t}}$$

**Proposition 4.2.** A European call option's gamma under the BS-BHM model is given as follows:

$$\text{gamma} = e^{\varphi + \frac{1}{2}\delta^2} \frac{1}{\delta S} \left[ \Phi'(d_1) + \frac{1}{\delta} \Phi''(d_1) \right] - \frac{K}{\delta S^2} \left[ \Phi'(-d_2) + \frac{1}{\delta} \Phi''(-d_2) \right] \quad (4.1.65)$$

*Proof.* For the BS-BHM model, gamma is computed as follows:

$$\begin{aligned} \text{gamma} &= \frac{\partial^2 (S e^{\varphi + \frac{1}{2}\delta^2} \Phi(d_1) - K \Phi(-d_2))}{\partial S^2} \\ &= \frac{\partial (e^{\varphi + \frac{1}{2}\delta^2} [\Phi(d_1) + \frac{1}{\delta} \Phi'(d_1)] + \frac{K}{\delta S} \Phi'(-d_2))}{\partial S} \\ &= \frac{\partial (e^{\varphi + \frac{1}{2}\delta^2} [\Phi(d_1) + \frac{1}{\delta} \Phi'(d_1)])}{\partial S} + \frac{\partial (\frac{K}{\delta S} \Phi'(-d_2))}{\partial S} \\ &= e^{\varphi + \frac{1}{2}\delta^2} \frac{\partial ([\Phi(d_1) + \frac{1}{\delta} \Phi'(d_1)])}{\partial S} + \frac{K}{\delta} \frac{\partial (\frac{1}{S} \Phi'(-d_2))}{\partial S} \\ &= e^{\varphi + \frac{1}{2}\delta^2} \left[ \frac{\partial (\Phi(d_1))}{\partial S} + \frac{1}{\delta} \frac{\partial (\Phi'(d_1))}{\partial S} \right] + \frac{K}{\delta} \left[ \Phi'(-d_2) \frac{\partial \frac{1}{S}}{\partial S} + \frac{1}{S} \frac{\partial (\Phi'(-d_2))}{\partial S} \right] \\ &= e^{\varphi + \frac{1}{2}\delta^2} \left[ \Phi'(d_1) \frac{\partial d_1}{\partial S} + \frac{1}{\delta} \Phi''(d_1) \frac{\partial d_1}{\partial S} \right] - \frac{K}{\delta} \left[ \Phi'(-d_2) \frac{1}{S^2} + \frac{1}{S} \Phi''(-d_2) \frac{\partial d_2}{\partial S} \right] \\ &= e^{\varphi + \frac{1}{2}\delta^2} \left[ \Phi'(d_1) + \frac{1}{\delta} \Phi''(d_1) \right] \frac{\partial d_1}{\partial S} - \frac{K}{\delta} \left[ \Phi'(-d_2) \frac{1}{S^2} + \frac{1}{S} \Phi''(-d_2) \frac{\partial d_1}{\partial S} \right] \\ &= e^{\varphi + \frac{1}{2}\delta^2} \frac{1}{\delta S} \left[ \Phi'(d_1) + \frac{1}{\delta} \Phi''(d_1) \right] - \frac{K}{\delta S^2} \left[ \Phi'(-d_2) + \frac{1}{\delta} \Phi''(-d_2) \right] \quad (4.1.66) \end{aligned}$$

Equation 4.1.66 gives the value for gamma for the BS-BHM information-based model.

The likelihood of variations in implied volatility is measured by vega. Vega measures the rate of variation in the asset with respect to changes in the assumed level of volatility assuming that the other parameters are unchanged at that time. Higher volatility results in options being more expensive because at some point there is a greater chance of reaching the strike price. It is defined as follows:

$$\text{vega} = \frac{\partial f}{\partial \sigma}$$

For the Black-Scholes model, it is given as:

$$\text{vega} = S \sqrt{T - t} \Phi(d_1)$$

**Proposition 4.3.** A European call option's vega under the BS-BHM model is given as

follows:

$$\begin{aligned}
\text{vega} &= (S + K) \left[ e^{\varphi + \frac{1}{2}\delta^2} \frac{\partial \Phi(d_1)}{\partial \gamma} \right. \\
&\quad + \Phi(d_1) e^{\varphi + \frac{1}{2}\delta^2} \left[ \frac{\tau v \sqrt{T}}{t} \sqrt{\left( \gamma^2 t^2 + \frac{t(T-t)}{T} \right)} \left[ \left( \frac{2\gamma^2}{\gamma^2 \tau + 1} \right)^{-2} + \left( \frac{1}{\gamma^2 \tau + 1} \right) \right] \right. \\
&\quad \left. \left. + \left( \frac{\gamma^2 t \tau v \sqrt{T}}{(\gamma^2 \tau + 1)} \right) \left( \gamma^2 t^2 + \frac{t(T-t)}{T} \right)^{-\frac{1}{2}} - 2\gamma v \sqrt{T} \left( \frac{1}{\gamma^2 \tau + 1} \right)^2 \right] \right] \quad (4.1.67)
\end{aligned}$$

*Proof.* For the information-based model, the parameter  $\gamma$  is seen to give the volatility. This implies, to compute the vega for the information-based model, a partial derivative of the price is obtained with respect to  $\gamma$  as follows:

$$\begin{aligned}
\text{vega} &= \frac{\partial f}{\partial \gamma} \\
&= \frac{\partial (S e^{\varphi + \frac{1}{2}\delta^2} \Phi(d_1) - K \Phi(-d_2))}{\partial \gamma} \\
&= \frac{\partial S e^{\varphi + \frac{1}{2}\delta^2} \Phi(d_1)}{\partial \gamma} - \frac{\partial (K \Phi(-d_2))}{\partial \gamma} \\
&= S \frac{\partial e^{\varphi + \frac{1}{2}\delta^2} \Phi(d_1)}{\partial \gamma} - K \frac{\partial \Phi(-d_2)}{\partial \gamma} \quad (4.1.68)
\end{aligned}$$

$$\frac{\partial e^{\varphi + \frac{1}{2}\delta^2} \Phi(d_1)}{\partial \gamma} = e^{\varphi + \frac{1}{2}\delta^2} \frac{\partial \Phi(d_1)}{\partial \gamma} + \Phi(d_1) \frac{\partial e^{\varphi + \frac{1}{2}\delta^2}}{\partial \gamma} \quad (4.1.69)$$

$$\frac{\partial \Phi(d_1)}{\partial \gamma} = \Phi(d_1) \frac{\partial d_1}{\partial \gamma} \quad (4.1.70)$$

$$\begin{aligned}
\frac{\partial d_1}{\partial \gamma} &= \frac{\partial \left( \frac{\log \left( \frac{S}{K} \right) + \varphi}{\delta} + \delta \right)}{\partial \gamma} \\
&= \frac{\partial \left( \frac{\varphi}{\delta} + \delta \right)}{\partial \gamma} \\
&= \frac{\partial \left( \frac{\varphi}{\delta} \right)}{\partial \gamma} + \frac{\partial (\delta)}{\partial \gamma} \quad (4.1.71)
\end{aligned}$$

$$\frac{\partial \left( \frac{\varphi}{\delta} \right)}{\partial \gamma} = \frac{1}{\delta} \frac{\partial \varphi}{\partial \gamma} + \varphi \frac{\partial \left( \frac{1}{\delta} \right)}{\partial \gamma} \quad (4.1.72)$$

$$\begin{aligned}
\frac{\partial \varphi}{\partial \gamma} &= \frac{\partial \left( rt - \frac{1}{2}v^2T + \frac{1}{2} \frac{v\sqrt{T}}{\gamma^2\tau+1} \right)}{\partial \gamma} \\
&= \frac{\partial \left( \frac{1}{2} \frac{v\sqrt{T}}{\gamma^2\tau+1} \right)}{\partial \gamma} \\
&= \frac{1}{2}v\sqrt{T} \frac{\partial \left( \frac{1}{\gamma^2\tau+1} \right)}{\partial \gamma} \\
&= -2\gamma v\sqrt{T} \left( \frac{1}{\gamma^2\tau+1} \right)^2
\end{aligned} \tag{4.1.73}$$

$$\begin{aligned}
\frac{\partial \left( \frac{1}{\delta} \right)}{\partial \gamma} &= \frac{\partial \left[ \left( \frac{\gamma\tau v\sqrt{T}}{t(\gamma^2\tau+1)} \right) \sqrt{\left( \gamma^2t^2 + \frac{t(T-t)}{T} \right)} \right]^{-1}}{\partial \gamma} \\
&= (-1) \left[ \left( \frac{\gamma\tau v\sqrt{T}}{t(\gamma^2\tau+1)} \right) \sqrt{\left( \gamma^2t^2 + \frac{t(T-t)}{T} \right)} \right]^{-2} \frac{\partial \left( \frac{\gamma\tau v\sqrt{T}}{t(\gamma^2\tau+1)} \right) \sqrt{\left( \gamma^2t^2 + \frac{t(T-t)}{T} \right)}}{\partial \gamma}
\end{aligned} \tag{4.1.74}$$

$$\begin{aligned}
\frac{\partial \left( \frac{\gamma\tau v\sqrt{T}}{t(\gamma^2\tau+1)} \right) \sqrt{\left( \gamma^2t^2 + \frac{t(T-t)}{T} \right)}}{\partial \gamma} &= \sqrt{\left( \gamma^2t^2 + \frac{t(T-t)}{T} \right)} \frac{\partial \left( \frac{\gamma\tau v\sqrt{T}}{t(\gamma^2\tau+1)} \right)}{\partial \gamma} \\
&\quad + \left( \frac{\gamma\tau v\sqrt{T}}{t(\gamma^2\tau+1)} \right) \frac{\partial \sqrt{\left( \gamma^2t^2 + \frac{t(T-t)}{T} \right)}}{\partial \gamma}
\end{aligned} \tag{4.1.75}$$

$$\frac{\partial \left( \frac{\gamma\tau v\sqrt{T}}{t(\gamma^2\tau+1)} \right)}{\partial \gamma} = \frac{\tau v\sqrt{T}}{t} \frac{\partial \left( \frac{\gamma}{\gamma^2\tau+1} \right)}{\partial \gamma} \tag{4.1.76}$$

$$\begin{aligned}
\frac{\partial \left( \frac{\gamma}{\gamma^2\tau+1} \right)}{\partial \gamma} &= \gamma \frac{\partial \left( \frac{1}{\gamma^2\tau+1} \right)}{\partial \gamma} + \left( \frac{1}{\gamma^2\tau+1} \right) \frac{\partial \gamma}{\partial \gamma} \\
&= -\left( \frac{2\gamma^2}{\gamma^2\tau+1} \right)^{-2} + \left( \frac{1}{\gamma^2\tau+1} \right)
\end{aligned} \tag{4.1.77}$$



Substituting equation 4.1.77 into equation 4.1.76 gives:

$$\frac{\partial \left( \frac{\gamma \tau v \sqrt{T}}{t(\gamma^2 \tau + 1)} \right)}{\partial \gamma} = \frac{\tau v \sqrt{T}}{t} \left[ \left( \frac{2\gamma^2}{\gamma^2 \tau + 1} \right)^{-2} + \left( \frac{1}{\gamma^2 \tau + 1} \right) \right] \quad (4.1.78)$$

$$\frac{\partial \sqrt{\left( \gamma^2 t^2 + \frac{t(T-t)}{T} \right)}}{\partial \gamma} = \gamma t^2 \left( \gamma^2 t^2 + \frac{t(T-t)}{T} \right)^{-\frac{1}{2}} \quad (4.1.79)$$

Substituting equation 4.1.79 and equation 4.1.78 into equation 4.1.75 leads to:

$$\begin{aligned} \frac{\partial \left( \frac{\gamma \tau v \sqrt{T}}{t(\gamma^2 \tau + 1)} \right) \sqrt{\left( \gamma^2 t^2 + \frac{t(T-t)}{T} \right)}}{\partial \gamma} &= \frac{\tau v \sqrt{T}}{t} \sqrt{\left( \gamma^2 t^2 + \frac{t(T-t)}{T} \right)} \left[ \left( \frac{2\gamma^2}{\gamma^2 \tau + 1} \right)^{-2} + \left( \frac{1}{\gamma^2 \tau + 1} \right) \right] \\ &+ \left( \frac{\gamma^2 t \tau v \sqrt{T}}{\gamma^2 \tau + 1} \right) \left( \gamma^2 t^2 + \frac{t(T-t)}{T} \right)^{-\frac{1}{2}} \end{aligned} \quad (4.1.80)$$

Substituting equation 4.1.80 into equation 4.1.74 gives:

$$\begin{aligned} \frac{\partial \left( \frac{1}{\delta} \right)}{\partial \gamma} &= (-1) \left( \frac{\gamma \tau v \sqrt{T}}{t(\gamma^2 \tau + 1)} \right)^{-2} \left[ \frac{\tau v \sqrt{T}}{t} \left( \gamma^2 t^2 + \frac{t(T-t)}{T} \right)^{-\frac{1}{2}} \left( \left( \frac{2\gamma^2}{\gamma^2 \tau + 1} \right)^{-2} + \left( \frac{1}{\gamma^2 \tau + 1} \right) \right) \right. \\ &\left. + \left( \frac{\gamma^2 t \tau v \sqrt{T}}{\gamma^2 \tau + 1} \right) \left( \gamma^2 t^2 + \frac{t(T-t)}{T} \right)^{-\frac{1}{2}} \right] \end{aligned} \quad (4.1.81)$$

Substituting equation 4.1.71 into equation 4.1.70 gives:

$$\frac{\partial \Phi(d_1)}{\partial \gamma} = \Phi(d_1) \left( \frac{\partial \left( \frac{\varphi}{\delta} \right)}{\partial \gamma} + \frac{\partial(\delta)}{\partial \gamma} \right) \quad (4.1.82)$$

Substituting equation 4.1.72 into equation 4.1.82 gives:

$$\frac{\partial \Phi(d_1)}{\partial \gamma} = \Phi(d_1) \left[ \left( \frac{1}{\delta} \frac{\partial \varphi}{\partial \gamma} + \varphi \frac{\partial \left( \frac{1}{\delta} \right)}{\partial \gamma} \right) + \frac{\partial(\delta)}{\partial \gamma} \right] \quad (4.1.83)$$

Substituting equation 4.1.73 into equation 4.1.83 gives:

$$\frac{\partial \Phi(d_1)}{\partial \gamma} = \Phi(d_1) \left[ \left( \frac{-2\gamma v \sqrt{T}}{\delta} \left( \frac{1}{\gamma^2 \tau + 1} \right)^2 + \varphi \frac{\partial \left( \frac{1}{\delta} \right)}{\partial \gamma} \right) + \frac{\partial(\delta)}{\partial \gamma} \right] \quad (4.1.84)$$

Substituting equation 4.1.81 into equation 4.1.84 gives:

$$\begin{aligned} \frac{\partial \Phi(d_1)}{\partial \gamma} = & \Phi(d_1) \left[ \left( \frac{-2\gamma v \sqrt{T}}{\delta} \left( \frac{1}{\gamma^2 \tau + 1} \right) \right)^2 \right. \\ & - \left( \frac{\gamma \tau v \sqrt{T}}{t(\gamma^2 \tau + 1)} \right)^{-2} \left[ \frac{\tau v \sqrt{T}}{t} \left( \gamma^2 t^2 + \frac{t(T-t)}{T} \right)^{-\frac{1}{2}} \left( \left( \frac{2\gamma^2}{\gamma^2 \tau + 1} \right)^{-2} + \left( \frac{1}{\gamma^2 \tau + 1} \right) \right) \right. \\ & \left. \left. + \left( \frac{\gamma^2 t \tau v \sqrt{T}}{(\gamma^2 \tau + 1)} \right) \left( \gamma^2 t^2 + \frac{t(T-t)}{T} \right)^{-1\frac{1}{2}} \right] + \frac{\partial(\delta)}{\partial \gamma} \right] \end{aligned} \quad (4.1.85)$$

$$\frac{\partial \delta}{\partial \gamma} = \frac{\partial \left( \frac{\gamma \tau v \sqrt{T}}{t(\gamma^2 \tau + 1)} \right) \sqrt{\left( \gamma^2 t^2 + \frac{t(T-t)}{T} \right)}}{\partial \gamma} \quad (4.1.86)$$

Substituting equation 4.1.80 into equation 4.1.86 gives:

$$\begin{aligned} \frac{\partial \delta}{\partial \gamma} = & \frac{\tau v \sqrt{T}}{t} \sqrt{\left( \gamma^2 t^2 + \frac{t(T-t)}{T} \right)} \left[ \left( \frac{2\gamma^2}{\gamma^2 \tau + 1} \right)^{-2} + \left( \frac{1}{\gamma^2 \tau + 1} \right) \right] \\ & + \left( \frac{\gamma^2 t \tau v \sqrt{T}}{(\gamma^2 \tau + 1)} \right) \left( \gamma^2 t^2 + \frac{t(T-t)}{T} \right)^{-\frac{1}{2}} \end{aligned} \quad (4.1.87)$$

Substituting equation 4.1.87 into equation 4.1.85 gives:

$$\begin{aligned} \frac{\partial \Phi(d_1)}{\partial \gamma} = & \Phi(d_1) \left[ \left( \frac{-2\gamma v \sqrt{T}}{\delta} \left( \frac{1}{\gamma^2 \tau + 1} \right) \right)^2 \right. \\ & - \left( \frac{\gamma \tau v \sqrt{T}}{t(\gamma^2 \tau + 1)} \right)^{-2} \left[ \frac{\tau v \sqrt{T}}{t} \left( \gamma^2 t^2 + \frac{t(T-t)}{T} \right)^{-\frac{1}{2}} \left( \left( \frac{2\gamma^2}{\gamma^2 \tau + 1} \right)^{-2} + \left( \frac{1}{\gamma^2 \tau + 1} \right) \right) \right. \\ & \left. \left. + \left( \frac{\gamma^2 t \tau v \sqrt{T}}{(\gamma^2 \tau + 1)} \right) \left( \gamma^2 t^2 + \frac{t(T-t)}{T} \right)^{-1\frac{1}{2}} \right] \right] \\ & + \frac{\tau v \sqrt{T}}{t} \sqrt{\left( \gamma^2 t^2 + \frac{t(T-t)}{T} \right)} \left[ \left( \frac{2\gamma^2}{\gamma^2 \tau + 1} \right)^{-2} + \left( \frac{1}{\gamma^2 \tau + 1} \right) \right] \\ & + \left( \frac{\gamma^2 t \tau v \sqrt{T}}{(\gamma^2 \tau + 1)} \right) \left( \gamma^2 t^2 + \frac{t(T-t)}{T} \right)^{-\frac{1}{2}} \end{aligned} \quad (4.1.88)$$

$$\begin{aligned} \frac{\partial e^{\varphi + \frac{1}{2}\delta^2}}{\partial \gamma} &= e^{\varphi + \frac{1}{2}\delta^2} \frac{\partial(\varphi + \frac{1}{2}\delta^2)}{\partial \gamma} \\ &= e^{\varphi + \frac{1}{2}\delta^2} \left[ \frac{1}{2} \frac{\partial \delta^2}{\partial \gamma} + \frac{\partial \varphi}{\partial \gamma} \right] \end{aligned} \quad (4.1.89)$$

$$\begin{aligned}\frac{\partial \delta^2}{\partial \gamma} &= 2 \frac{\tau v \sqrt{T}}{t} \sqrt{\left(\gamma^2 t^2 + \frac{t(T-t)}{T}\right)} \left[ \left(\frac{2\gamma^2}{\gamma^2 \tau + 1}\right)^{-2} + \left(\frac{1}{\gamma^2 \tau + 1}\right) \right] \\ &\quad + \left(\frac{\gamma^2 t \tau v \sqrt{T}}{\gamma^2 \tau + 1}\right) \left(\gamma^2 t^2 + \frac{t(T-t)}{T}\right)^{-\frac{1}{2}}\end{aligned}\quad (4.1.90)$$

Substituting equation 4.1.90 and equation 4.1.73 into equation 4.1.89 leads to:

$$\begin{aligned}\frac{\partial e^{\varphi + \frac{1}{2}\delta^2}}{\partial \gamma} &= e^{\varphi + \frac{1}{2}\delta^2} \left[ \frac{\tau v \sqrt{T}}{t} \sqrt{\left(\gamma^2 t^2 + \frac{t(T-t)}{T}\right)} \left[ \left(\frac{2\gamma^2}{\gamma^2 \tau + 1}\right)^{-2} + \left(\frac{1}{\gamma^2 \tau + 1}\right) \right] \right. \\ &\quad \left. + \left(\frac{\gamma^2 t \tau v \sqrt{T}}{\gamma^2 \tau + 1}\right) \left(\gamma^2 t^2 + \frac{t(T-t)}{T}\right)^{-\frac{1}{2}} - 2\gamma v \sqrt{T} \left(\frac{1}{\gamma^2 \tau + 1}\right)^2 \right]\end{aligned}\quad (4.1.91)$$

Substituting equation 4.1.91 and equation 4.1.73 into equation 4.1.88 leads to:

$$\begin{aligned}\frac{\partial e^{\varphi + \frac{1}{2}\delta^2} \Phi(d_1)}{\partial \gamma} &= e^{\varphi + \frac{1}{2}\delta^2} \frac{\partial \Phi(d_1)}{\partial \gamma} \\ &\quad + \Phi(d_1) e^{\varphi + \frac{1}{2}\delta^2} \left[ \frac{\tau v \sqrt{T}}{t} \sqrt{\left(\gamma^2 t^2 + \frac{t(T-t)}{T}\right)} \left[ \left(\frac{2\gamma^2}{\gamma^2 \tau + 1}\right)^{-2} + \left(\frac{1}{\gamma^2 \tau + 1}\right) \right] \right. \\ &\quad \left. + \left(\frac{\gamma^2 t \tau v \sqrt{T}}{\gamma^2 \tau + 1}\right) \left(\gamma^2 t^2 + \frac{t(T-t)}{T}\right)^{-\frac{1}{2}} - 2\gamma v \sqrt{T} \left(\frac{1}{\gamma^2 \tau + 1}\right)^2 \right]\end{aligned}\quad (4.1.92)$$

Thus:

$$\begin{aligned}rho &= (S + K) \left[ e^{\varphi + \frac{1}{2}\delta^2} \frac{\partial \Phi(d_1)}{\partial \gamma} \right. \\ &\quad + \Phi(d_1) e^{\varphi + \frac{1}{2}\delta^2} \left[ \frac{\tau v \sqrt{T}}{t} \sqrt{\left(\gamma^2 t^2 + \frac{t(T-t)}{T}\right)} \left[ \left(\frac{2\gamma^2}{\gamma^2 \tau + 1}\right)^{-2} + \left(\frac{1}{\gamma^2 \tau + 1}\right) \right] \right. \\ &\quad \left. \left. + \left(\frac{\gamma^2 t \tau v \sqrt{T}}{\gamma^2 \tau + 1}\right) \left(\gamma^2 t^2 + \frac{t(T-t)}{T}\right)^{-\frac{1}{2}} - 2\gamma v \sqrt{T} \left(\frac{1}{\gamma^2 \tau + 1}\right)^2 \right] \right]\end{aligned}\quad (4.1.93)$$

An option's rho measures the rate of variation in the asset with respect to changes in the risk-free rate of interest assuming that the other parameters are unchanged at that time. It tests the effect of interest-rate fluctuations on the price of an option. Higher interest rates usually cause call options to be more costly, all other factors being equal. It's value is obtained from:

$$rho = \frac{\partial f}{\partial r}$$

For the Black-Scholes model, it is given as:

$$rho = K(T - t)e^{-r(T-t)}N(d_2)$$

**Proposition 4.4.** *A European call option's rho under the BS-BHM model is as follows:*

$$rho = tSe^{\varphi + \frac{1}{2}\delta^2} \left[ \Phi(d_1) + \frac{1}{\delta} \Phi'(d_1) \right] + K \frac{t}{\delta} \Phi'(-d_2) \quad (4.1.94)$$

*Proof.* For the BS-BHM model, rho is computed as follows:

$$\begin{aligned} rho &= \frac{\partial (Se^{\varphi + \frac{1}{2}\delta^2} \Phi(d_1) - K\Phi(-d_2))}{\partial r} \\ &= \frac{\partial Se^{\varphi + \frac{1}{2}\delta^2} \Phi(d_1)}{\partial r} - \frac{\partial K\Phi(-d_2)}{\partial r} \\ &= Se^{\frac{1}{2}\delta^2} \frac{\partial e^\varphi \Phi(d_1)}{\partial r} - K \frac{\partial \Phi(-d_2)}{\partial r} \\ &= Se^{\frac{1}{2}\delta^2} \left[ \Phi(d_1) \frac{\partial e^\varphi}{\partial r} + e^\varphi \frac{\partial \Phi(d_1)}{\partial r} \right] + K\Phi'(-d_2) \frac{\partial d_2}{\partial r} \\ &= Se^{\frac{1}{2}\delta^2} \left[ e^\varphi \Phi(d_1) \frac{\partial \varphi}{\partial r} + e^\varphi \Phi'(d_1) \frac{\partial d_1}{\partial r} \right] + K\Phi'(-d_2) \frac{\partial d_1}{\partial r} \\ &= Se^{\varphi + \frac{1}{2}\delta^2} \left[ \Phi(d_1) \frac{\partial \varphi}{\partial r} + \Phi'(d_1) \frac{\partial d_1}{\partial r} \right] + K\Phi'(-d_2) \frac{\partial d_1}{\partial r} \end{aligned} \quad (4.1.95)$$

$$\begin{aligned} \frac{\partial \varphi}{\partial r} &= \frac{\partial \left( rt - \frac{1}{2}v^2T + \frac{1}{2} \frac{v\sqrt{T}}{\gamma^2\tau+1} \right)}{\partial r} \\ &= t \end{aligned} \quad (4.1.96)$$

$$\begin{aligned} \frac{\partial d_1}{\partial r} &= \frac{\partial \left( \frac{\log\left(\frac{S}{K}\right) + \varphi}{\delta} + \delta \right)}{\partial r} \\ &= \frac{\partial \left( \frac{\log\left(\frac{S}{K}\right) + \varphi}{\delta} \right)}{\partial r} \\ &= \frac{\partial \left( \frac{\varphi}{\delta} \right)}{\partial r} \\ &= \frac{1}{\delta} \frac{\partial \varphi}{\partial r} \\ &= \frac{t}{\delta} \end{aligned} \quad (4.1.97)$$

Substituting equation 4.1.96 and equation 4.1.97 into equation 4.1.95 gives:

$$rho = Ste^{\varphi + \frac{1}{2}\delta^2} \left[ \Phi(d_1) + \frac{1}{\delta} \Phi'(d_1) \right] + K \frac{t}{\delta} \Phi'(-d_2) \quad (4.1.98)$$

Theta measures the rate of variation in the asset as time progresses assuming that the other parameters are unchanged at that time. The probability of an option being profitable or in-the-money decreases as time passes. It is defined as follows:

$$theta = \frac{\partial f}{\partial t}$$

In this case,  $t$  denotes the time that has elapsed since the start of the derivative contract. For the Black-Scholes model, theta is given as follows:

$$theta = -S\Phi(d_1) \frac{\sigma}{2\sqrt{T-t}} - rKe^{-r(T-t)}\Phi(d_2)$$

For the BS-BHM model:

$$\begin{aligned} theta &= \frac{\partial (Se^{\varphi + \frac{1}{2}\delta^2} \Phi(d_1) - K\Phi(-d_2))}{\partial t} \\ &= \frac{\partial (Se^{\varphi + \frac{1}{2}\delta^2} \Phi(d_1))}{\partial t} - \frac{\partial (K\Phi(-d_2))}{\partial t} \\ &= S \frac{\partial (e^{\varphi + \frac{1}{2}\delta^2} \Phi(d_1))}{\partial t} - K \frac{\partial (\Phi(-d_2))}{\partial t} \\ &= S \left[ \Phi(d_1) \frac{\partial (e^{\varphi + \frac{1}{2}\delta^2})}{\partial t} + e^{\varphi + \frac{1}{2}\delta^2} \frac{\partial \Phi(d_1)}{\partial t} \right] + K \Phi'(-d_2) \frac{\partial d_2}{\partial t} \\ &= S \left[ \Phi(d_1) \frac{\partial (e^{\varphi + \frac{1}{2}\delta^2})}{\partial t} + e^{\varphi + \frac{1}{2}\delta^2} \Phi'(d_1) \frac{\partial d_1}{\partial t} \right] + K \Phi'(-d_2) \frac{\partial d_1}{\partial t} \end{aligned} \quad (4.1.99)$$

#### 4.2. Comparison of volatility in a stochastic volatility model vs volatility in an information-based asset pricing model in a multivariate framework

This section makes use of non-linear filtering to extract volatility in the Heston model and the information-based asset pricing model. The system of dynamic equations in the models are non-linear. This makes it impossible to use linear filtering methods such as the Kalman filter. The non-linear filtering methods used in this study are the extended Kalman filter and the particle filter.

##### 4.2.1. Preliminary concepts on non-linear filtering

The extended Kalman filter is an extension of the Kalman filter where Jacobian matrices are used to linearise the system of dynamic equations.

The state transition equation is as follows:

$$x_k = f(x_{k-1}, b_{k-1})$$

while the measurement equation is given as:

$$y_k = h(x_k, c_k)$$

The extended Kalman filter Jacobian matrices are:

$$A = \frac{\partial f_i}{\partial x_j}(\hat{x}_{k-1}, 0)$$

$$W = \frac{\partial f_i}{\partial b_j}(\hat{x}_{k-1}, 0)$$

$$H = \frac{\partial h_i}{\partial x_j}(\tilde{x}_k, 0)$$

$$V = \frac{\partial h_i}{\partial c_j}(\tilde{x}_k, 0)$$

The prediction error is given by:

$$\tilde{e}_{x_k} \approx x_k - \tilde{x}_k, \tag{4.2.1}$$

while the measurement error is:

$$\tilde{e}_{y_k} \approx y_k - \tilde{y}_k, \tag{4.2.2}$$

Using equations 4.2.1 and 4.2.2, an estimate for  $x_k$  is obtained by:

$$\begin{aligned}\hat{x}_k &= \tilde{x}_k + K_k \tilde{e}_{y_k} \\ &= \tilde{x}_k + K_k (y_k - \tilde{y}_k)\end{aligned}\quad (4.2.3)$$

The particle filter which is based on monte carlo simulation is an approximate bayesian filtering algorithm. It can be used where the system of dynamic equations is non-linear and non-gaussian. The rationale underlying the particle filtering technique can be illustrated by considering an integral of the form:

$$\int g(x)p(x)dx = E[g(x)] \quad (4.2.4)$$

To evaluate the integral 4.2.4, an approximation can be made by simulating  $n$  values,  $x^{(1)}, \dots, x^{(n)}$  from the density function  $p(x)$  whose domain integration is performed. It may be challenging to sample from  $p(x)$  which leads to importance sampling where another density function, in this case  $q(x)$  is sampled from such that:

$$\begin{aligned}\int g(x)p(x)dx &= \int g(x)\frac{p(x)}{q(x)}q(x)dx \\ &= E[g(x)w(x)]\end{aligned}\quad (4.2.5)$$

where  $w(x) = \frac{p(x)}{q(x)}$  is referred to as a weight.

An approximation to equation 4.2.5 is made as follows:

$$E[g(x)w(x)] \approx \frac{1}{N} \sum_{i=1}^N g(x^{(i)})w(x^{(i)}), \quad (4.2.6)$$

For this approach to be valid,  $q(\cdot)$  must have the same domain as  $p(\cdot)$

In most cases, the discrete state transition distribution,  $p(x_k|x_{k-1})$  is used as the importance function because it is easy to draw particles from it. The generation of samples should be done randomly. A better approach is to make use of the recent observations,  $y_k$  since they carry information about the state  $x_k$  by taking the importance function as  $p(x_k|x_{k-1}^{(i)}, y_k)$ .

These particles are then used to approximate the distribution of the unobserved states. At a discrete time,  $k$ , a sample of  $n$  particles is given as follows:

$$z_k^{(1)}, z_k^{(2)}, \dots, z_k^{(n)}.$$

The probability of a particle being sampled depends on the weight,  $w_k^{(i)}$  it has been assigned.

The unobservable state vector  $z_k$ , is driven by noise denoted by  $m_k$  and the observable vector  $y_k$  is driven by the observation noise denoted by  $n_k$ .

The weight  $w_k^{(i)}$  is obtained from:

$$\hat{w}_k^{(i)} \approx w_{k-1}^{(i)} \frac{p(y_k | z_{0:k}^{(i)}) p(z_k^{(i)} | z_{0:k-1}^{(i)})}{q(z_k^{(i)} | z_{k-1}^{(i)}, y_k)} \quad (4.2.7)$$

The weights are then normalised at time  $k$  as follows:

$$\tilde{w}_k^{(i)} = \frac{\hat{w}_k^{(i)}}{\sum_{l=1}^n \hat{w}_k^{(l)}} \quad (4.2.8)$$

The unobserved state can then be obtained as follows:

$$\hat{z}_{k|k} = \sum_{i=1}^n \tilde{w}_k^{(i)} z_k^{(i)} \quad (4.2.9)$$

Numerous iterations are performed to approximate the state distributions based on the random samples obtained from the set of random numbers used in the monte carlo simulation. Particle degeneration can be observed when the effective sample size denoted by  $N_{eff}$  is less than  $\frac{n}{2}$ , when this occurs, the particles are resampled as follows:

$$N_{eff} = \frac{1}{\sum_{j=1}^n (\tilde{w}_k^{(j)})^2} \quad (4.2.10)$$

#### 4.2.2. Non-linear filtering in the Heston model

The Brownian motion driving the variance process is correlated with the Brownian motion driving the asset process in the Heston model. In order to remove correlation from the two Brownian motions, cholesky decomposition is used.

Using the extended Kalman filter, the measurement equation is given as follows:

$$\begin{aligned} \ln S_k = \ln S_{k-1} &+ \left( \mu - \frac{\rho}{\eta} \right) \Delta k + \frac{\rho}{\eta} V_k + \left[ \frac{\rho}{\eta} (\kappa \Delta k - 1) - \frac{1}{2} \Delta k \right] V_{k-1} \\ &+ \sqrt{1 - \rho^2} \sqrt{\Delta k} \sqrt{V_{k-1}} W_{k-1} \end{aligned}$$

The state transition equations are given by the variance processes:

$$\begin{pmatrix} V_k \\ V_{k-1} \end{pmatrix} = \begin{pmatrix} \kappa \theta \Delta k \\ 0 \end{pmatrix} + \begin{pmatrix} 1 - \kappa \Delta k & 0 \\ 1 & 0 \end{pmatrix} \begin{pmatrix} V_{k-1} \\ V_{k-2} \end{pmatrix} + \begin{pmatrix} \eta \sqrt{\Delta k} \sqrt{V_{k-1}} \\ 0 \end{pmatrix} Z_{k-1}$$



The Heston model's Jacobian matrices are given as:

$$A = 1 - \kappa \Delta k$$

$$W = \sigma \sqrt{V_{k-1}} \sqrt{\Delta k}$$

In order to compute  $H$ , two parameters,  $v_1 = \sqrt{V_0}$  and  $v_2 = \sqrt{\theta}$  are used giving the following Jacobian matrices:

$$H_1 = \frac{\partial h(\hat{x}_{k|k-1}, 0)}{\partial v_1} = \frac{\partial h(\hat{x}_{k|k-1}, 0)}{\partial V_0} 2\sqrt{V_0}$$

$$H_2 = \frac{\partial h(\hat{x}_{k|k-1}, 0)}{\partial v_2} = \frac{\partial h(\hat{x}_{k|k-1}, 0)}{\partial \theta} 2\sqrt{\theta}$$

Substituting  $h(\hat{x}_{k|k-1}, 0)$  with the Heston model option price leads to:

$$h(\hat{x}_{k|k-1}, 0) = S e^{-q\tau} P_1 - K e^{-r\tau} P_2$$

This results in:

$$H_1 = \frac{\partial (S e^{-q\tau} P_1 - K e^{-r\tau} P_2)}{\partial V_0} 2\sqrt{V_0}$$

$$= S e^{-q\tau} \frac{\partial P_1}{\partial V_0} 2\sqrt{V_0} - K e^{-r\tau} \frac{\partial P_2}{\partial V_0} 2\sqrt{V_0}$$

where

$$\frac{\partial P_j}{\partial V_0} = \frac{1}{\pi} \int_0^\infty \operatorname{Re} \left[ \frac{e^{-i\phi \ln K} f_j(\phi; S_k, V_k) B_j(\tau, \phi)}{i\phi} \right] d\phi$$

and

$$H_2 = \frac{\partial (S e^{-q\tau} P_1 - K e^{-r\tau} P_2)}{\partial \theta} 2\sqrt{\theta}$$

$$= S e^{-q\tau} \frac{\partial P_1}{\partial \theta} 2\sqrt{\theta} - K e^{-r\tau} \frac{\partial P_2}{\partial \theta} 2\sqrt{\theta}$$

where

$$\frac{\partial P_j}{\partial \theta} = \frac{1}{\pi} \int_0^\infty \operatorname{Re} \left[ \frac{e^{-i\phi \ln K} f_j(\phi; S_k, V_k) \partial A_j(\tau, \phi) / \partial \theta}{i\phi} \right] d\phi$$

$$\frac{\partial A_j(\phi, \tau)}{\partial \theta} = \frac{\kappa}{\sigma^2} \left[ (b_j - \rho \sigma \phi i + d_j) \tau - 2 \ln \left( \frac{1 - g_j e^{d_j \tau}}{1 - g_j} \right) \right]$$

In order to apply particle filtering to the Heston model, let  $S_t$  denote the observed asset price at time  $t$  and  $y_t = \log \left( \frac{S_t}{S_0} \right)$ . The system of dynamic equations given by equation 3.1.21 and equation 3.1.22 are used to obtain the state space model to be used in non-linear filtering.

Applying Ito's lemma to equation 3.1.21 gives:

$$dy_t = \left( \mu - \frac{1}{2}V_t \right) dt + \sqrt{V_t} dB_t \quad (4.2.11)$$

This implies that:

$$dB_t = \frac{1}{\sqrt{V_t}} \left( dy_t - \left( \mu - \frac{1}{2}V_t \right) dt \right) \quad (4.2.12)$$

The aim is to estimate the variance process  $V_t$ , for each fixed  $t$ , based on the observations  $\{y_s\}_{0 \leq s \leq t}$ .

Let:

$$dZ_t = \sqrt{1 - \rho^2} d\tilde{Z}_t + \rho dB_t \quad (4.2.13)$$

Substituting for the value of  $dB_t$  in equation 4.2.13 from equation 4.2.12:

$$dZ_t = \sqrt{1 - \rho^2} d\tilde{Z}_t + \frac{\rho}{\sqrt{V_t}} \left( dy_t - \left( \mu - \frac{1}{2}V_t \right) dt \right) \quad (4.2.14)$$

where  $\tilde{Z}_t$  and  $B_t$  are uncorrelated. Substituting  $dZ_t$  in equation 3.1.22:

$$dV_t = \kappa(\theta - V_t)dt + \eta\sqrt{V_t}\sqrt{1 - \rho^2}d\tilde{Z}_t + \rho\eta \left( dy_t - \left( \mu - \frac{1}{2}V_t \right) dt \right) \quad (4.2.15)$$

The Heston model is discretized to obtain its discrete-time representation so as to be able to apply this filtering technique. Equation 4.2.11 and equation 4.2.15 are discretized using the Euler scheme as follows:

$$\begin{aligned} V_k &= V_{k-1} + \kappa(\theta - V_{k-1})\Delta t - \rho\eta \left( \mu - \frac{1}{2}V_{k-1} \right) \Delta t \\ &\quad + \eta\sqrt{V_{k-1}}\sqrt{1 - \rho^2}\Delta\tilde{Z}_k + \rho\eta(y_k - y_{k-1}) \end{aligned} \quad (4.2.16)$$

Similarly;

$$y_k = y_{k-1} + \left( \mu - \frac{1}{2}V_{k-1} \right) \Delta t + \sqrt{V_{k-1}}\Delta B_k \quad (4.2.17)$$

Equations 4.2.16 and 4.2.17 represent the state transition and measurement equations respectively which make up the state space model.

The weight  $w_k^{(i)}$  at time  $k$  is obtained from:

$$w_k^{(i)} = w_{k-1}^{(i)} \frac{p(y_k | v_{0:k}^{(i)}, y_{0:k-1}) p(v_k^{(i)} | v_{0:k-1}^{(i)}, y_{0:k-1})}{q(v_k^{(i)} | v_{k-1}^{(i)}, y_k)} \quad (4.2.18)$$

The importance function is given as:

$$q(v_k | v_{k-1}, y_k) = p(v_k | v_{k-1}, y_k) \quad (4.2.19)$$

The mean and variance of equation 4.2.16 are:

$$\mu_p = V_{k-1} + \kappa(\theta - V_{k-1})\Delta t - \rho\eta\left(\mu - \frac{1}{2}V_{k-1}\right)\Delta t + \rho\eta(y_k - y_{k-1})$$

and:

$$\sigma_p^2 = \eta^2 V_{k-1}^{(i)} (1 - \rho^2) \Delta t$$

respectively.

Thus:

$$p(v_k | v_{k-1}, y_k) \sim N(\mu_p, \sigma_p) \quad (4.2.20)$$

The next step is to obtain an estimate for  $p(v_k | v_{0:k-1}, y_{0:k-1})$ . Substituting equation 4.2.17 into equation 4.2.16 :

$$V_k = V_{k-1} + \kappa(\theta - V_{k-1})\Delta t + \eta\sqrt{V_{k-1}}\sqrt{1 - \rho^2}\Delta\tilde{Z}_k + \rho\eta\sqrt{V_{k-1}}\Delta B_k \quad (4.2.21)$$

The mean and variance of equation 4.2.21 are:

$$\mu_q = V_{k-1} + \kappa(\theta - V_{k-1})\Delta t$$

and:

$$\sigma_q^2 = \eta^2 V_{k-1} \Delta t$$

respectively.

Thus:

$$p(v_k | v_{0:k-1}, y_{0:k-1}) \sim N(\mu_q, \sigma_q^2) \quad (4.2.22)$$

The likelihood function is given as:

$$p(y_k | v_{0:k}, y_{0:k-1}) = p(y_k | v_k, v_{k-1}, y_{k-1}) \quad (4.2.23)$$

The mean of equation 4.2.17 is:

$$\mu_r = y_{k-1} + \left( \mu - \frac{1}{2} V_{k-1} \right) \Delta t$$

and the variance of equation 4.2.17 is:

$$\sigma_r^2 = V_{k-1} \Delta t$$

Thus:

$$p(y_k | v_k, v_{k-1}, y_{k-1}) \sim N(\mu_r, \sigma_r^2) \quad (4.2.24)$$

The posterior density function can be approximated as follows:

$$\hat{x}_{k|k} = \sum_{i=1}^n \tilde{w}_k^{(i)} x_k^{(i)}$$

### 4.2.3. Non-linear filtering in an information-based framework

Starting with the extended Kalman filter approach, let  $V_t$  represent the variable which is unobserved.

The Brownian motion driving the asset process is assumed to be independent of the Brownian motion driving the variance process.

The Euler-Maruyama scheme discretization approach can be used to obtain the measurement and state transition equations by applying it to the SDEs. For a given model:

$$dX_t = a(X_t)dt + \sigma(X_t)dW_t \quad (4.2.25)$$

The scheme discretizes equation 4.2.25 as follows:

$$X_k = X_{k-1} + a(X_{k-1})\Delta k + \sigma(X_{k-1})\sqrt{\Delta k}W_{k-1}$$

over an interval  $[0, T]$ , and it's discretized as  $0 = k_1 < k_2 < \dots < k_m = T$  with increments equally spaced  $\Delta k$ .

By discretizing equation 3.2.14, the following measurement equation is obtained:

$$S_k = S_{k-1} + rS_{k-1}\Delta k + v_{k-1}P_{(k-1)T}V_{k-1}\sqrt{\Delta k}W_{k-1} \quad (4.2.26)$$

The discretized variance process is as follows:

$$V_k = V_{k-1} - v_{k-1}^2 V_{k-1}^2 \Delta k + v_{k-1}\kappa_{k-1}\sqrt{\Delta k}W_{k-1} \quad (4.2.27)$$

Let:

$$f_i(\hat{x}_{k-1}, 0) = V_{k-1} - v_{k-1}^2 V_{k-1}^2 \Delta k + v_{k-1}\kappa_{k-1}\sqrt{\Delta k}W_{k-1} \quad (4.2.28)$$

and

$$h_i(\tilde{x}_k, 0) = S_0\Phi(d_1) - Ke^{-(\delta + \frac{\sigma^2}{2})}\Phi(d_2) \quad (4.2.29)$$

The Jacobian matrices are derived as follows:

$$\begin{aligned} A &= \frac{\partial}{\partial V_{k-1}}(V_{k-1} - v_{k-1}^2 V_{k-1}^2 \Delta k + v_{k-1}\kappa_{k-1}\sqrt{\Delta k}W_{k-1}) \\ &= 1 - 2v_{k-1}^2 V_{k-1} \Delta k \end{aligned} \quad (4.2.30)$$

$$\begin{aligned} W &= \frac{\partial}{\partial W_{k-1}}(V_{k-1} - v_{k-1}^2 V_{k-1}^2 \Delta k + v_{k-1}\kappa_{k-1}\sqrt{\Delta k}W_{k-1}) \\ &= v_{k-1}\kappa_{k-1}\sqrt{\Delta k} \end{aligned} \quad (4.2.31)$$

An estimate for the unobserved state is obtained as follows:

$$x_k \approx \tilde{x}_k + (1 - 2v_{k-1}^2 V_{k-1} \Delta k)(x_{k-1} - \hat{x}_{k-1}) + Wb_{k-1} \quad (4.2.32)$$

In the information-based asset pricing model,  $H$  is obtained as follows:

$$H = \frac{\partial h(\hat{x}_{k|k-1}, 0)}{\partial \gamma} \quad (4.2.33)$$

Substituting  $h(\hat{x}_{k|k-1}, 0)$  with the BS-BHM model option price gives:

$$h(\hat{x}_{k|k-1}, 0) = S_0 e^{\varphi + \frac{1}{2}\delta^2} \Phi(d_1) - K\Phi(-d_2) \quad (4.2.34)$$

This results in:

$$H = \frac{\partial \left( S_0 e^{\varphi + \frac{1}{2}\delta^2} \Phi(d_1) - K\Phi(-d_2) \right)}{\partial \gamma}$$

$$\begin{aligned}
H = (S + K) & \left[ e^{\varphi + \frac{1}{2}\delta^2} \frac{\partial \Phi(d_1)}{\partial \gamma} \right. \\
& + \Phi(d_1) e^{\varphi + \frac{1}{2}\delta^2} \left[ \frac{\tau v \sqrt{T}}{t} \sqrt{\left( \gamma^2 t^2 + \frac{t(T-t)}{T} \right)} \left[ \left( \frac{2\gamma^2}{\gamma^2 \tau + 1} \right)^{-2} + \left( \frac{1}{\gamma^2 \tau + 1} \right) \right] \right. \\
& \left. \left. + \left( \frac{\gamma^2 t \tau v \sqrt{T}}{\gamma^2 \tau + 1} \right) \left( \gamma^2 t^2 + \frac{t(T-t)}{T} \right)^{-\frac{1}{2}} - 2\gamma v \sqrt{T} \left( \frac{1}{\gamma^2 \tau + 1} \right)^2 \right] \right] \quad (4.2.35)
\end{aligned}$$

The study also extracts volatility from the information-based asset pricing model using particle filtering. A particle filter algorithm is applied to the discretized representation of the asset price process and the variance process. An assumption is made that the noise process driving the asset price process is independent of the noise process driving the variance process.

The model dynamics will first be discretized so as to make them suitable for the application of particle filtering. To discretize the asset price process, equation 3.2.14 is integrated over the interval  $[k, k + \Delta k]$ , leading to:

$$\begin{aligned}
\int_k^{k+\Delta k} dS_s &= \int_k^{k+\Delta k} r S_s ds + \int_k^{k+\Delta k} P_{sT} v_s V_s dW_s \\
\int_k^{k+\Delta k} dS_s &= S_{k+\Delta k} - S_k \\
\int_k^{k+\Delta k} r S_s ds &= r S_k \Delta k \\
\int_k^{k+\Delta k} P_{sT} v_s V_s dW_s &= P_{kT} v_k V_k (W_{k+\Delta k} - W_k) \\
&= P_{kT} v_k V_k \sqrt{\Delta k} Z
\end{aligned}$$

where  $Z \sim N[0, 1]$

Thus, the discretized asset price process is as follows:

$$S_{k+\Delta k} = S_k + r S_k \Delta k + P_{kT} v_k V_k \sqrt{\Delta k} Z \quad (4.2.36)$$

Making  $\Delta k$  to be the subject in equation 4.2.36 gives:

$$\Delta k = \frac{S_{k+\Delta k} - S_k - P_{kT} v_k V_k \sqrt{\Delta k} Z}{r S_k} \quad (4.2.37)$$

To discretize the variance process, equation 3.2.11 is integrated over the interval  $[k, k + \Delta k]$ ,

giving:

$$\begin{aligned}\int_k^{k+\Delta k} dV_s &= - \int_k^{k+\Delta k} g_s^2 V_s^2 ds + \int_k^{k+\Delta k} g_s \kappa_s d\tilde{W}_s \\ \int_k^{k+\Delta k} dV_s &= V_{k+\Delta k} - V_k \\ - \int_k^{k+\Delta k} g_s^2 V_s^2 ds &= -g_k^2 V_k^2 \Delta k\end{aligned}$$

$$\begin{aligned}\int_k^{k+\Delta k} g_s \kappa_s dW_s &= g_k \kappa_k \sqrt{\tilde{W}_{k+\Delta k} - \tilde{W}_k} \\ &= g_k \kappa_k \sqrt{\Delta k} \tilde{Z}\end{aligned}$$

Thus, the discretized variance process is as follows:

$$V_{k+\Delta k} = V_k - g_k^2 V_k^2 \Delta k + g_k \kappa_k \sqrt{\Delta k} \tilde{Z} \quad (4.2.38)$$

where  $\tilde{Z} \sim N[0, 1]$

The mean and variance of equation 4.2.38 are:

$$\mu_b = V_k - g_k^2 V_k^2 \Delta k$$

and:

$$\sigma_b^2 = g_k^2 \kappa_k^2 \Delta k \tilde{Z}$$

respectively.

Thus  $q(z_k | z_{k-1})$  has a normal distribution with mean  $\mu_b$  and variance  $\sigma_b^2$ , that is:

$$q(z_k | z_{k-1}) \sim N(\mu_b, \sigma_b^2) \quad (4.2.39)$$

To obtain an estimate for  $p(z_k | z_{0:k-1})$ . Equation 4.2.37 is substituted into equation 4.2.38 leading to:

$$V_{k+\Delta k} = V_k - g_k^2 V_k^2 \left( \frac{S_{k+\Delta k} - S_k - P_{sT} g_k V_k \sqrt{\Delta k} \tilde{Z}}{r S_k} \right) + g_k \kappa_k \sqrt{\Delta k} \tilde{Z} \quad (4.2.40)$$

The mean and variance of equation 4.2.40 are:

$$\mu_d = V_k - g_k^2 V_k^2 \left( \frac{S_{k+\Delta k} - S_k}{r S_k} \right)$$

and

$$\sigma_d^2 = (g_k^2 V_k^2)^2 \left( \frac{P_{sT} g_k^2 V_k^2 \Delta k Z}{r^2 S_k^2} \right) + g_k^2 \kappa_k^2 \Delta k \tilde{Z}$$

respectively.

Thus:

$$p(z_k | z_{0:k-1}) \sim N(\mu_d, \sigma_d^2) \quad (4.2.41)$$

The likelihood function is as follows:

$$p(y_k | z_{0:k}) = p(y_k | z_k, z_{k-1}) \quad (4.2.42)$$

The mean and variance of equation 4.2.36 are:

$$\mu_f = S_k + r S_k \Delta k$$

and

$$\sigma_f^2 = g_k^2 V_k^2 \Delta k Z$$

respectively.

Thus, the likelihood function has a normal distribution with mean  $\mu_f$  and variance  $\sigma_f^2$ , that is:

$$p(y_k | z_k, z_{k-1}) \sim N(\mu_f, \sigma_f^2) \quad (4.2.43)$$

Multi-asset stochastic volatility models make use of simulation-based estimation techniques which are able to estimate the volatility sequentially. This implies that particle filtering can also be used to extract volatility for the multi-asset information-based stochastic volatility model as follows:

Let  $p_t$  be a vector representing the log of the ratio of asset prices, such that  $p_t = [p_{1t}, \dots, p_{nt}]^\top$  that is for  $i = 1, \dots, n$ :

$$p_{it} = \log \left( \frac{S_{it}}{S_{i,t-1}} \right)$$



where  $S_{it}$  denotes the price of the  $i^{th}$  asset at time  $t$ .  
 $p_t$  follows a normal distribution given as follows:

$$p_t = \mu + \epsilon_t, \quad \epsilon_t \sim N_n(0, \Sigma_t),$$

where  $\mu$  is a vector denoting the mean of  $p_t$ ,  $\epsilon_t$  is an innovation vector and  $\Sigma_t$  denotes the volatility covariance matrix generated by an inverse Wishart process given by:

$$\Sigma_t^{-1} | \Sigma_{t-1} \sim W(k, k^{-1} A \Sigma_{t-1}^{-1} A^\top)$$

$A$  is a  $n \times n$  autoregressive parameter and  $W(k, k^{-1} A \Sigma_{t-1}^{-1} A^\top)$  denotes a Wishart distribution. This study obtains an estimate for the conditional covariance matrix of  $p_t$  which is known as the volatility matrix.

Let  $y_{1:k} = \{y_1, \dots, y_k\}$  be a vector representing the observations upto and including time  $k$ . Similarly, let  $\Sigma_{0:k} = \{\Sigma_0, \Sigma_1, \dots, \Sigma_k\}$  be a vector representing the covariance matrices upto and including time  $k$ .  $q(\Sigma_{0:k} | y_{1:k})$  denotes an importance function from which simulation can be performed from.

The sequential monte carlo method begins by generating  $\Sigma_k^{(1)}, \dots, \Sigma_k^{(n)}$  from  $q(\Sigma_k | \Sigma_{k-1}^i, y_k)$  and computing the non-normalised weights:

$$w_k^{(i)} = \frac{p(y_k | \Sigma_k^{(i)}) p(\Sigma_k^{(i)} | \Sigma_{k-1}^{(i)})}{q(\Sigma_k^{(i)} | \Sigma_{k-1}^{(i)}, y_k)} \tilde{w}_{k-1}^{(i)}$$

The posterior density function for  $\Sigma_k$  can be approximated as follows

$$p(\Sigma_{0:k} | y_{1:k}) \approx \sum_{i=1}^n \tilde{w}_k^{(i)} \Sigma_k^{(i)}$$

## 5. Data Analysis and Results

The data used in this study was obtained from daily SPX European call options data from yahoo finance (<https://www.yahoofinance.com/>) starting from 28.01.2019 to 21.06.2019 and Dow Jones Euro Stoxx 50 obtained from *ivolatility.com* from 15.01.2019 to 20.09.2019.

R statistical software and Python programming language are used for analysis and graphical representation of the results obtained in the study. The historical option prices are for SPX European call options with a total of 250 observations while those for the Dow Jones Euro Stoxx 50 had a total of 245 observations.

The summary of the data from SPX call options is given in table 1.

	Strike Price	Current Price	Implied Volatility
Minimum :	1300	0.0500	0.0000
1st Quartile :	2144	1.1630	0.1440
Median :	2762	88.4500	0.2266
Mean :	2604	339.9730	0.5638
3rd Quartile :	2976	679.9380	0.6914
Maximum :	4100	1478.9000	2.4790
Skewness :	-0.1356	0.9953	1.4782
Kurtosis :	-0.3954	-0.2731	0.9520

Table 1: SPX options data summary

Table 1 shows the descriptive statistics for the daily figures for the SPX call options. These include the minimum, quartiles, median, mean, maximum, skewness and kurtosis for the strike price, current price and implied volatility.

The strike prices are seen to be fairly symmetrical since the skewness value is  $-0.1356$  which lies between  $-0.5$  and  $0.5$ .

The current prices are moderately positively skewed since  $0.5 < 0.9953 < 1$ .

The implied volatilities are seen to be highly positively skewed since  $1.4782 > 1$  which implies that they have a long tail that extends to the right. This is consistent with the fact that data that is skewed to the right in most cases will have the mean being greater than the median as shown in the table where the mean value given by  $0.5638$  is greater than the median given by  $0.2266$ .

The datasets of the strike price, current price and implied volatility have lighter tails since the kurtosis of all the three datasets is less than 3.

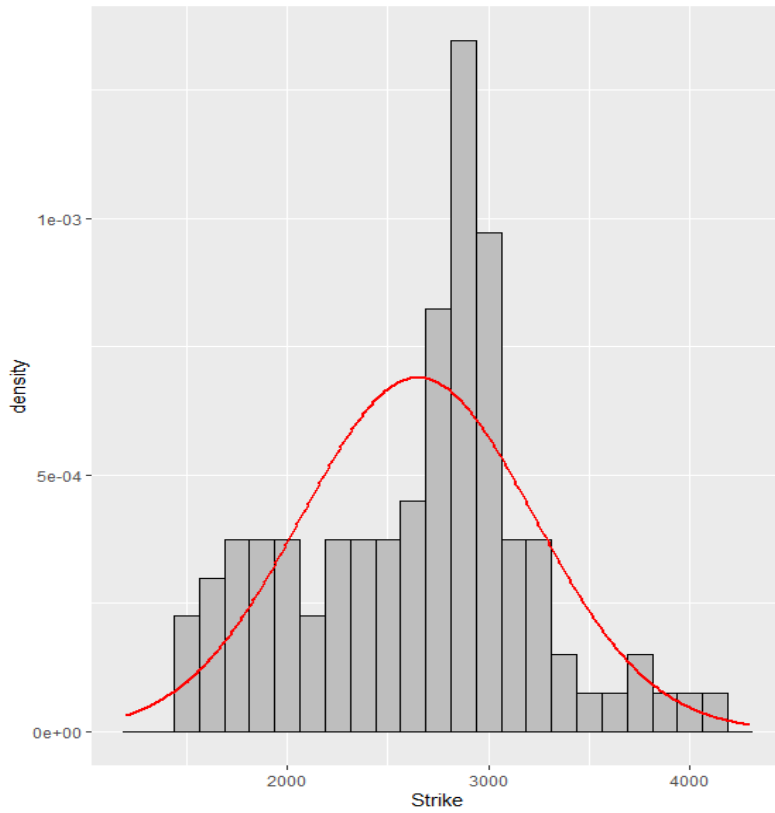


Figure 2: Histogram of the SPX option strike prices

Figure 2 displays a histogram for the strike prices which further illustrates the notion that the strike prices are fairly symmetrical as most of the values lie near the mean of 2,604.

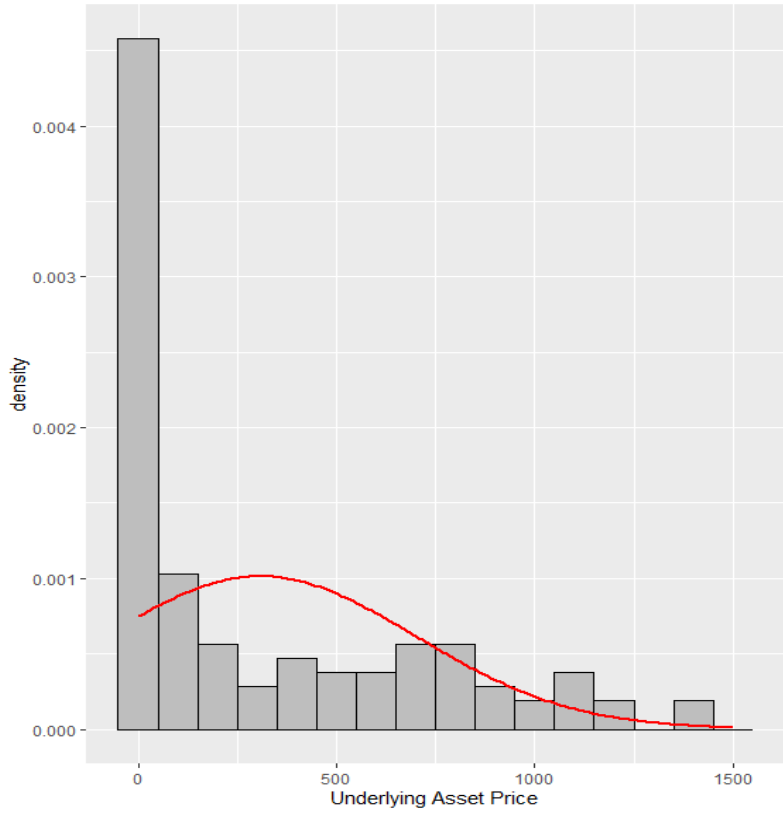


Figure 3: Histogram of the SPX option underlying asset price

The histogram in figure 3 emphasizes the fact that the underlying asset prices are positively skewed since most of the values lie on the right.

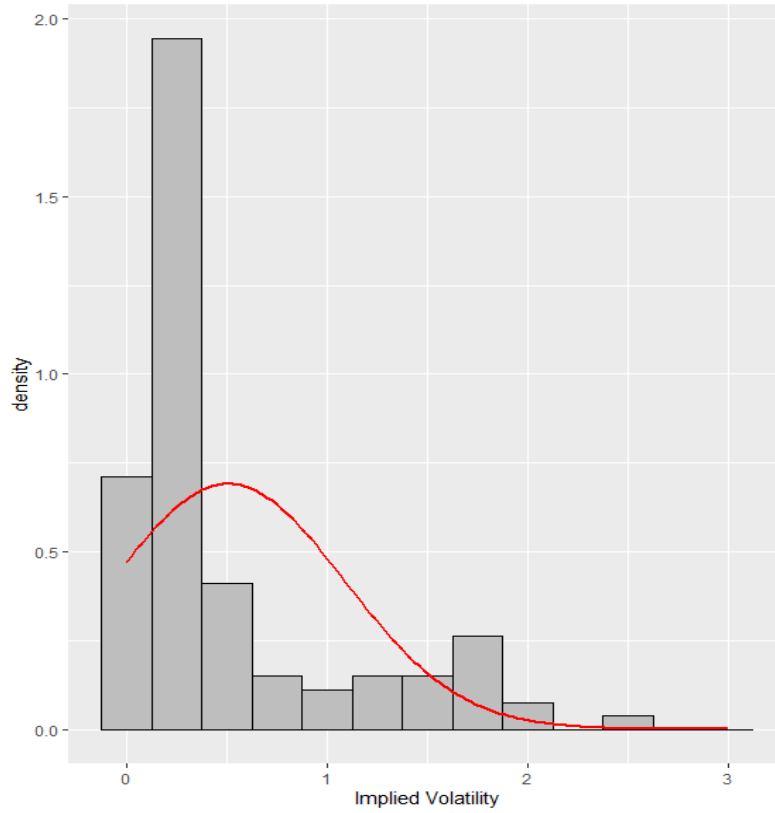


Figure 4: Histogram of the SPX option implied volatility

Figure 4 shows that the implied volatilities are positively skewed since most of the values lie on the right.

The summary of the data from Dow Jones Euro Stoxx 50 call options is given in table 2.

	Strike Price	Current Price	Empirical Price
Minimum :	500	3067	0.001
1st Quartile :	1550	3067	0.001
Median :	1925	3067	796.55
Mean :	1843	3067	731.019
3rd Quartile :	2225	3067	1091.2
Maximum :	2500	3067	2066.2
Skewness :	-0.7008	0	-0.02446
Kurtosis :	2.7656	0	2.2744

Table 2: Dow Jones Euro Stoxx 50 options data summary

Table 2 shows the descriptive statistics for the daily figures for the Dow Jones Euro Stoxx 50 call options. These include the minimum, mean, median, quartiles, maximum, skewness and kurtosis for the strike price, current price and the empirical price.

The strike prices are seen to be moderately negatively skewed since the skewness value is  $-0.7008$  which lies between  $-1$  and  $-0.5$ .

The datasets of the strike price, current price and empirical price have lighter tails since the kurtosis of all the three datasets is less than 3.

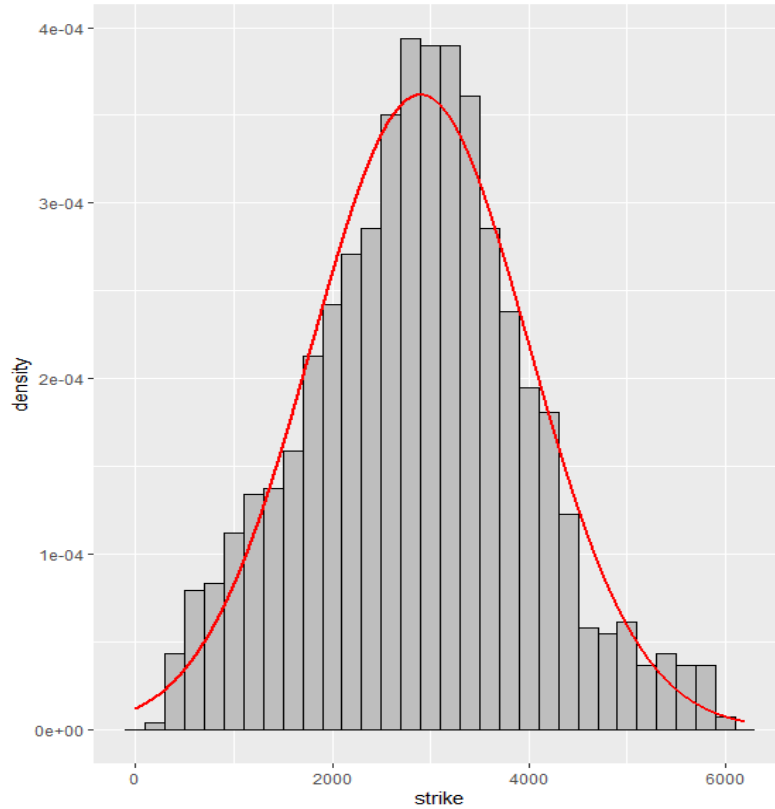


Figure 5: Histogram of the Dow Jones Euro Stoxx 50 option strike prices

The histogram in figure 5 further illustrates the notion that the strike prices are moderately negatively skewed as most of the values lie near the mean value of 1, 843.

For the multi-asset options, monte carlo simulation is used to obtain the data used in analysis.

### *5.1. Modelling volatility in a multi-asset framework*

A numerical illustration is made between a European call option under the Heston model and that under the Black-Scholes model. The results from the two models are compared to the actual price based on data relating to Dow Jones Euro Stoxx 50 European call options. For the multi-asset option, two assets are considered.

#### *5.1.1. Asset pricing model with constant volatility*

To illustrate the Black-Scholes model, the study compares the result obtained using monte carlo simulation to that obtained using the Black-Scholes model option pricing formula. For monte carlo simulation,  $S = 100$ ,  $\sigma = 0.2$ ,  $K = 100$ ,  $T = 1$ , and  $r = 0.01$ .



### Monte carlo simulation Black-Scholes model

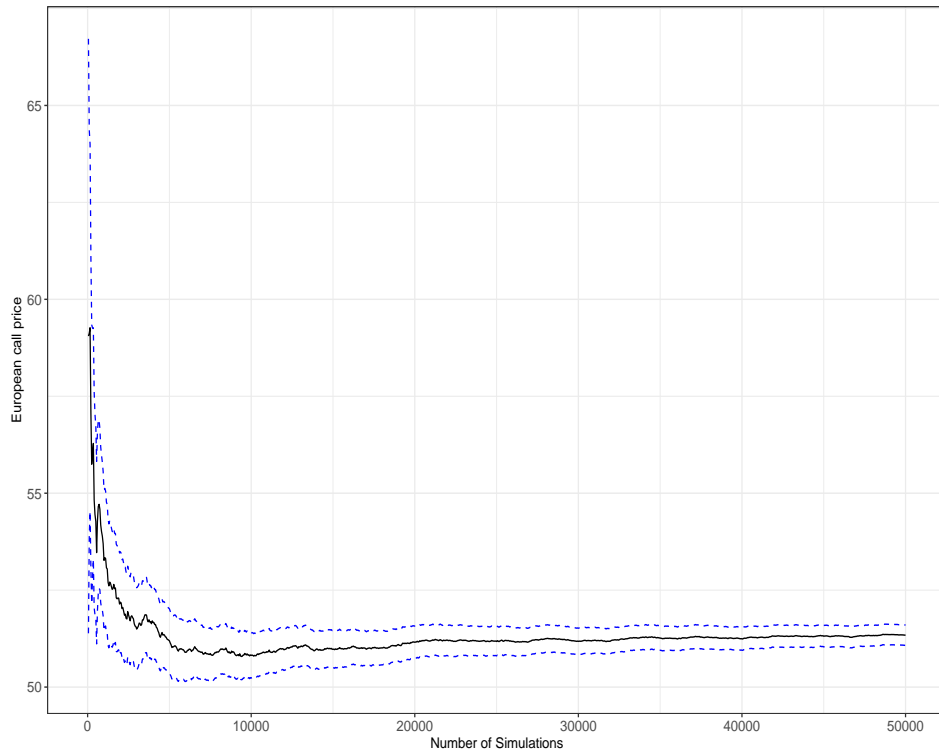


Figure 6: Simulated Black-Scholes model option prices

Figure 6 shows that the variation in the simulated European call option price in the Black-Scholes model reduces significantly with an increase in the number of simulations. The black line denotes the Black-Scholes model price while the upper and lower blue line denote the upper and lower bound respectively.

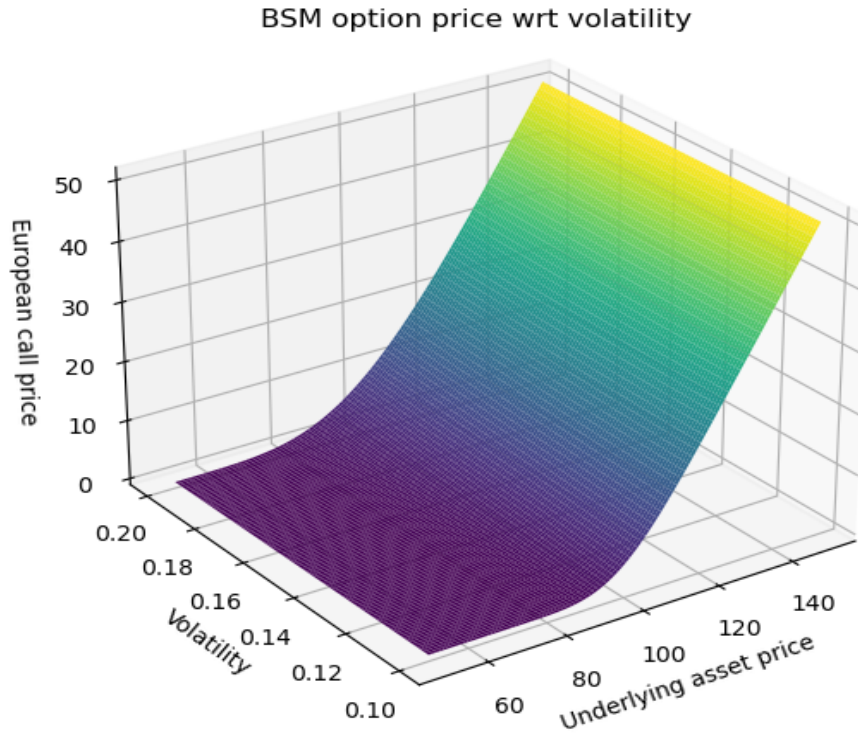


Figure 7: Black-Scholes model surface wrt volatility

Figure 7 shows the features of the Black-Scholes model surface based on monte carlo simulation. The value of the underlying asset price ranges from 50 to 150, time varies from 0.01 to 1 and volatility ranges from 0.1 to 0.2.

The figure disapproves the assumption of the Black-Scholes model of constant volatility, if the volatility is constant, then the implied volatility surface should be flat. However, looking at the simulated values, this is not the case as the volatility rates are seen to vary.

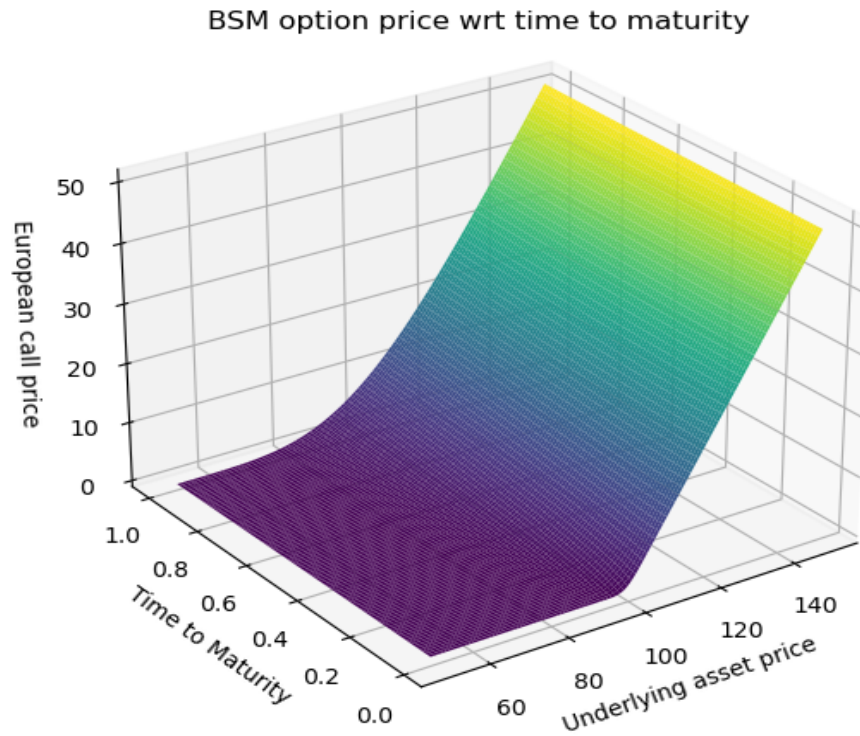


Figure 8: Black-Scholes model surface wrt time to maturity

Figure 8 shows the Black-Scholes model European call price with respect to time to maturity based on monte carlo simulation. A longer time to maturity implies an increased certainty in the call option being exercised, this causes a smoother curve.

European call option prices are also computed using data from Dow Jones Euro Stoxx 50.

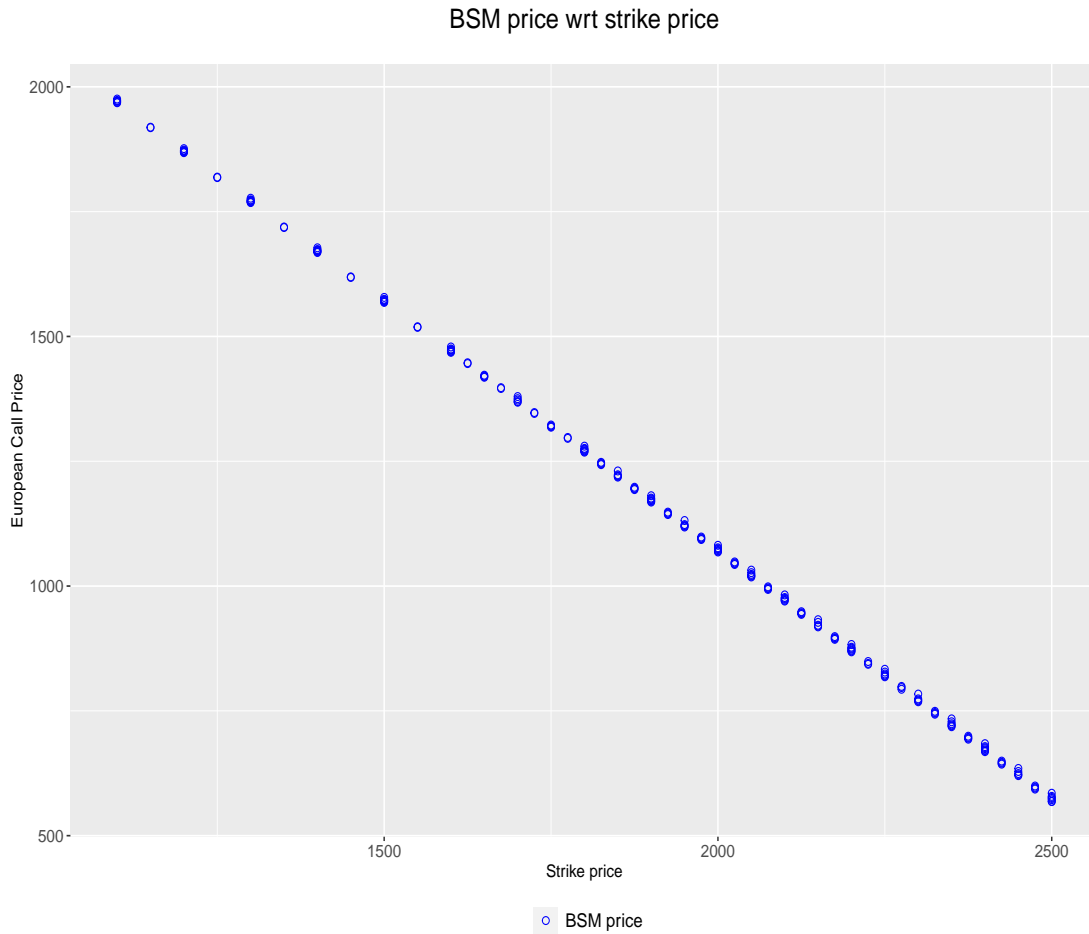


Figure 9: Black-Scholes model price wrt strike price

Figure 36 shows the Black-Scholes model prices plotted against the strike prices, the prices are seen to decrease as the strike prices increase.

A comparison between the Black-Scholes model option price and the empirical option price is given in figure 10.

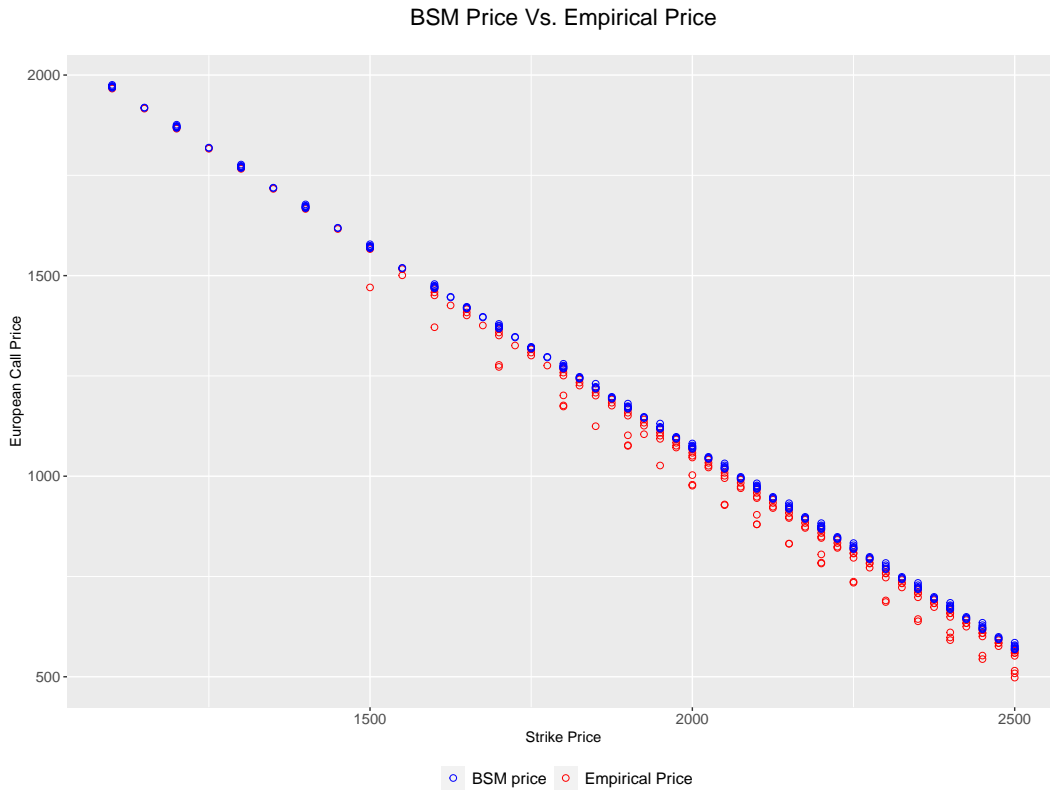


Figure 10: Comparison of the Black-Scholes model option prices and the empirical option prices

From figure 10, the prices under the Black-Scholes model are relatively similar to those from the empirical data. The call prices are relatively similar between the strike prices 1,500 to 2,500.

For the multi-asset European call option, two assets having equal weights and a correlation coefficient of 0.4 are considered.  $r$  is 0.01.

Multi-Asset European Call Option			
K	$S_{1,0}$	$S_{2,0}$	BSM price
237	190	180	5.50
235	195	185	7.39
232	200	190	9.48
226	205	195	13.87
221	210	200	18.63

Table 3: The multi-asset Black-Scholes model option prices

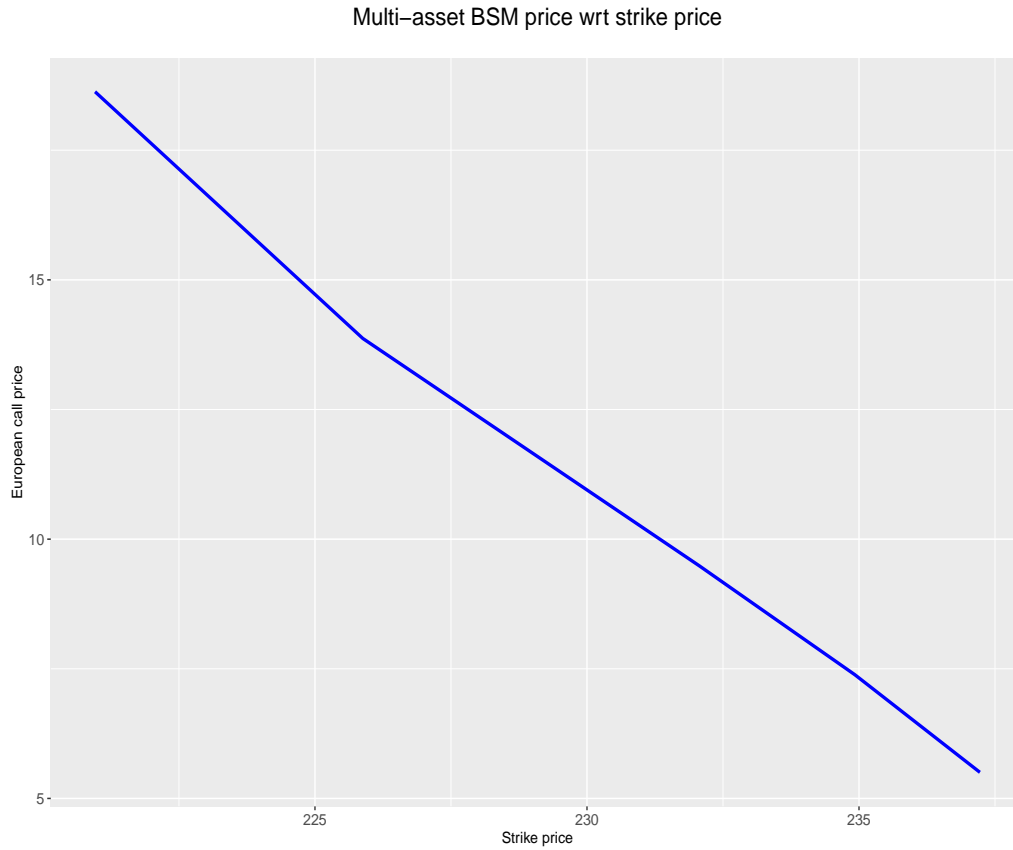


Figure 11: The multi-asset Black-Scholes model option prices

Figure 11 illustrates that there's a general reduction in the option price as the strike price increases for the multi-asset model.

### 5.1.2. Asset pricing model with stochastic volatility

For the Heston model, the estimated parameters used were from Albrecher et al., where  $\nu_0 = 0.0175$ ,  $\kappa = 1.5768$ ,  $\eta = 0.0398$ ,  $\lambda = 0.5751$  and  $\rho = -0.5711$ , (Albrecher et al., 2007). This study compares the result obtained using monte carlo simulation to that obtained using the closed form Heston option pricing formula.

### Monte carlo simulation Heston model

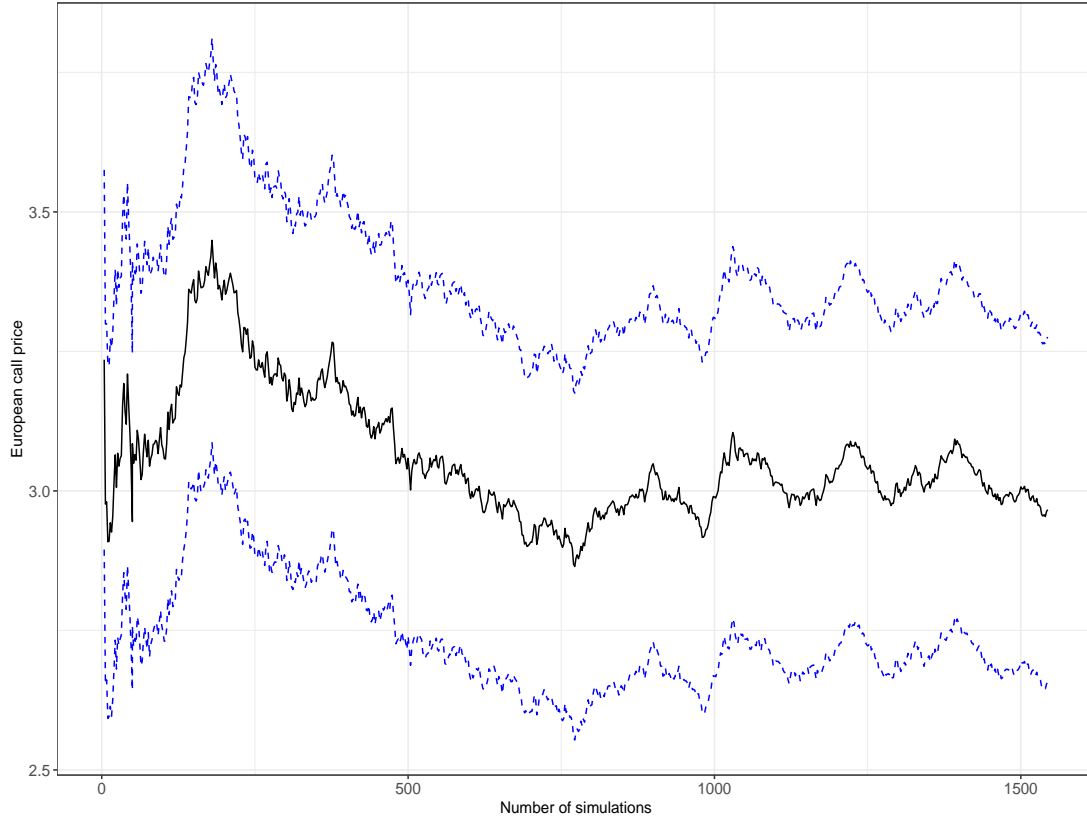


Figure 12: Simulated Heston model option price

Figure 12 shows the simulated European call option price under the Heston model. There's increased variation in the prices as compared to the simulated option price under the Black-Scholes model as given in figure 6.



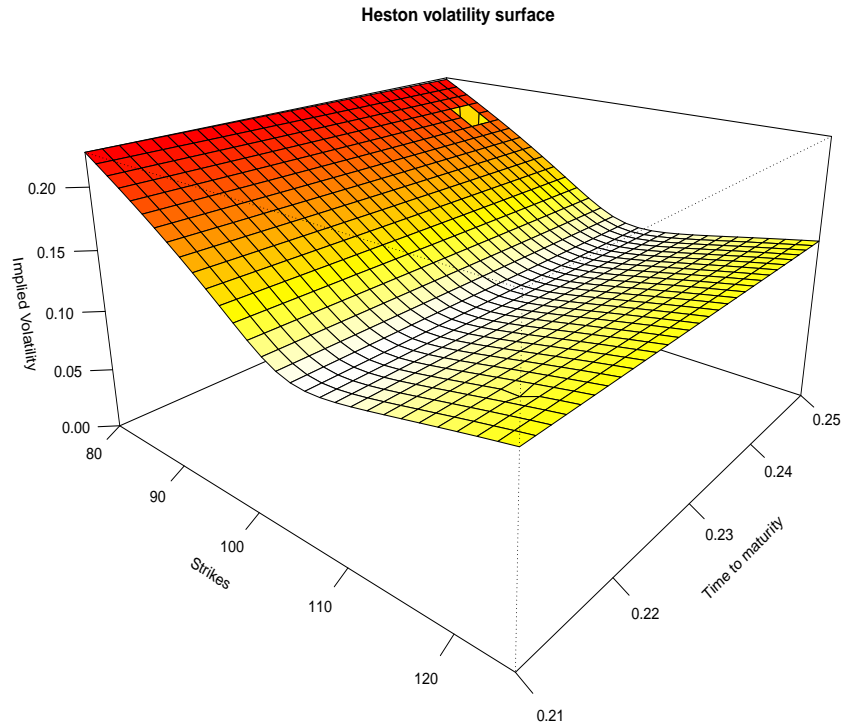


Figure 13: Heston model volatility surface

Figure 13 illustrates the Heston surface, the lower strike prices are seen to have higher implied volatilities as compared to those with higher strike prices.

To illustrate the use of Wishart process in multi-asset option pricing, the study considers the case of two assets with parameter values as given in Da Fonseca et al., 2007:

$$M = \begin{pmatrix} -2.5 & -1.5 \\ -1.5 & -2.5 \end{pmatrix}, \quad Q = \begin{pmatrix} 0.21 & -0.14 \\ 0.14 & 0.21 \end{pmatrix}$$

$\eta = 7.14286$ ,  $r = 0$ ,  $\rho = -0.6$  and

$$\Sigma_0 = \begin{pmatrix} 0.09 & -0.036 \\ -0.036 & 0.09 \end{pmatrix}$$

The price obtained for the multi-asset Heston model using the discounted characteristic function of the Wishart model is as follows:

Underlying asset price	European call price
1,500	68.29
1,800	14.71

Table 4: The multi-asset Heston model option prices

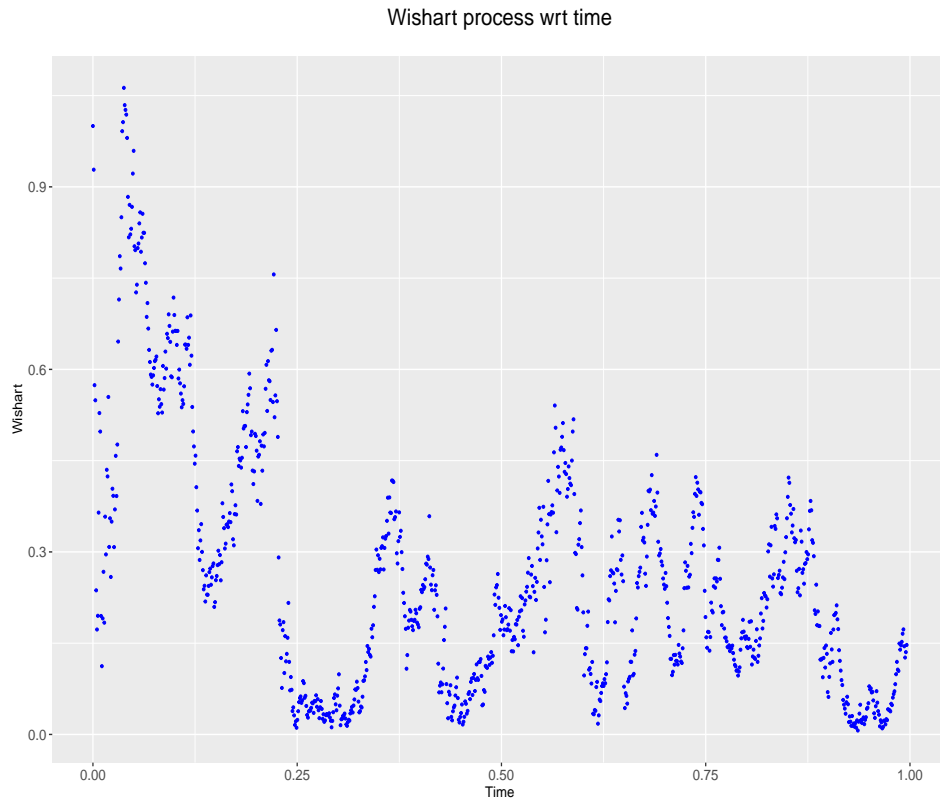


Figure 14: Wishart processes

Figure 14 shows the progression of the Wishart processes with time. The highest values for the Wishart process lie between time 0 and time 0.25.

## 5.2. Asset pricing in an information-based framework

Dow Jones Euro Stoxx 50 options data is used in this section to obtain option prices based on the information-based asset pricing framework.

The RMSE test will then be used to determine the goodness of fit of the multi-asset information-based stochastic volatility model prices to the multi-asset Black-Scholes model prices as follows:

$$RMSE = \sqrt{\sum_{k=1}^n \frac{(A_k - R_k)^2}{n}}$$

where  $A_k$  is the multi-asset Black-Scholes model price and  $R_k$  is the multi-asset information-based stochastic volatility model price.

### 5.2.1. BS-BHM model

Comparing the prices obtained from the BS-BHM model to the observed prices, figure 15 shows that the BS-BHM model prices are higher than the observed prices.

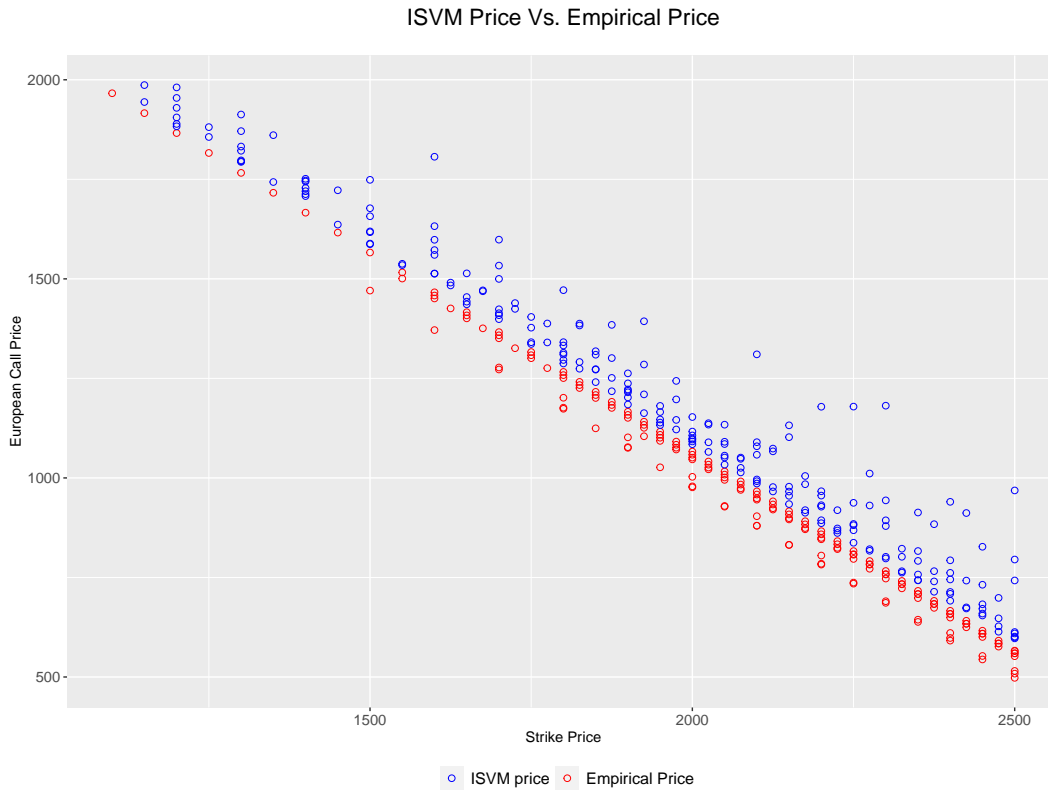


Figure 15: BS-BHM model option prices vs. empirical option prices,  $\gamma = 0.3$

The information flow rate,  $\gamma$  causes a variation in the fit.

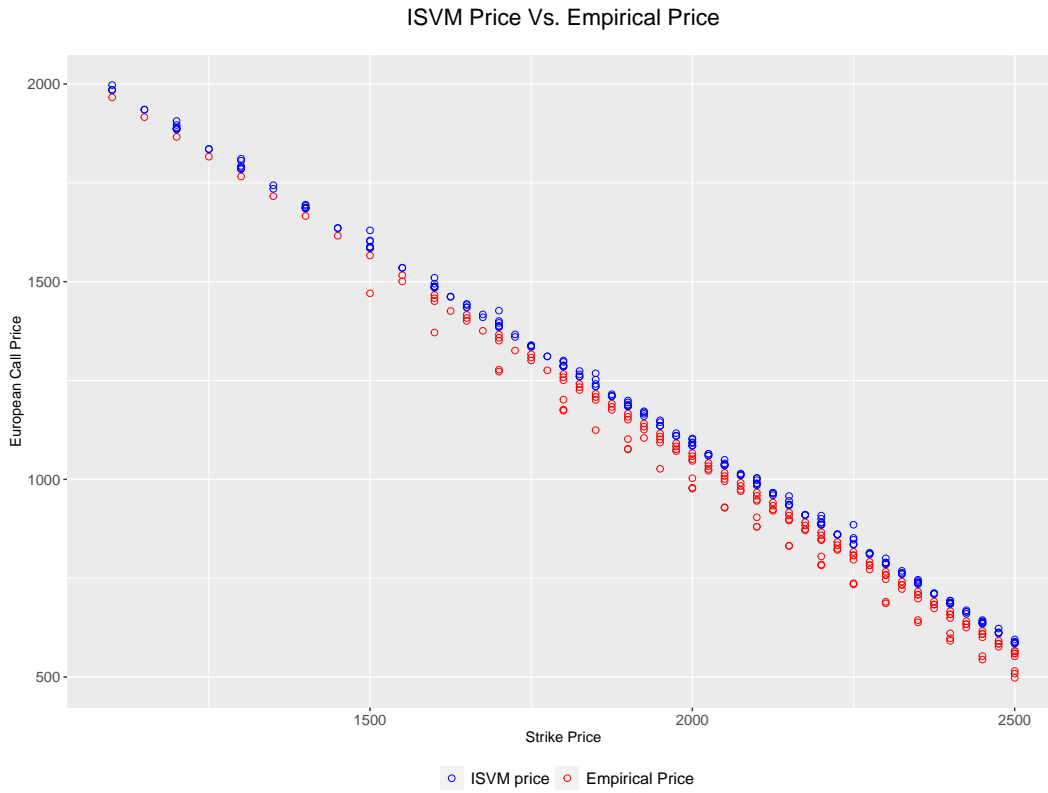


Figure 16: BS-BHM model option prices vs. empirical option prices,  $\gamma = 0.25$

In figure 16,  $\gamma$  has a mean value of 0.25. A reduction in the value of  $\gamma$  from 0.3 to 0.25 causes an improved fit of the BS-BHM model to the empirical data.

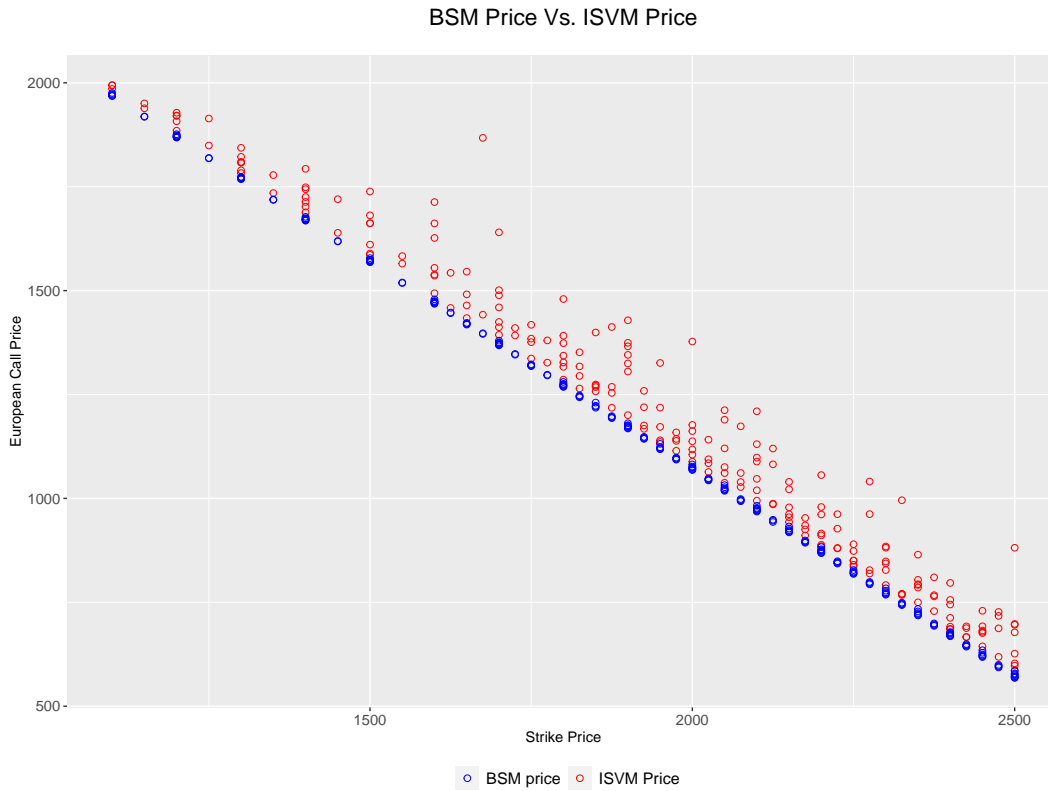


Figure 17: Black-Scholes model vs. BS-BHM model option prices,  $\gamma = 0.3$ .

Comparing the BS-BHM model and the Black-Scholes model option price in figure 17, the BS-BHM model provides a higher price than the Black-Scholes model. The values between the two models are closer when  $\gamma$  is varied from 0.3 to 0.25, as shown in figure 18. The price under the BS-BHM model is higher than that under the Black-Scholes model as illustrated in 17. Figure 18 shows that the two models give relatively similar prices when  $\gamma$  is varied from 0.3 to 0.25.

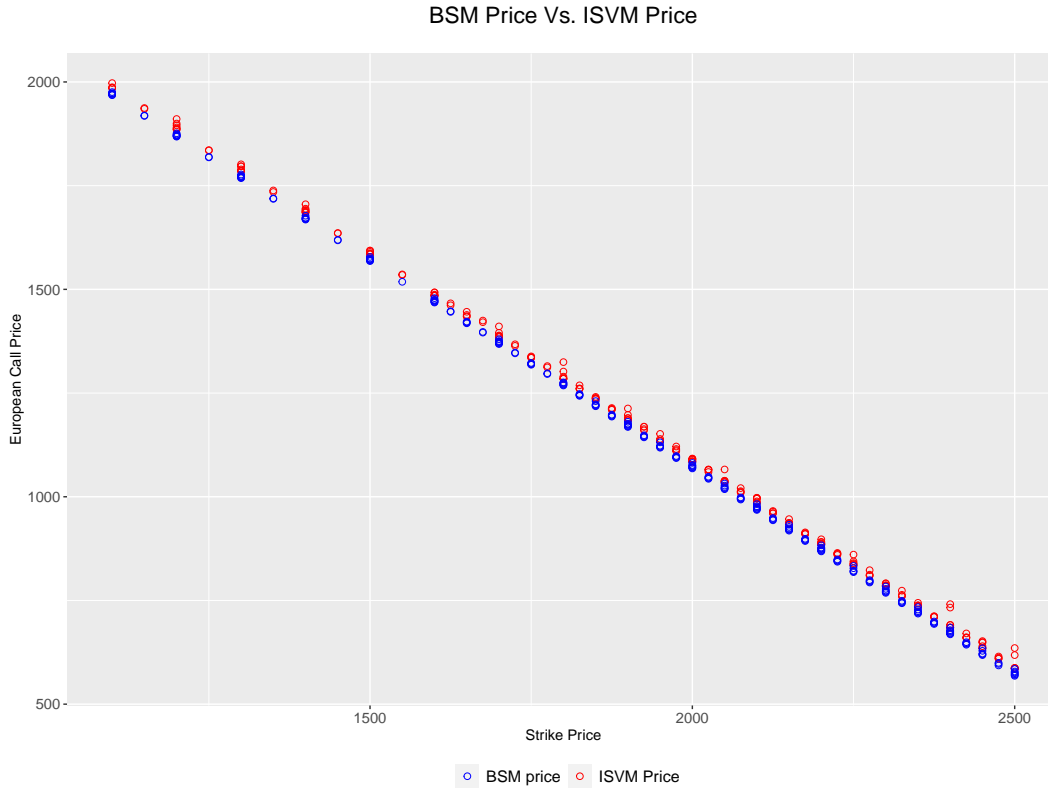


Figure 18: Black-Scholes model vs. BS-BHM model option prices,  $\gamma = 0.25$ .

The study shows that with a suitably chosen information flow rate parameter, the goodness of fit of the BS-BHM model to the empirical data improves significantly.

For the multi-asset European call option, two assets having equal weights and a correlation coefficient of 0.4 are considered.  $r$  is 0.01.

Multi-Asset European Call Option				
K	$S_{1,0}$	$S_{2,0}$	BS-BHM model Price	BSM price
237	190	180	5.85	5.50
235	195	185	7.61	7.39
232	200	190	9.55	9.48
226	205	195	13.86	13.87
221	210	200	18.14	18.63

Table 5: Comparison of the multi-asset option prices between the BS-BHM model & the Black-Scholes model

From table 5, the prices produced from the BS-BHM multi-asset model are comparatively similar to those produced from the Black-Scholes multi-asset model. For higher strike rates, the prices for the BS-BHM model are higher, and for lower strike prices, the Black-Scholes

model prices are higher.

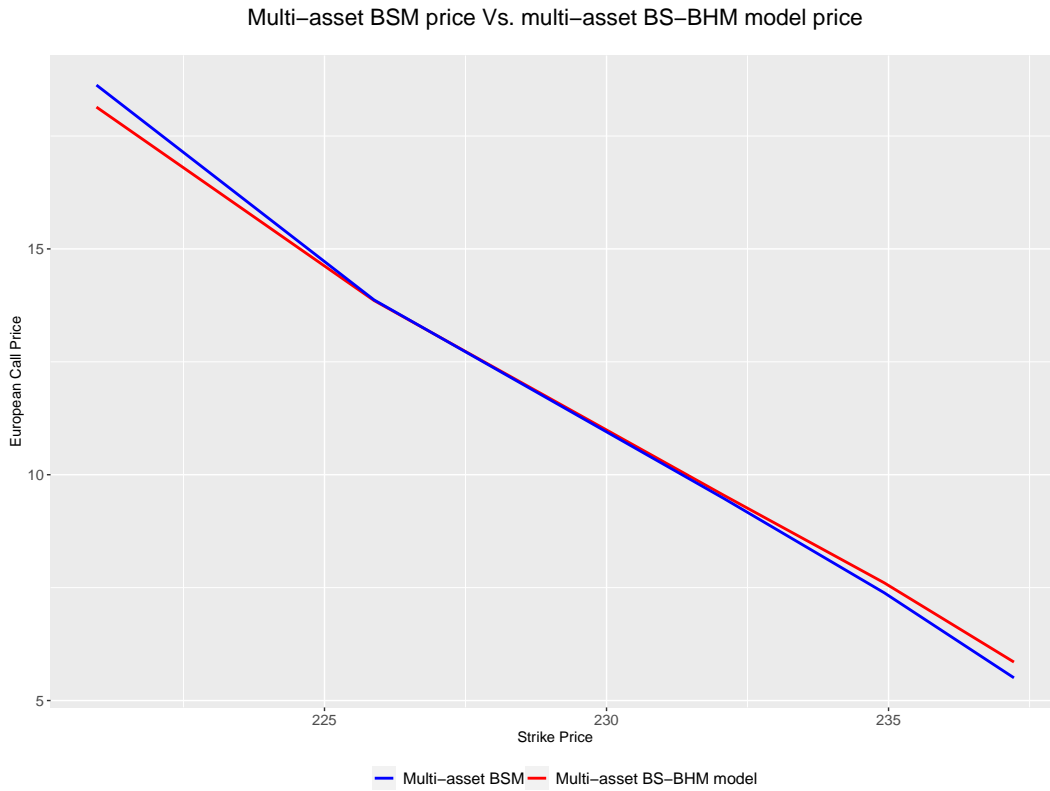


Figure 19: Comparison of the multi-asset BS-BHM model and the multi-asset BSM

Figure 19 shows that the prices under the multi-asset BS-BHM model are relatively similar to those obtained from the multi-asset BSM. The RMSE value is 0.2874.



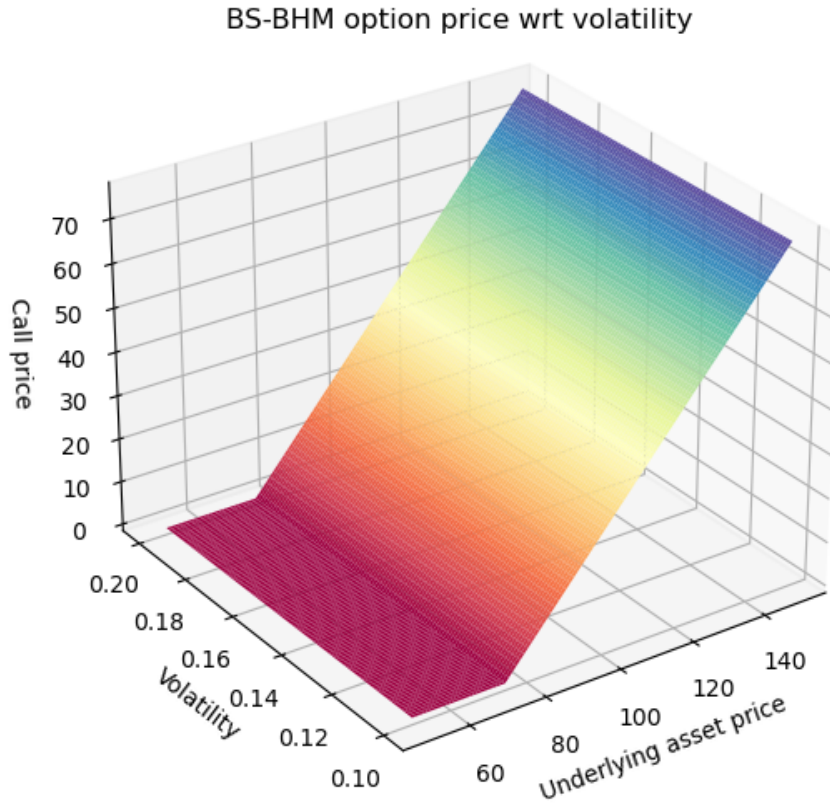


Figure 20: BS-BHM model volatility surface

Figure 20 shows the features of the BS-BHM model surface based on monte carlo simulation. This figure illustrates that volatility in the BS-BHM model is stochastic as the volatility is seen to be varying.

### 5.2.2. *BS-BHM updated model*

It is evident from the figure 21 that the values from the BS-BHM updated model are comparatively higher for all strike prices considered than for the empirical European call option prices.

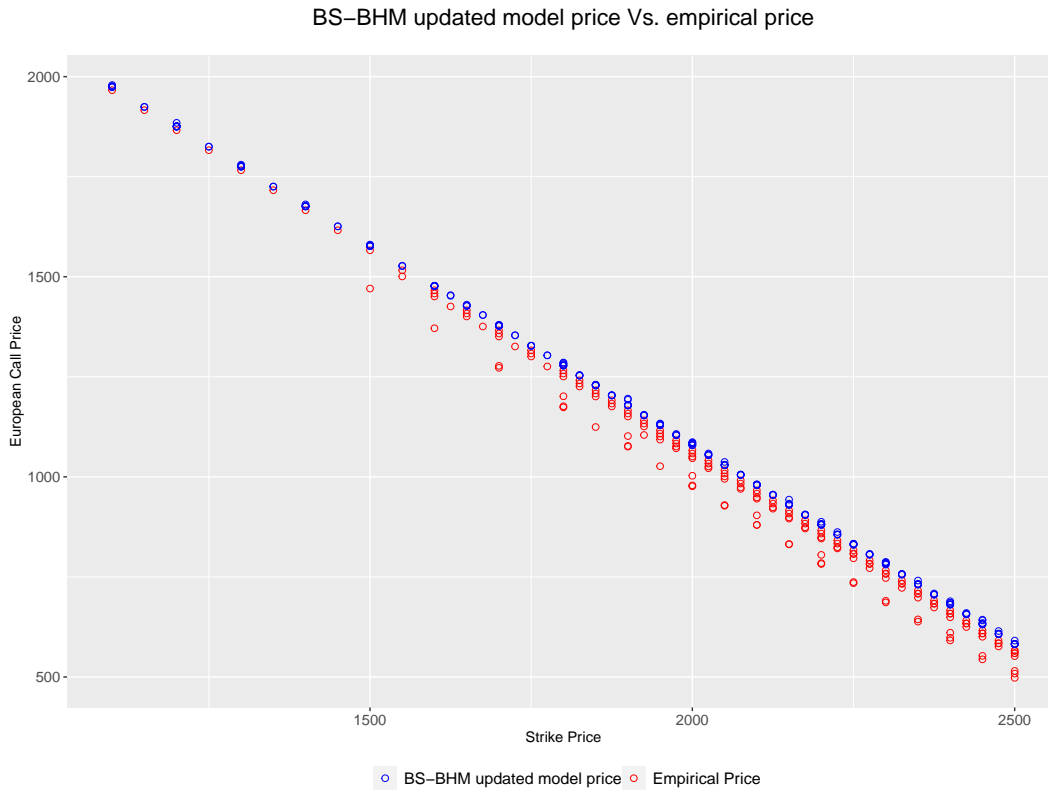


Figure 21: BS-BHM updated model option prices vs. empirical option prices,  $\gamma = 0.3$

$\gamma$  is taken to have a mean value of 0.3 in figure 21.

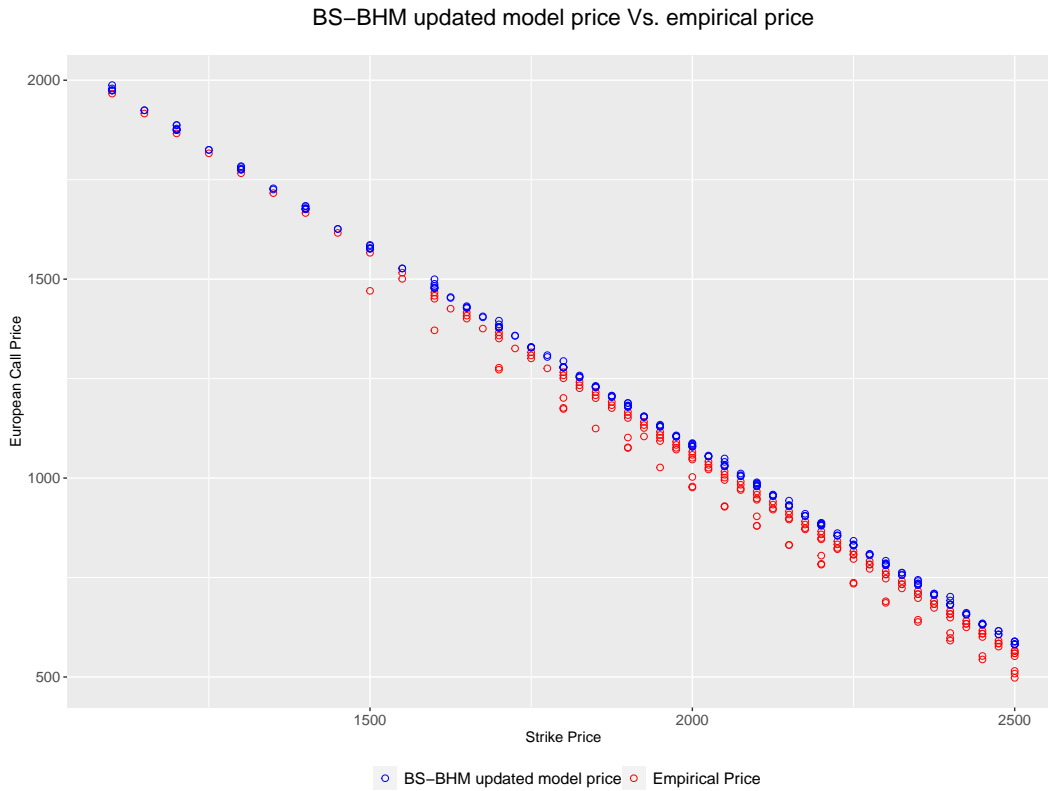


Figure 22: BS-BHM updated model option prices vs. empirical option prices,  $\gamma = 0.25$

Figure 22 illustrates the effect of a variation in  $\gamma$  from a mean value of 0.3 to 0.25. The fit of the BS-BHM updated model price to the empirical data is very similar to that in figure 21. This implies that  $\gamma$  has a less significant impact on the option prices in the BS-BHM updated model as compared to the BS-BHM model.

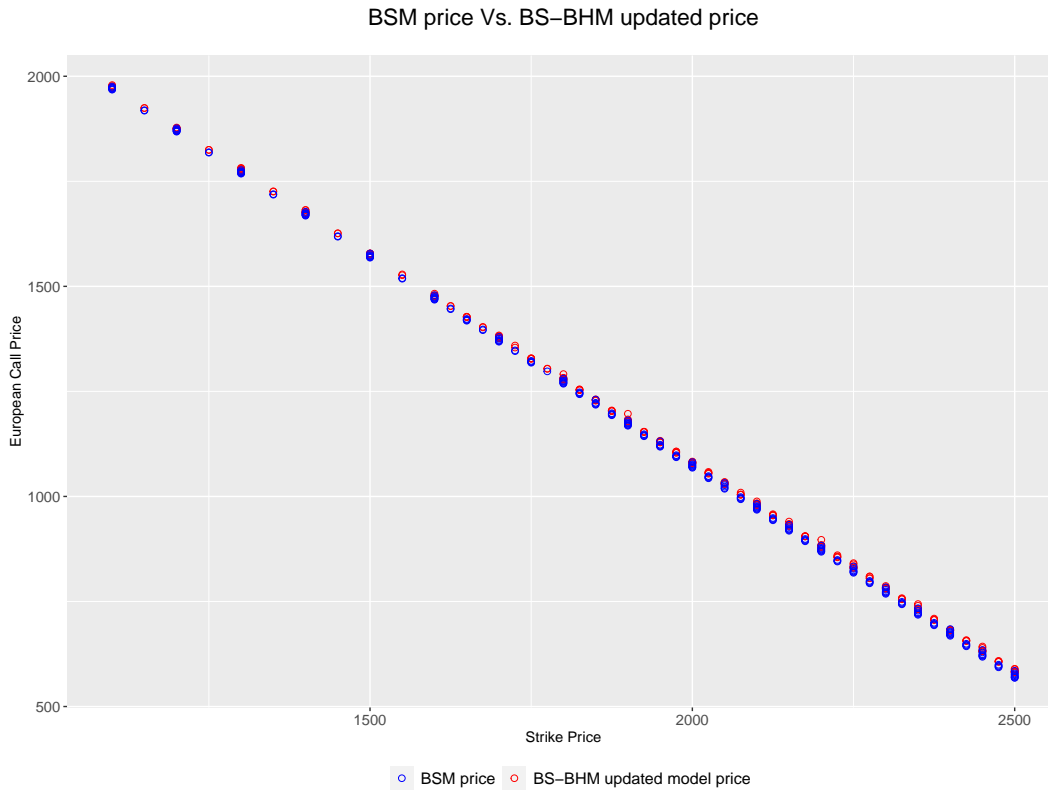


Figure 23: Black-Scholes model vs. BS-BHM updated model option prices,  $\gamma = 0.3$ .

Comparing the BS-BHM updated model and the Black-Scholes model option price in figure 23, the BS-BHM updated model provides slightly higher prices than the Black-Scholes model.

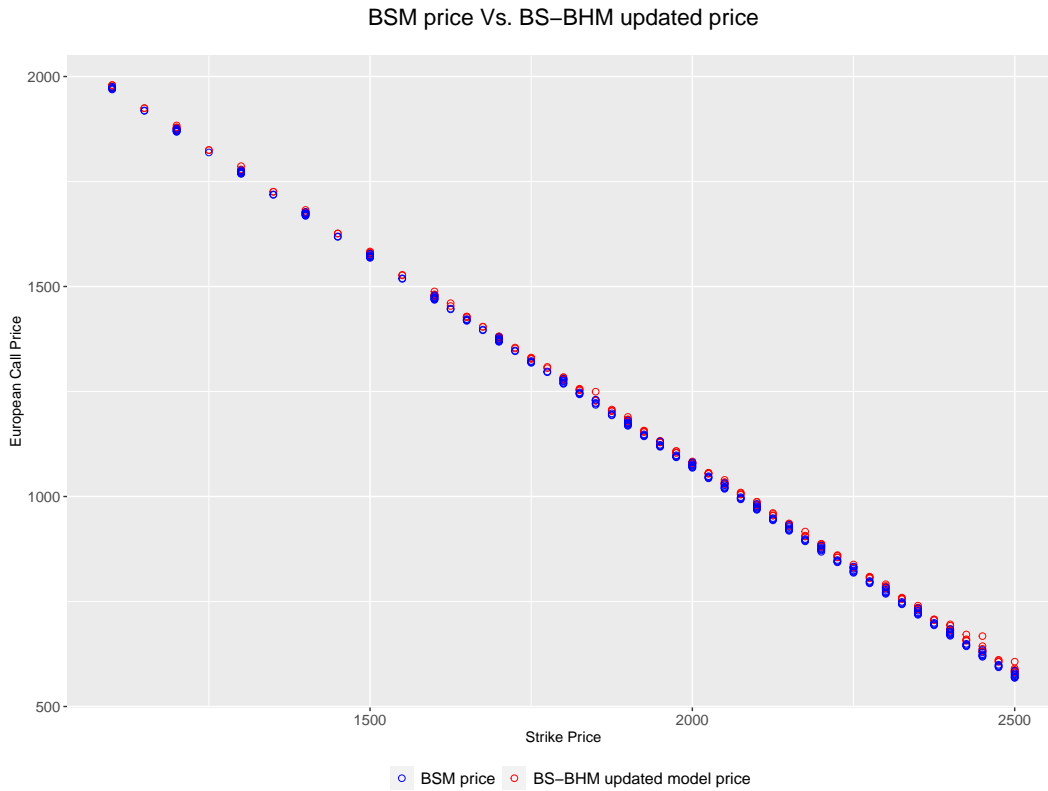


Figure 24: Black-Scholes model vs. BS-BHM updated model option prices,  $\gamma = 0.25$ .

The prices for the models are very similar when  $\gamma$  is varied from 0.3 to 0.25, as shown in figure 24.

For the multi-asset European call option, two assets having equal weights and a correlation coefficient of 0.4 are considered.  $r$  is 0.01.

Multi-Asset European Call Option				
K	$S_{1,0}$	$S_{2,0}$	BS-BHM updated model price	BSM price
237	190	180	5.90	5.50
235	195	185	7.57	7.39
232	200	190	9.67	9.48
226	205	195	13.61	13.87
221	210	200	18.38	18.63

Table 6: Comparison of the multi-asset option prices between the BS-BHM updated model & the Black-Scholes model

From table 6, the prices produced from the BS-BHM updated multi-asset model are comparatively similar to those produced from the Black-Scholes multi-asset model. For higher strike rates, the prices for the BS-BHM updated model are higher, and for lower strike prices, the Black-Scholes model prices are higher.



Figure 25: Comparison of the multi-asset BS-BHM updated and the multi-asset BSM

Figure 25 shows that the prices under the multi-asset BS-BHM updated are relatively similar to those obtained from the multi-asset BSM. The RMSE value is 0.2674.

Comparing the RMSE obtained in the multi-asset BS-BHM model to the multi-asset BS-BHM updated model, the RMSE value in the BS-BHM updated model is lower which indicates it provides a closer fit to the multi-asset BSM as compared to the multi-asset BS-BHM model.

BS-BHM updated model price wrt volatility

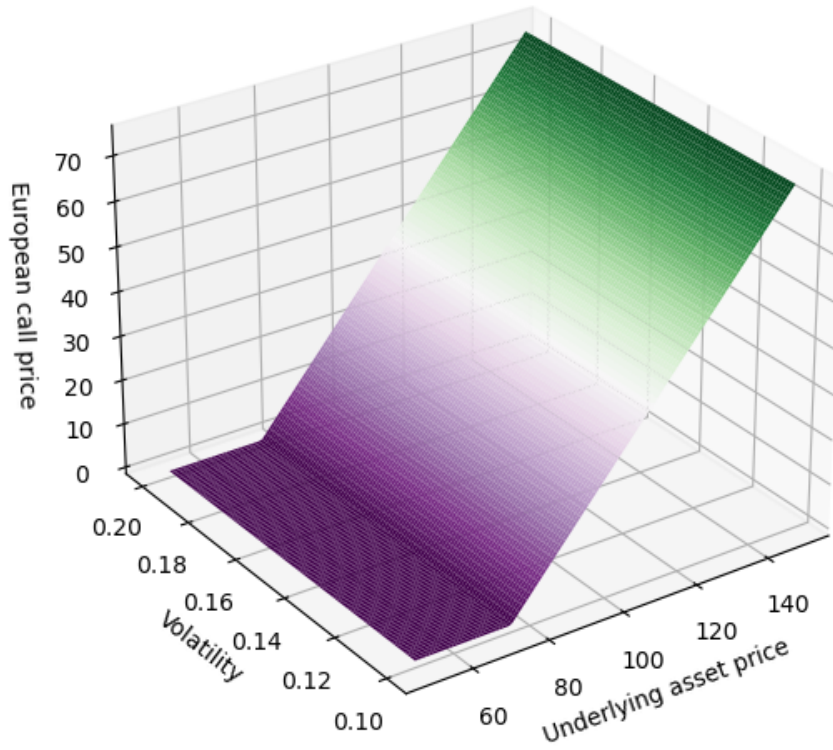


Figure 26: BS-BHM updated volatility surface

Figure 26 shows the features of the BS-BHM updated surface based on monte carlo simulation. This figure illustrates that volatility in the BS-BHM updated model is stochastic.



### *5.3. Estimation of model parameters*

#### *5.3.1. Maximum likelihood estimation*

The estimation of parameters using maximum likelihood estimation is done using daily historical data for SPX call options.

For the Black-Scholes model, the estimate for  $\sigma$  is found to be 0.46283.

For the information-based model, the estimates for the parameters  $\gamma$  and  $\nu$  are 0.071 and  $\nu = 0.001874$  respectively.

#### *5.3.2. Method of moments*

The data used here relates to SPX call options daily data obtained from yahoo finance.

The method of moments is used to estimate  $\nu$  and  $\gamma$ .

Estimation using the method of moments produces an estimate for the volatility parameter,  $\hat{\nu} = 0.005047805$  and  $\hat{\gamma} = 0.07104789$ .

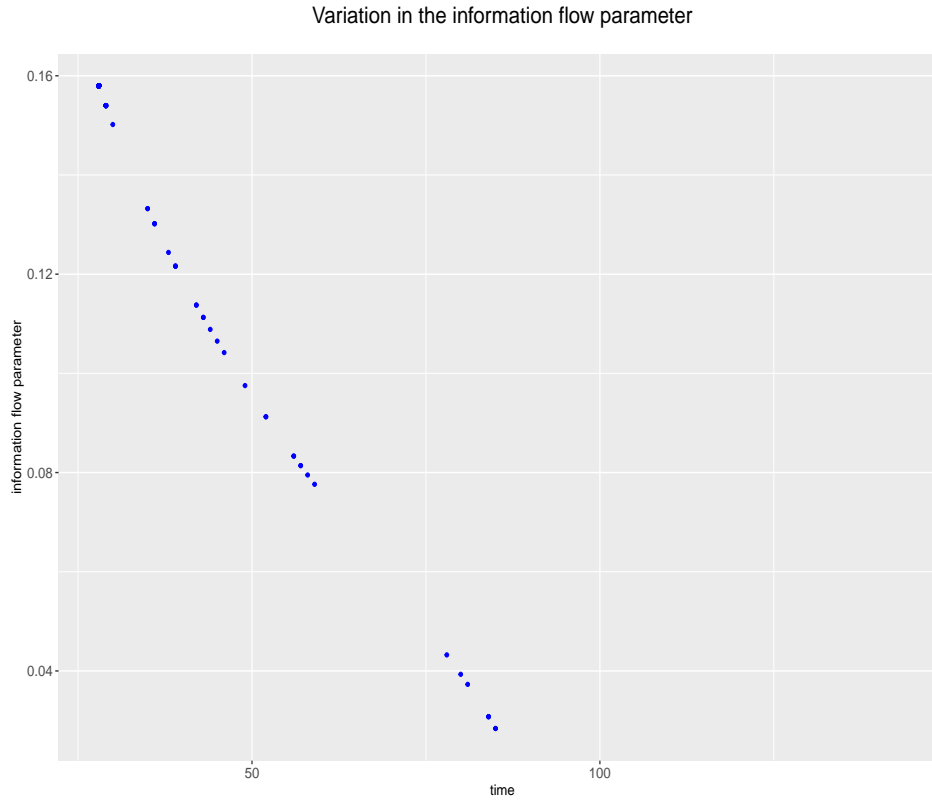


Figure 27: Information flow rate wrt time

Figure 27 shows that the value of the information flow parameter decreases as time increases. This is due to the fact that as the maturity period approaches, the rate at which information about the expected cashflow is revealed decreases as most of the information has already been revealed to the market participants.

### 5.3.3. Measurement of parameter sensitivity

The parameter values used are as follows:  $K$  takes the values 90, 100 and 110,  $S = 100$ ,  $r = 0.05$ ,  $v = 0.56$ ,  $T = 3$ ,  $t = 1$  and  $\gamma = 0.2$ .

Figure 28 shows that delta is positive for European call options. Delta tends to one when an option gets further in-the-money and it tends to zero the more the option gets further out-of-the-money.

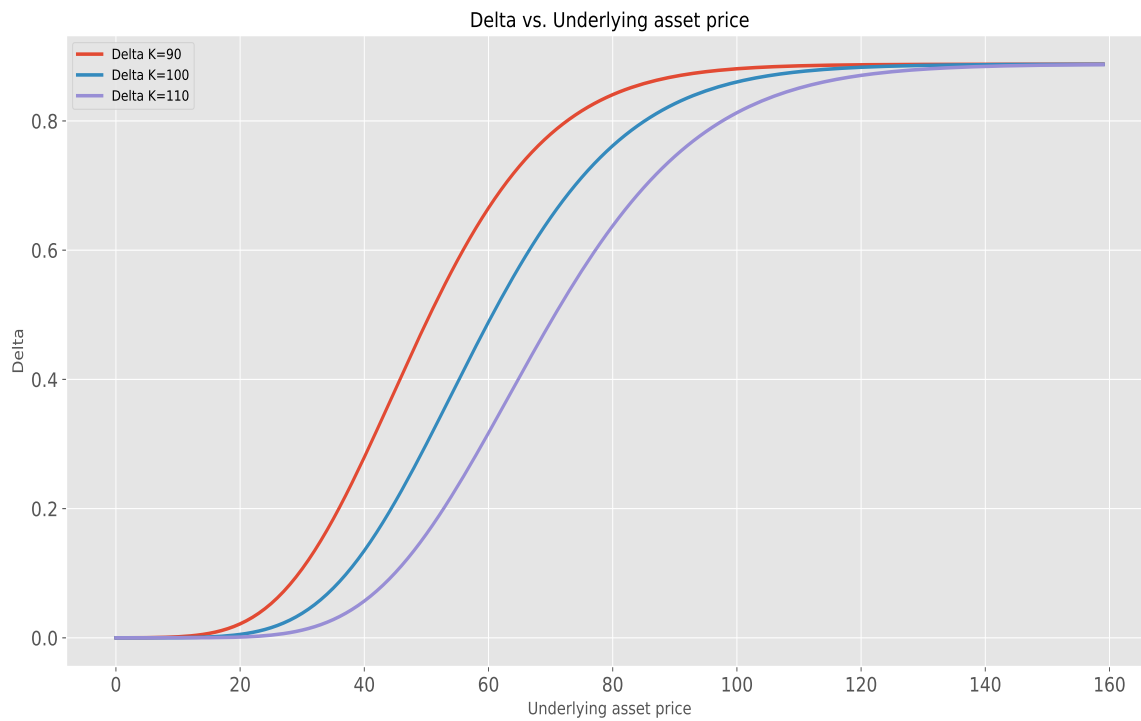


Figure 28: Sensitivity of the option price wrt Delta

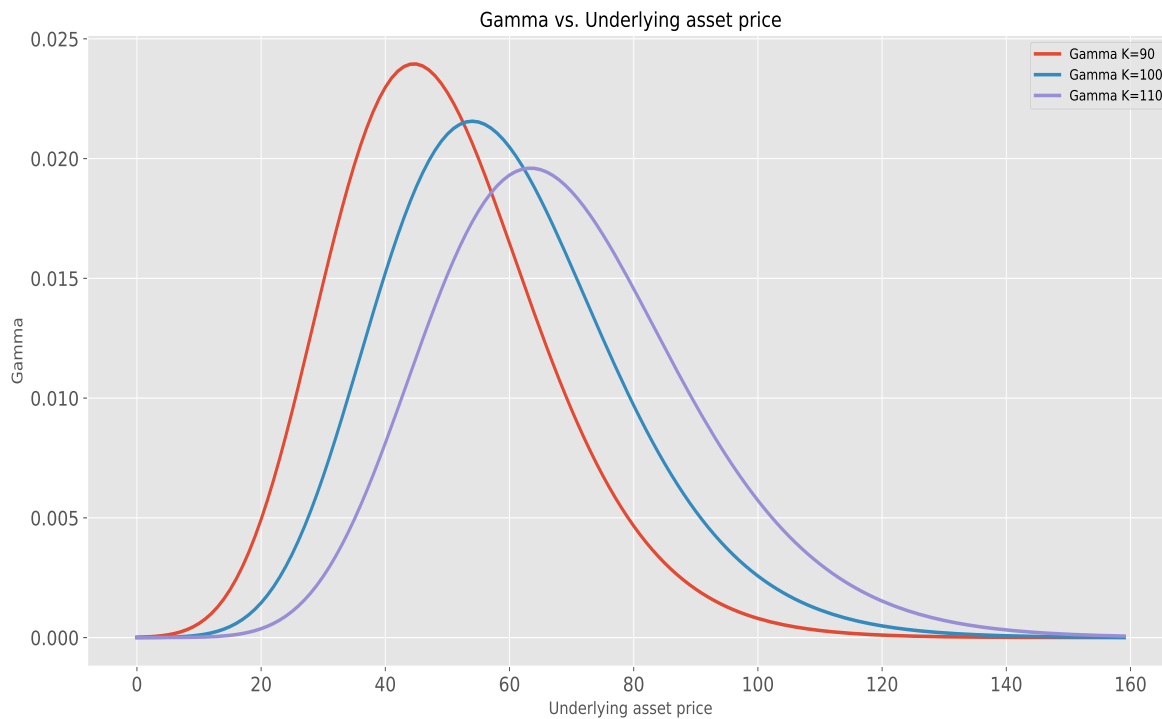


Figure 29: Sensitivity of the option price wrt Gamma

Figure 29 shows that Gamma measures the curvature or convexity of the relationship between the asset price and the underlying asset price.

The higher the value of Gamma, the higher the options sensitivity to the underlying asset price.

As an option gets further in-the-money or out-of-the-money, gamma reduces and tends to zero.

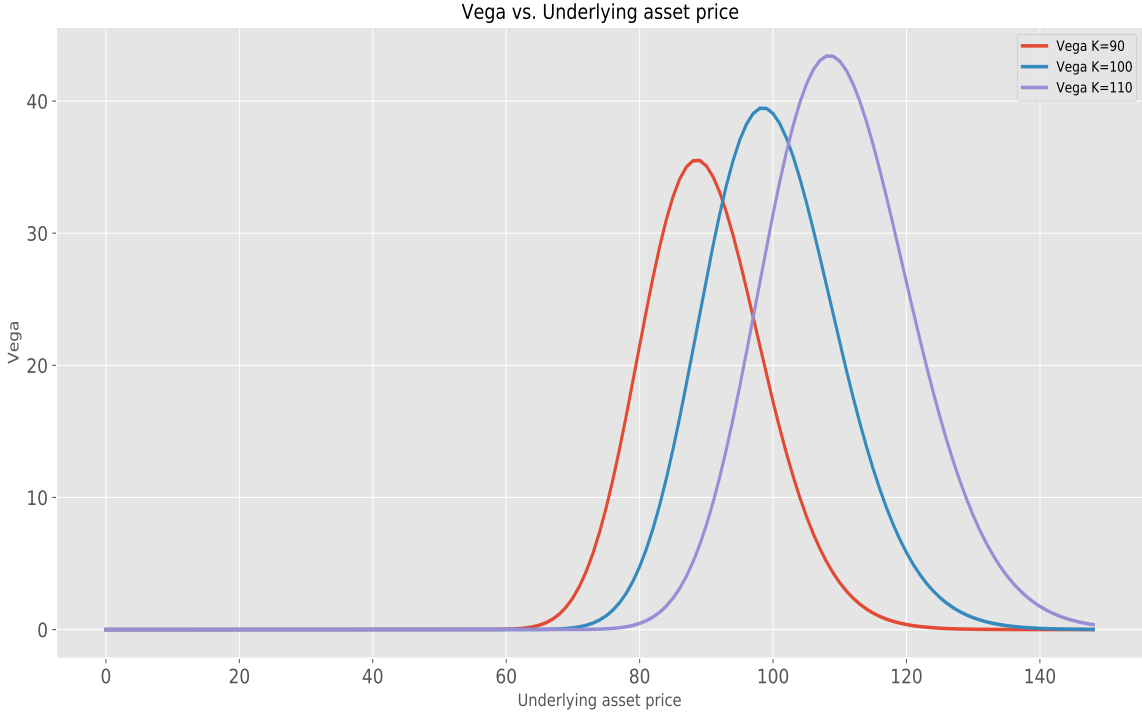


Figure 30: Sensitivity of the option price wrt Vega

Figure 30 shows that the vega of at-the-money options are the highest. This implies that the option price is most sensitive to variations in volatility at this point.

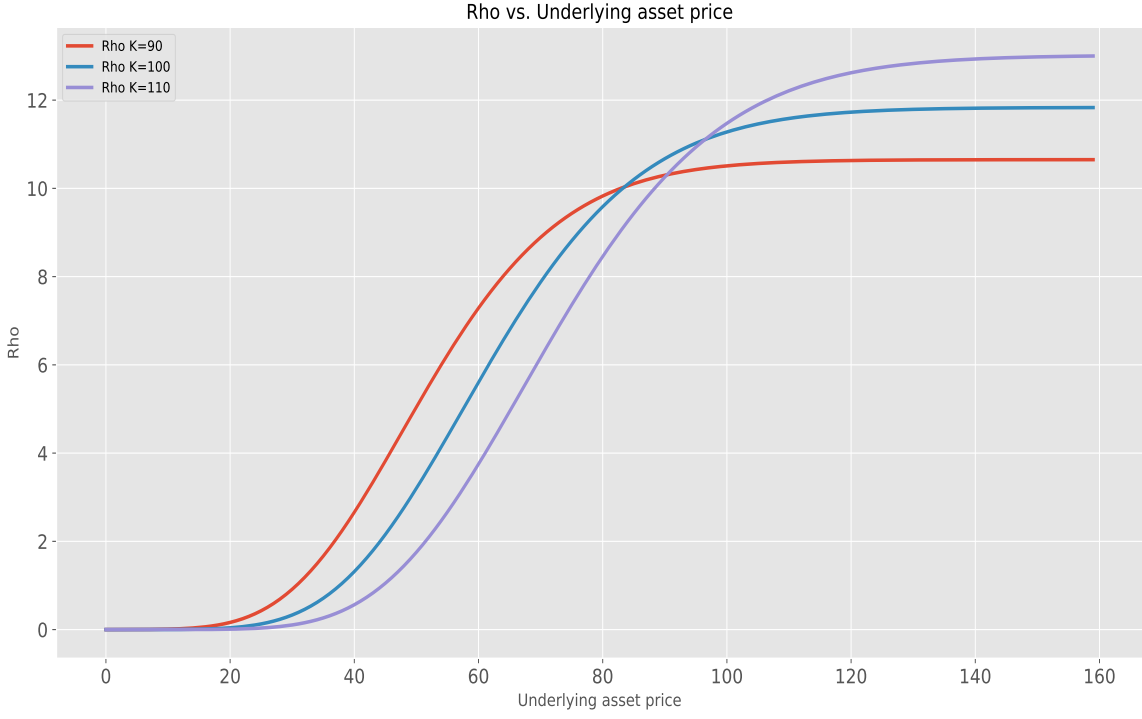


Figure 31: Sensitivity of the option price wrt Rho

The lower the value of Rho, the less sensitive the option price is to changes in interest rates as shown in figure 31.

For options that are in-the-money, Rho is larger and gradually decreases as the option moves to become out-of-the-money.

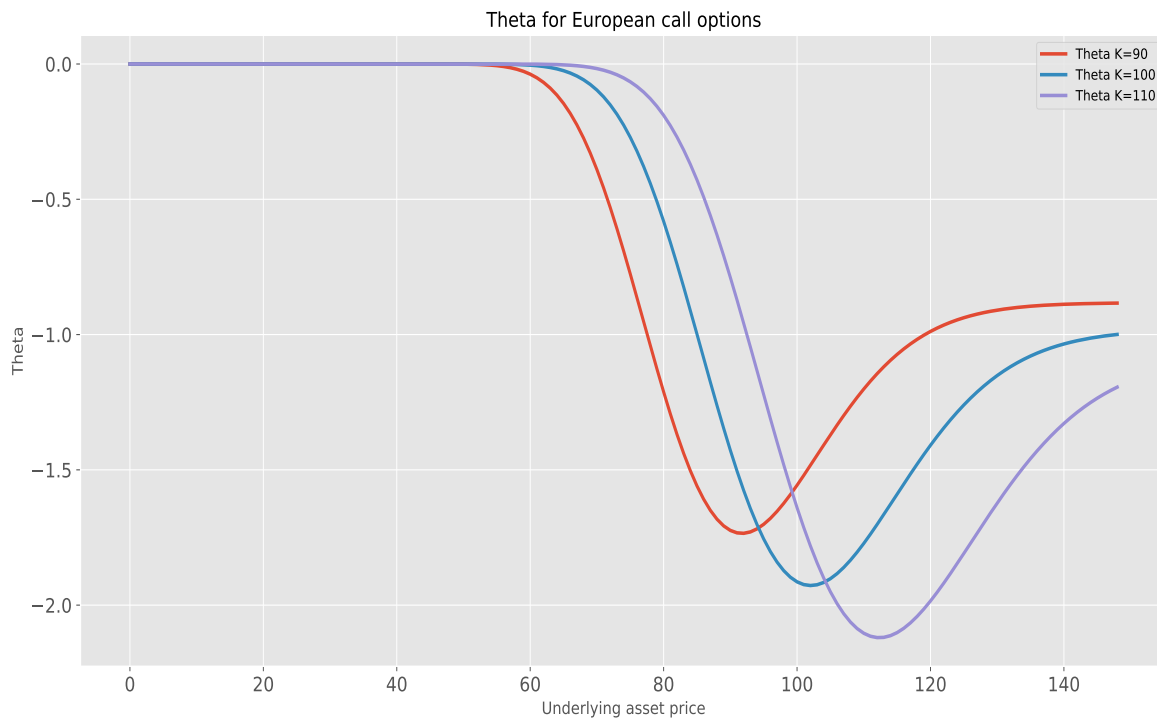


Figure 32: Sensitivity of the option price wrt Theta

Figure 32 illustrates that the value of theta is lowest when the option is at the money, this is because the profitability of an option reduces over time.

#### 5.4. Comparison of volatility in a stochastic volatility model vs volatility in an information-based asset pricing model

A numerical illustration of volatility extraction in the Heston model and the information-based asset pricing framework is looked at in this section. Volatility extraction is done using non-linear filtering in particular using the extended Kalman filter and the particle filter approach. A comparison will then be done between the results obtained from the particle filter and the extended Kalman filter.

The RMSE test will be used to assess the goodness of fit of the simulated estimates to the estimates obtained using non-linear filtering as follows:

$$RMSE = \sqrt{\sum_{k=1}^n \frac{(O_k - E_k)^2}{n}}$$

$O_k$  is the simulated volatility and  $E_k$  is the estimated volatility based on non-linear filtering.

##### 5.4.1. Volatility extraction in the Heston model

The estimated parameters used are as follows:  $v_0 = 0.0175$ ,  $\kappa = 1.5768$ ,  $\eta = 0.0398$ ,  $\theta = 0.5751$ ,  $r = 0.01$  and  $\rho = -0.5711$ .

The measurement equation is given by:

$$y_k = \left( r - \frac{\rho}{\eta} \right) \Delta k + \frac{\rho}{\eta} V_k + \left[ \frac{\rho}{\eta} (\kappa \Delta k - 1) - \frac{1}{2} \Delta k \right] V_{k-1} + \sqrt{1 - \rho^2} \sqrt{\Delta k} \sqrt{V_{k-1}} B_{k-1} \quad (5.4.1)$$

$$= \left( 0.01 + \frac{0.5711}{0.0398} \right) \Delta k - \frac{0.5711}{0.0398} V_k - \left[ \frac{0.5711}{0.0398} (1.5768 \Delta k - 1) + \frac{1}{2} \Delta k \right] V_{k-1} + \sqrt{1 + 0.5711^2} \sqrt{\Delta k} \sqrt{V_{k-1}} B_{k-1} \quad (5.4.2)$$

The state transition equations are given by:

$$V_k = \kappa \theta \Delta k + (1 - \kappa \Delta k) V_{k-1} + \eta \sqrt{\Delta k} V_{k-1} Z_{k-1} = 1.5768 \times 0.5751 \Delta k + (1 - 1.5768 \Delta k) V_{k-1} + 0.0398 \sqrt{\Delta k} V_{k-1} Z_{k-1} \quad (5.4.3)$$

The initial mean is given by  $\hat{x}_0 = 0.0175$  and the initial covariance is  $\hat{P}^- = 0.0398^2 \times 0.0175 \Delta k$ .  $V_0$  denotes the initial variance level.



The Jacobian matrices in the extended Kalman filter are obtained as follows:

$$\begin{aligned} A_k &= 1 - \kappa \Delta k \\ &= 1 - 1.5768 \Delta k \end{aligned} \tag{5.4.4}$$

$$W_k = 0.0398 \sqrt{V_{k-1}} \sqrt{\Delta k} \tag{5.4.5}$$

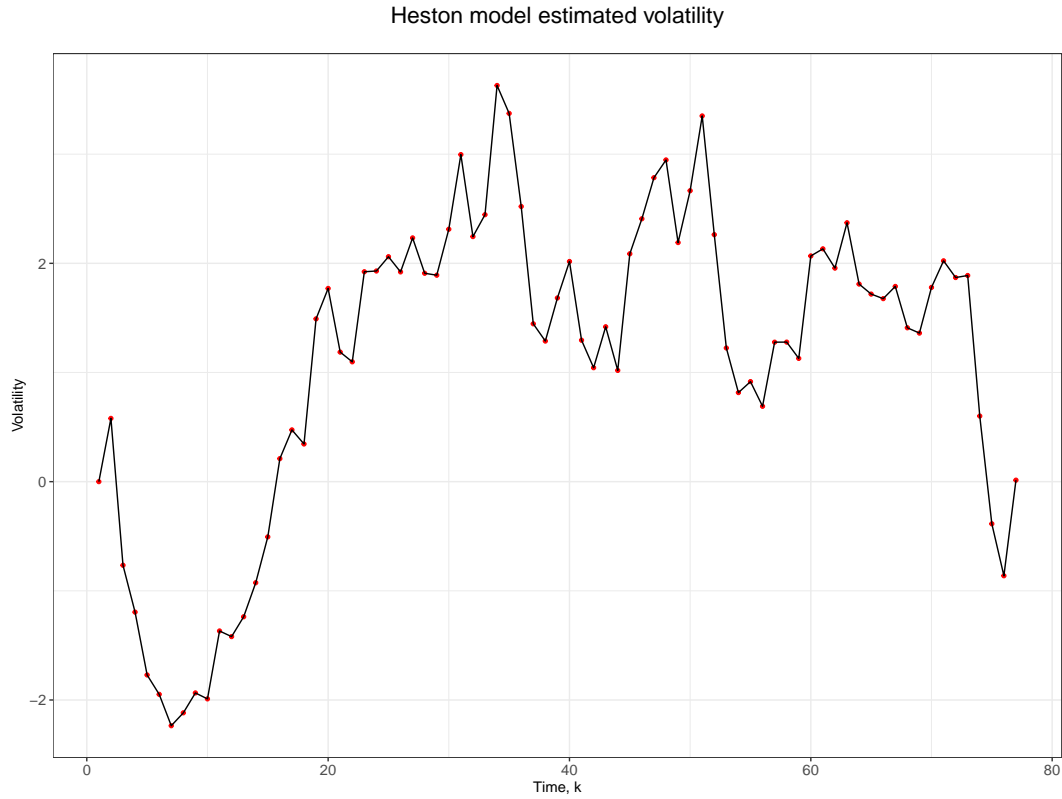


Figure 33: Heston model's simulated volatility

Figure 33 shows the simulated volatility based on monte carlo simulation using the Heston model. 75 time steps,  $k$  were considered in the simulation.

The volatility estimates from the extended Kalman filter approach against the simulated volatility are given in figure 34.

Heston EKF estimated volatility Vs. simulated volatility

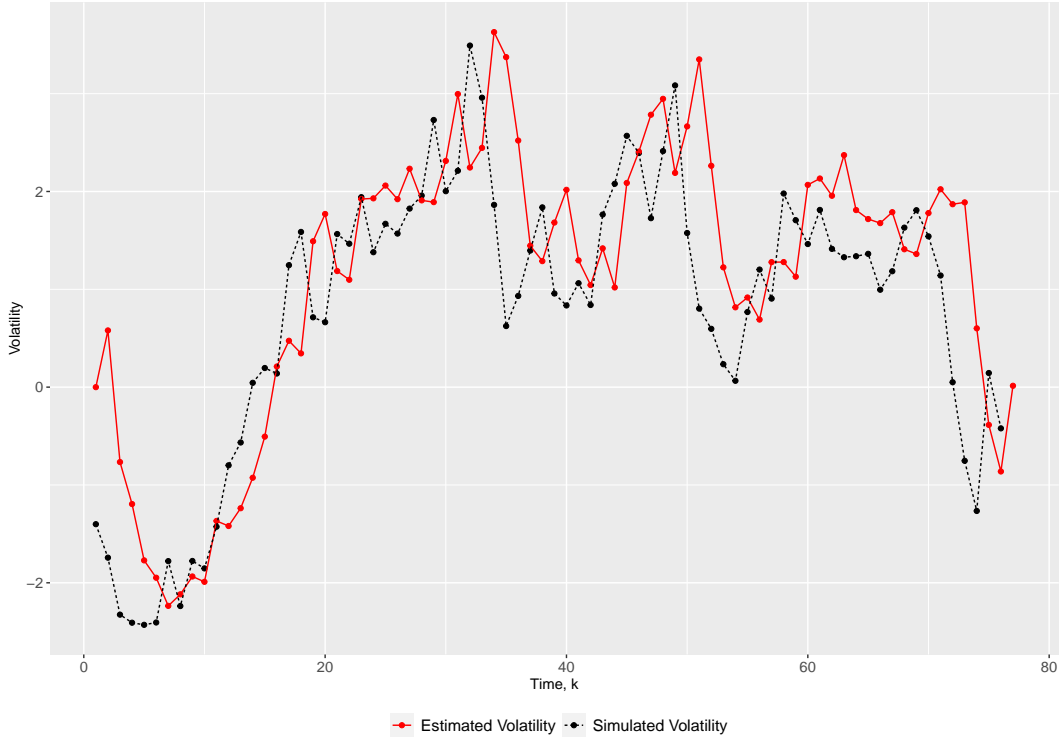


Figure 34: Heston model's simulated volatility vs. estimated volatility using the EKF

Figure 34 shows that the extended Kalman filter approach produces estimated volatility rates that are relatively close to the simulated volatility rates. The RMSE is 0.6475.

In order to apply particle filtering to the Heston model, the weight  $w_k^{(i)}$  at time  $k$  is obtained as follows:

$$w_k^{(i)} = w_{k-1}^{(i)} \frac{p(y_k | v_{0:k}^{(i)}, y_{0:k-1}) p(v_k^{(i)} | v_{0:k-1}^{(i)}, y_{0:k-1})}{p(v_k^{(i)} | v_{k-1}^{(i)}, y_k)}$$

$$p(v_k | v_{k-1}, y_k) \sim N(\mu_p, \sigma_p)$$

$$\begin{aligned} \mu_p &= V_{k-1} + \kappa(\theta - V_{k-1})\Delta t - \rho\eta\left(\mu - \frac{1}{2}V_{k-1}\right)\Delta t + \rho\eta(y_k - y_{k-1}) \\ &= V_{k-1} + 1.5768(0.5751 - V_{k-1})\Delta t + 0.5711 \times 0.0398\left(\mu - \frac{1}{2}V_{k-1}\right)\Delta t \\ &\quad - 0.5711 \times 0.0398(y_k - y_{k-1}) \end{aligned}$$

$$\begin{aligned} \sigma_p^2 &= \eta^2 V_{k-1}^{(i)} (1 - \rho^2) \Delta t \\ &= 0.0398^2 V_{k-1}^{(i)} (1 - 0.5711^2) \Delta t \end{aligned}$$

$$\begin{aligned}
p(v_k | v_{0:k-1}, y_{0:k-1}) &\sim N(\mu_q, \sigma_q^2) \\
\mu_q &= V_{k-1} + \kappa(\theta - V_{k-1})\Delta t \\
&= V_{k-1} + 1.5768(0.5751 - V_{k-1})\Delta t \\
\sigma_q^2 &= \eta^2 V_{k-1} \Delta t \\
&= 0.0398^2 V_{k-1} \Delta t
\end{aligned}$$

$$\begin{aligned}
p(y_k | v_{0:k}, y_{0:k-1}) &= p(y_k | v_k, v_{k-1}, y_{k-1}) \\
p(y_k | v_k, v_{k-1}, y_{k-1}) &\sim N(\mu_r, \sigma_r^2) \\
\mu_r &= y_{k-1} + \left(r - \frac{1}{2}V_{k-1}\right)\Delta t \\
&= y_{k-1} + \left(0.01 - \frac{1}{2}V_{k-1}\right)\Delta t \\
\sigma_r^2 &= V_{k-1} \Delta t
\end{aligned}$$

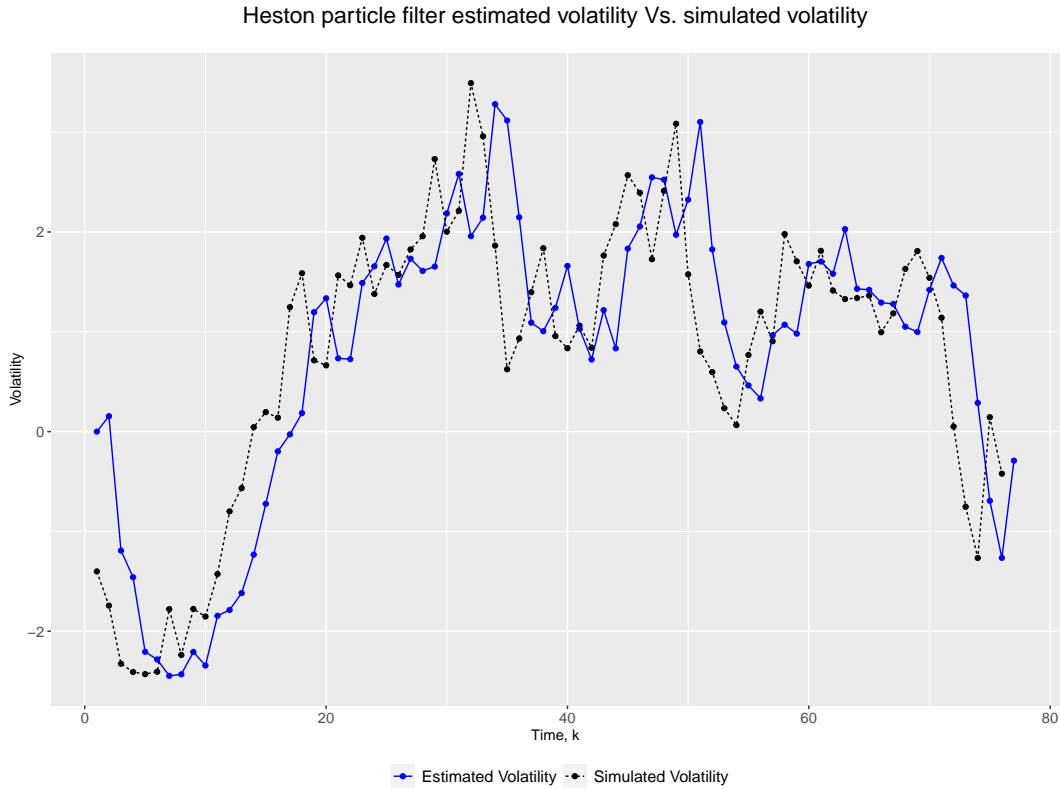


Figure 35: Heston model’s simulated volatility vs. estimated volatility using the particle filter

Figure 35 illustrates the progression over time between the particle filter volatility estimate and the simulated volatility in the Heston model. The estimated volatility using particle filter gives a relatively close fit to the simulated volatility rates and the RMSE is 0.6356. Under the Heston model, the RMSE value from the particle filter estimates is lower than that from the extended Kalman filter estimates. This implies that the particle filter is a better estimate to use for volatility estimation in the Heston model.

Comparing figure 34 to figure 35, it is evident that the estimated volatility rates obtained from the particle filter approach provide a closer fit to the simulated volatility rates than the estimated volatility rates from the extended Kalman filter approach in the Heston model.

#### 5.4.2. Volatility extraction in the information-based asset pricing model

Simulated volatility rates are generated using monte carlo simulation. The values of  $v_{k-1}$  and  $\kappa_{k-1}$  are taken to be constants with estimated values 0.5 and 0.2 respectively with  $r = 0.01$ .

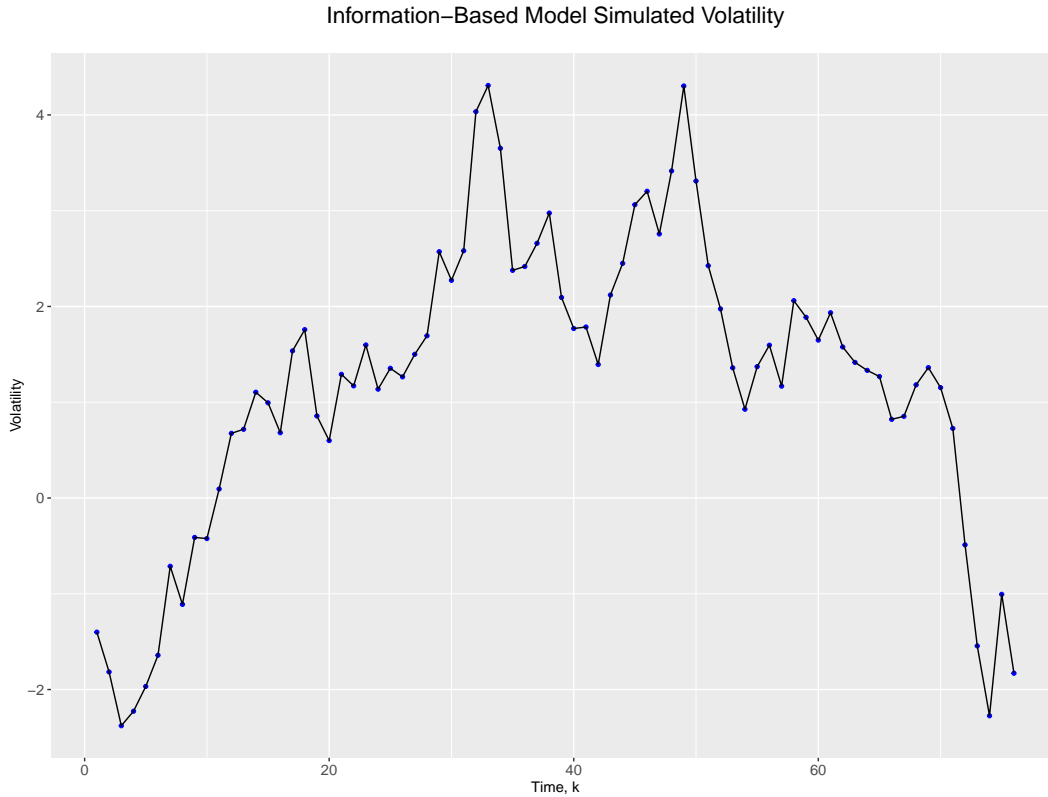


Figure 36: Information-based asset pricing model's simulated volatility

Figure 36 shows the simulated volatility based on monte carlo simulation. 75 time steps,  $k$  were considered in the simulation.

Starting with the extended Kalman filter approach the measurement noise is taken to be 0.01 and the state process noise is taken to be  $5 \times 10^{-6}$ , these two values make up the value of  $R$  and  $Q$  respectively.

Making use of Jacobian matrices:

$$\begin{aligned} A &= 1 - 2v_{k-1}^2 V_{k-1} \Delta k \\ &= 1 - V_{k-1} \Delta k \end{aligned}$$

and

$$\begin{aligned} W &= v_{k-1} \kappa_{k-1} \sqrt{\Delta k} \\ &= 0.1 \sqrt{\Delta k} \end{aligned}$$

The volatility process which is the subject of modelling is represented by the state transition

equation given by:

$$V_k = V_{k-1} - 0.25V_{k-1}^2\Delta k + 0.1\sqrt{\Delta k}B_{k-1}$$

and the measurement equation is as follows:

$$S_k = S_{k-1} + 0.1S_{k-1}\Delta k + 0.5P_{(k-1)T}V_{k-1}\sqrt{\Delta k}W_{k-1}$$

$\hat{x}_0 = 0$ ,  $P_0 = 1$  and  $R \sim N[0, 0.01]$ .

The volatility estimates from the extended Kalman filter approach against the simulated volatility are given in figure 37. The Jacobian matrices are as follows:

$$A = -2g_{k-1}^2V_{k-1}\Delta k$$

$$W = g_{k-1}\kappa_{k-1}\sqrt{\Delta k}$$

$$H = 0$$

$$U = P_{kT}\frac{\lambda T}{T - k}$$

$\tilde{z}_k$  is used to approximate the unobserved variables while  $\tilde{y}_k$  is used as an approximation to the observed variables leading to:

$$z_k \approx \tilde{z}_k + A(z_{k-1} - \hat{z}_{k-1}) + Wm_{k-1},$$

and

$$y_k \approx \tilde{y}_k + H(x_k - \tilde{z}_k) + Vn_k.$$

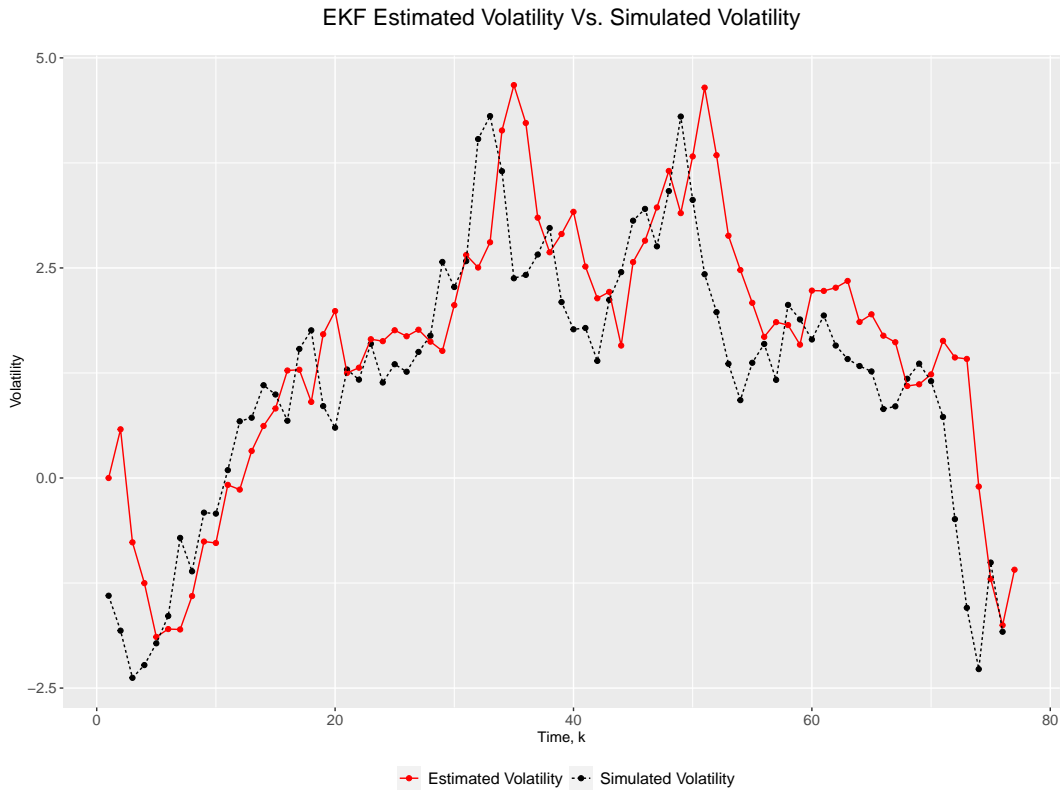


Figure 37: Information-based framework simulated volatility vs. estimated volatility using the EKF

Figure 37 shows that the extended Kalman filter approach produces estimated volatility rates that are relatively close to the simulated volatility rates. The RMSE value is 0.6324. Using the particle filter approach in the information-based stochastic volatility model, the following result is obtained:



Particle Filter Estimated Volatility Vs. Simulated Volatility

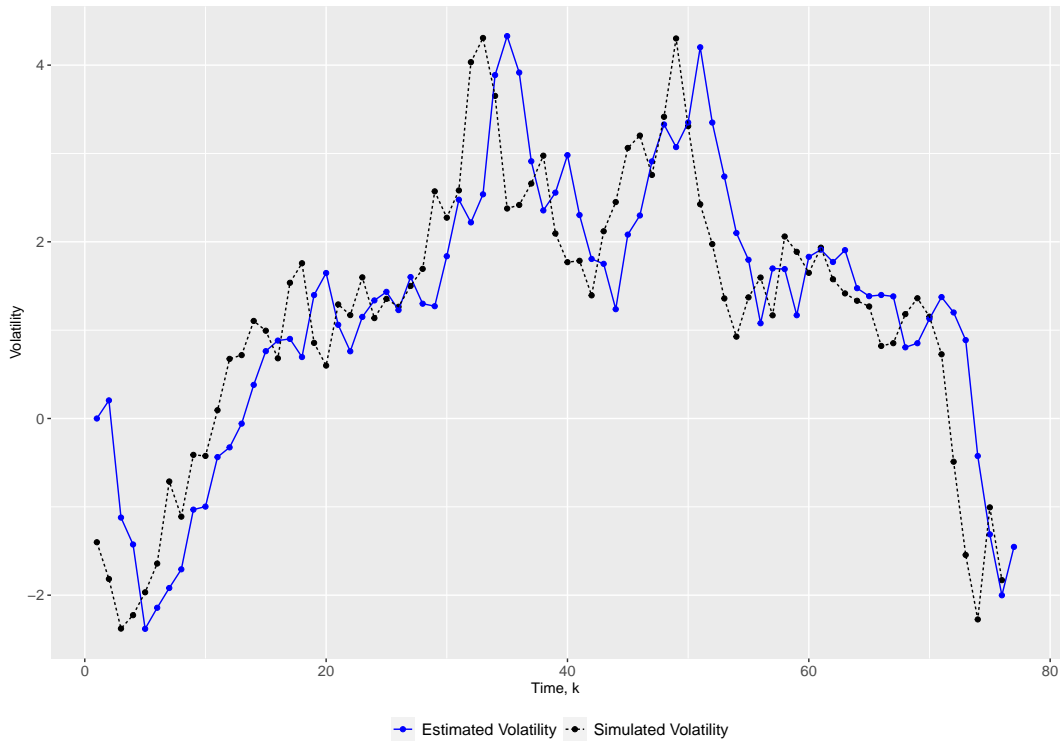


Figure 38: Information-based framework simulated volatility vs. estimated volatility using the particle filter

Figure 38 illustrates the progression over time between the particle filter volatility estimate and the simulated volatility. The estimated volatility using particle filter gives a relatively close fit to the simulated volatility rates. RMSE value is 0.6194 which is lower than the value obtained from the extended Kalman filter estimates. This implies that the particle filter is a better approach to volatility estimation in the information-based stochastic volatility model. Comparing figure 37 to figure 38, it is evident that the estimated volatility rates obtained from the particle filter approach provide a closer fit to the simulated volatility rates than the estimated volatility rates from the extended Kalman filter approach.

Model	Filter	RMSE
Heston:	EKF	0.6475
	Particle	0.6356
ISVM:	EKF	0.6324
	Particle	0.6194

Table 7: RMSE values for the non-linear filters

Table 7 shows the RMSE for the information-based stochastic volatility model are lower for both the extended Kalman filter and the particle filter estimates as compared to the Heston model. This means the results from the filters are more accurate from the information-based stochastic volatility model as compared to the Heston model.

## 6. Conclusion and Recommendation

The information-based asset pricing framework is an improvement over the Heston model and the Black-Scholes model as it views the dynamics of the asset as an emergent phenomenon as opposed to being pre-specified. This research uses the notion of comonotonicity and wishart processes to extend the information-based asset pricing framework to the multi-asset scenario.

The first objective of using a stochastic volatility model in a multivariate framework is achieved by looking at the multi-asset Heston model. Wishart processes are used to obtain the joint dynamics for the asset process and the variance process. The dynamics are then discretized to allow for numerical simulation. A volatility-in-mean effect is added to capture the tendency for the volatility and the asset prices moving together and the Laplace transform is then used to solve the pricing equation for the multi-asset option.

The study looks at the second objective of modelling the dynamics of an asset where the volatility parameter depends on time and information by considering two approaches of the information-based asset pricing framework: the BS-BHM model and the BS-BHM updated model. The price is obtained using risk-neutral pricing in the single-asset case. The derived price takes a similar representation to the Black-Scholes model. This outcome motivates the use of the notion of comonotonicity which is applied in deriving the price for the Black-Scholes model in the multi-asset case.

For the single asset case, the derived information-based stochastic volatility model prices are consistently greater than their true price for all the strike prices considered. The numerical results suggest that the information-based stochastic volatility model values are close to the Black-Scholes model prices. Two assets are considered for the multi-asset option and the results illustrate that the prices from the multi-asset information-based stochastic volatility model give a close fit to the multi-asset Black-Scholes model prices.

In pricing the derivatives of an asset where the volatility parameter depends on time and information in objective three, the RMSE for the BS-BHM updated model takes a value of 0.2674, this is lower than that of the BS-BHM model which is equal to 0.2874. This indicates that the BS-BHM updated model is a better model to be used in the information-based asset pricing framework. A lower RMSE value is indicative of a model that gives a higher accuracy between the true prices and the model prices.

A change in the information flow parameter has a significant impact on the prices obtained in the BS-BHM model. A variation in the parameter value from 0.3 to 0.25 resulted in a better fit of the BS-BHM model to the empirical prices. The study noted that the BS-BHM updated model was less sensitive to changes in the information flow rate as compared to the BS-BHM model. A recommendation is made for further research on determining the optimal

information flow rate parameter to be used in asset pricing.

Objective four is achieved by estimating the model parameters using the method of moments and maximum likelihood estimation. The result obtained by this study is different from that obtained by Mutijah et al., in their estimation of the model parameters using the method of moments, (Mutijah et al., 2013). This is due to an imprecision made by Mutijah et al. in equating the population moments to the sample moments in their work. Further research can be done in this area by considering the case where the information flow rate parameter depends on time. An assumption is made in this research that the information flow rate parameter is a constant.

The study also finds that, regardless of the model's disadvantage of assuming that volatility does not change and pre-specifying the asset price dynamics, the option prices under the Black-Scholes model provide a good fit to the observed price. This research made use of a constant interest rate, further research is needed on the use of a varying interest rate in an information-based stochastic volatility model.

Wishart processes are used to derive the joint dynamics that determine the price for the multi-asset information-based stochastic volatility model. Ito's formula is first applied to the variance process so that it can be written in a form that is consistent with the CIR process. The multi-asset information-based stochastic volatility model has fewer parameters as compared to the multi-asset Heston model, this makes the multi-asset information-based stochastic volatility model easier to implement. In both cases, the multi-asset case reduces to the respective single asset model by a suitable choice of parameter values.

A volatility matrix is introduced in the asset price equation to take account of the risk premium and capture the tendency of the asset price and volatility to move together in the Wishart processes. The volatility matrix parameter takes the value of zero in the multi-asset information-based stochastic volatility model which in effect means that there's no account for the risk premium and the tendency of the asset price and volatility to move together is not captured. This work recommends for further research in this area to ensure that a non-zero risk premium can be introduced in the multi-asset case of the information-based stochastic volatility model.

To assess the sensitivity of the model to changes in the parameter values, the study makes use of Greeks. Greeks can be used as an effective risk management tool through hedging. By making use of Greeks such as an option's delta and gamma, a trader can be able to hedge his portfolio to minimize his risk exposure. Due to the volatile nature of financial markets occasioned by the variations in the factors that affect the option price such as the interest rate, underlying asset price and volatility, the need for sound risk management practices become essential for option traders.

In order to compare the volatility obtained in an asset where information is incorporated and that where information is fixed as outlined in objective five, non-linear filtering is used. An assumption is made that the Weiner process driving the asset process and the Weiner process driving the variance process are uncorrelated in the information-based stochastic volatility model. Further studies need to be carried out in cases where the two Weiner processes are correlated and whether cholesky decomposition can be used to decorrelate them.

Volatility has become a popular area of financial research because the inaccurate volatility estimates lead to inaccurate prices of financial instruments. This may lead to significant financial losses being incurred by financial institutions, and in the long run, it may result in insolvency. In order to avoid such scenarios, it is vital to use accurate estimates of volatility in asset pricing.

This research finds that the particle filter approach to estimating volatility in the information-based model produces volatility rates that are a close fit to the simulated volatility rates. The estimated volatility rates obtained using the extended Kalman filter approach also provide a relatively close fit to the simulated volatility rates. However, the particle filter is seen to provide estimated volatility rates that give a better fit to the simulated volatility than the extended Kalman filter approach.

Despite giving fairly accurate estimates, the particle filter approach to estimating volatility suffers from the setback that the particle weight variance increases continuously with time. This is referred to as particle degradation which implies that as iteration continues, the insignificant particles will consume a significant amount of computation time, which will not only cause resource wastage, but also affect the final estimates, decreasing the accuracy of the process.

The resampling technique is adopted in this study to reduce the problem of degradation. However, this only reduces the problem of degradation. Further research needs to be done on how to eliminate this problem from the particle filtering approach. The extended Kalman filter is considered to be a practical method to be applied in modeling volatility as the current volatility only depends on the previous volatility.

## List of References

X. Wang, X. He, Y. Bao, & Y. Zhao, (2018), "Parameter estimates of Heston stochastic volatility model with MLE and consistent EKF algorithm." *Science China Information Sciences* 61(4).

C. Ewald, A. Zhang, & Z. Zong, (2018), "On the calibration of the Schwartz two-factor model to WTI crude oil options and the extended Kalman Filter." *Annals of Operations Research*.

T. Li, G. Villarrubia, S. Sun, J. Corchado, & J. Bajo, (2015), "Resampling methods for particle filtering: identical distribution, a new method, and comparable study." *Frontiers of Information Technology & Electronic Engineering* 16(11), 969–984.

F. Karamé, (2018), "A new particle filtering approach to estimate stochastic volatility models with Markov-switching." *Econometrics and Statistics*.

P. Wu, & R. Elliott, (2017), "A simple efficient approximation to price basket stock options with volatility smile". *Annals of Finance* 13(1) 1–29.

Y. Ait-Sahalia, C. Li, & C.X. Li, (2020) "Closed-form implied volatility surfaces for stochastic volatility models with jumps". *Journal of Econometrics*.

J., Dhaene, A., Kukush and D., Linders (2020) "Comonotonic asset prices in arbitrage-free markets," *Journal of Computational and Applied Mathematics* 364, 377-427.

R., Carmona and V., Durrleman (2006) "Generalizing the black-scholes formula to multivariate contingent claims," *Journal of Computational Finance* 9, 43-67.

G., Dimitroff, S., Lorenz and A., Szimayer (2011) "A parsimonious multi-asset Heston model: calibration and derivative pricing," *International Journal of Theoretical and Applied Finance* 14(8), 1299-1333.

D., Brody, L., Hughston and A., Macrina (2008) "Information-based asset pricing," *International Journal of Theoretical and Applied finance* 11, 107-142.

G., Deelstra, J., Liinev and M., Vanmaele (2004) "Pricing of arithmetic basket options by conditioning," *Insurance: Mathematics and Economics* 34(1), 1-23.

A., Macrina (2006) "An Information-Based Framework for Asset Pricing: X-Factor Theory and its Applications," PhD Thesis, King's College London.

J., Cox, J., Ingersoll and S., Ross (1985) "A Theory of the Term Structure of Interest Rates," *Econometrica* 53, 385–407.

D., Bernhardt and M., Eckblad (2013) "Stock market crash of 1987," Federal Reserve Bank of Chicago.

X., Chen, G., Deelstra, J., Dhaene and M., Vanmaele (2008) "Static super-replicating strategies for a class of exotic options," *Insurance, Mathematics and Economics* 42(3), 1067-1085

- D., Linders (2013) "Pricing index options in a multivariate Black and Scholes model," Research report AFI-1383, FEB, KU Leuven.
- F., Black and M., Scholes (1973) "The Pricing of Options and Corporate Liabilities," *Journal of Political Economy* 81(3), 637–654.
- S., Heston (1993) "A Closed-Form Solution for Options with Stochastic Volatility with Applications to Bond and Currency Options," *The Review of Financial Studies* 6(2), 327-343.
- J., Da Fonseca, M., Grasselli and C., Tebaldi (2008) "A multifactor volatility Heston model," *Quantitative Finance* 8, 591-604.
- L.P., Bos and A.F., Ware (2000) "How to solve multiasset Black-Scholes with time-dependent volatility and correlation," *Journal of Computational Finance* 4(2), 99-107.
- C., Gouriéroux and R., Sufana (2010) "Derivative pricing with multivariate stochastic volatility," *Journal of Business and Economic Statistics* 28(3), 438-451.
- M., Bru (1991) "Wishart processes," *Journal of Theoretical Probability* 4, 725-743.
- P., Christoffersen, S., Heston and K., Jacobs (2009) "The shape and term structure of the index option smirk: Why multifactor stochastic volatility models work so well," *Management Science* 55(12), 1914-1932.
- M.C., Recchioni and A., Scoccia (2014) "An Analytically Tractable Multi-asset Stochastic Volatility Model," *Applied Mathematical Sciences* 8(27), 1339-1355.
- T., Khraisha and K., Arthur (2018) "Can we have a general theory of financial innovation processes?" A conceptual review. *Financial Innovation* 4(1), 4.
- D., Brody, L., Hughston and A., Macrina (2011) "Modelling Information Flows in Financial Markets," *Advanced Mathematical Methods for Finance* 133–153.
- A., Macrina and P.A., Parbhoo (2010) "Securities Pricing with Information-Sensitive Discounting," KIER Working Papers 695, Kyoto University, Institute of Economic Research.
- R.C., Merton (1973) "Theory of Rational Option Pricing," *Bell Journal of Economics and Management Science* 4 (1), 141–183.
- A.V., Thakor (2015) "The Financial Crisis of 2007–2009: Why Did It Happen and What Did We Learn?" *Review of Corporate Finance Studies* 4(2), 155-205.
- A., Javaheri, D., Lautier and A., Galli (2003) "Filtering in finance," Wilmott Magazine, Chichester, UK, 67–83.
- P., Wilmott (2005), "Paul Wilmott Introduces Quantitative Finance" Chichester, John Wiley and Sons Inc.
- C., Ball and W., Torous (2000) "Stochastic correlation across international stock markets" *Journal of Empirical Finance* 7, 373-388.
- M., Loretan and W., English (2000) "Evaluating correlation breakdowns during periods of market volatility," Mimeo, Federal Reserve Board.

C., Gouriéroux (2006) "Wishart Processes for Stochastic Risk," *Econometric Reviews, special issue on Stochastic Volatility* 25, 1-41.

P., Gauthier and D., Possamai (2009) "Efficient simulation of the Wishart model," SSRN eLibrary.

P., Kloeden and E., Platen (1999) "Numerical Solution of Stochastic Differential Equations," Springer.

A., Lewis (2005) "Option Valuation under Stochastic Volatility: With Mathematica Code," Newport Beach, Finance Press 2, 22-57.

M., Davis and A., Etheridge (2006) "Louis Bachelier's Theory of Speculation: The Origins of Modern Finance," Princeton University Press.

P., Samuelson (1965) "Proof that properly anticipated prices fluctuate randomly," *Industrial Management Review* 6, 41-9.

P., Samuelson, and R., Merton (1969) "A Complete Model of Warrant Pricing that Maximizes Utility." *Industrial Management Review* 10, 17-46.

D., Hobson and L., Rogers (1998) "Complete Models with Stochastic Volatility," *Mathematical Finance* 8, 27-48.

R.C., Blattberg and N.J., Gonedes (1974) "A comparison of the stable and Student distributions as statistical models for stock prices," *Journal of Business* 47, 244-280.

L.O., Scott (1987) "Option pricing when the variance changes randomly: theory, estimation and an application," *Journal of Financial and Quantitative Analysis* 22, 419-438.

J. Hull and White (1987). "The Pricing of Options on Assets with Stochastic Volatilities". *The Journal of Finance* 42(2), 281-300.

Das, Sanjiv, and R. Sundaram, (1999) "Of smiles and smirks: A term structure perspective", *Journal of Financial and Quantitative Analysis* 34, 211-240.

B. David, F. Silverio, L. Kai and W. Liuren, (1997) "Accounting for Biases in Black-Scholes". CRIF Working Paper series.

C. Gouriéroux (2006) "Continuous Time Wishart Process for Stochastic Risk". *Econometric Reviews*, 25(2), 177-217.

L. Teng, M. Ehrhardt, and M. Gunther (2018) "Numerical simulation of the heston model with stochastic correlation". *International Journal of Financial Studies* 6(1).

J. Zuzana, (2018) "Drawbacks and Limitations of Black-Scholes Model for Options Pricing". *Journal of Financial Studies and Research*.

H. Albrecher, P. Mayer, W. Schoutens, and J. Tistaert (2007) "The little Heston Trap". *Wilmott*, 83-92.

J., Da Fonseca, M., Grasselli, and C., Tebaldi (2007) "Option pricing when correlations are stochastic: an analytical framework," *Review of Derivatives Research* 10, 151-180.

Mutijah, Guritno and Gunardi, (2012), "A Black Scholes Model from an Information-



Based Perspective” International Conference on Statistics in Science, Business and Engineering.

Mutijah, Guritno and Gunardi, (2013), “Estimation of Parameters on the BS-BHM Updated Model.” *Journal Applied Mathematical Sciences* 7(72).

Mutijah, Guritno and Gunardi, (2016), “Pricing of European options under BS-BHM-updated model and its properties” *AIP Conference Proceedings* 1707.

F. D. Rouah, *The Heston Model and its Extensions in Matlab and C#*, Wiley, 2013.

H. Chen, C. Hu, & W. Yeh, *Option pricing and the Greeks under Gaussian fuzzy environments*. *Soft Computing*. 2019.

K. Shafi, N. Latif, S. Shad, Z. Idrees, & S. Gulzar, *Estimating option greeks under the stochastic volatility using simulation*. *Physica A: Statistical Mechanics and Its Applications*. 2018.

Song-Ping Zhu & Xin-Jiang He, *A new closed-form formula for pricing European options under a skew Brownian motion*, *The European Journal of Finance*. 2017.